TECHNISCHE
UNIVERSITÄT
MÜNCHEN

Signatures of CP-Violating Electroweak Penguins in Flavor Physics

Felix Schwab

Max-Planck-Institut für Physik
(Werner-Heisenberg-Institut)
Föhringer Ring 6
D-80805 München
Email: schwab@mppmu.mpg.de

Max-Planck-Institut
für Physik
(Werner-Heisenberg-Institut)

Physik-Department
Technische Universität München
Institut für Theoretische Physik
Lehrstuhl Univ.-Prof. Dr. Andrzej J. Buras

Signatures of CP-Violating Electroweak Penguins in Flavor Physics

Felix Schwab

Vollständiger Abdruck der von der Fakultät für Physik der Technischen Universität München zur Erlangung des akademischen Grades eines

Doktors der Naturwissenschaften (Dr. rer. nat.)

genehmigten Dissertation.

Vorsitzender:		Univ-Prof. Dr. L. Oberauer
Prüfer der Dissertation:	1.	Univ-Prof. Dr. A. J. Buras
	2.	Priv.-Doz. Dr. A. H. I. Hoang

Die Dissertation wurde am 20.4.06 bei der Technischen Universität München eingereicht und durch die Fakultät für Physik am 27.6.06 angenommen.

"Yes There Are Two Paths You Can Go By,
But In The Long Run,
There's Still Time To Change The Road You're On."
Led Zeppelin, Stairway To Heaven

Signatures of CP-Violating Electroweak Penguins in Flavor Physics

Abstract

We study several non-leptonic decays in a scenario of enhanced electroweak penguins. Beginning with the decays $B \to \pi\pi$, we find them to be well described within the SM. Some anomalous signatures can be explained in our scenario by hadronic interference effects. We also determine the CKM angle γ from $B \to \pi\pi$, which we find as $\gamma = 74 \pm 6^\circ$. The small discrepancy with the values obtained from unitarity triangle fits can be attributed to small new physics effects in $B^0_d - \bar{B}^0_d$ mixing. We then predict the CP violating asymmetries for $B^0_d \to \pi^0\pi^0$. Taking the hadronic parameters and γ from the $B \to \pi\pi$ system, we use the SU(3) flavor symmetry of strong interaction to fix the corresponding hadronic parameters in the $B \to \pi K$ system. We find agreement in the predictions for those observables that are only marginally affected by electroweak penguins, while the description of those quantities where they play a significant role is only moderately good. We then determine the electroweak penguin parameters required to describe the data and find an enhanced electroweak penguin contribution with a large CP violating phase. Exploring next the implications of a simple scenario, where new physics effects enter only in the electroweak penguins, we find that the possible enhancement of these amplitudes is already strongly constrained by the measurement of the inclusive decay $b \to s l^+ l^-$. Therefore, we discuss the implications of future developments in the $B \to \pi K$ data for several rare K and B decays, where the strongest modification can be seen in the decays $K^+ \to \pi^+ \nu\bar{\nu}$ and especially $K_{\rm L} \to \pi^0 \nu\bar{\nu}$, which can be enhanced by an order of magnitude with respect to its standard model value. Other prominent signals of these scenarios are an enhancement of $K_L \to \pi^0 l^+ l^-$ and a strong departure of $\sin 2\beta|_{K\pi\nu\bar{\nu}}$ from its standard model value, as well as a rather strong sensitivity of the CP asymmetries $\mathcal{A}_{\rm CP}^{\rm dir}(B_d \to \pi^0 K^0)$, $\mathcal{A}_{\rm CP}^{\rm mix}(B_d \to \pi^0 K^0)$, $\mathcal{A}_{\rm CP}^{\rm dir}(B^\pm \to \pi^0 K^\pm)$ to the values of the electroweak penguin parameters. We then comment also on the CP asymmetries of $B \to \phi K_S$. Next, we analyze in detail the rare decays $K_{\rm L} \to \pi^0 \nu\bar{\nu}$ and $K^+ \to \pi^+ \nu\bar{\nu}$, where the theoretical uncertainties are very small, since the hadronic matrix elements can be extracted from tree-level decays. Here, we focus in the standard model prediction for both decays, which we analyze in the present and make projections for the predictions in the future. This demonstrates not only the significance of CKM uncertainties, but also the impact of the NNLO corrections to the charm component. We then investigate the potential of both decays to constrain the unitarity triangle, where we again project onto some future measurements. We find that clean and precise determinations of $\bar{\eta}$ and $\sin 2\beta$ become possible and that the complete unitarity triangle can be constructed within the SM to a respectable precision.

Contents

Chapter 1

Introduction

The goal of particle physics is to find an ultimate description of nature. This ultimate description, that is hoped to lie at the heart of all processes, may be either a physical theory, or simply a basic principle. On the way to this final aim, particle physicists have by now arrived at the standard model (SM) of particle physics [1–3], which is, in a sense, both: From the underlying principles of relativity, quantum theory and gauge invariance one has constructed a theory that incorporates strong, electromagnetic and weak interactions, thereby describing phenomena from the binding and decay of the atomic nucleus to everyday electricity. However, the fourth known force, namely gravity, has not been included, and is still a challenge for field theory. Furthermore, there are a number of unknown parameters in the model, that should, at best, come out of the final theory. Despite these shortcomings, the SM has so far passed every test successfully.

Nevertheless, there are some hints as to which kind of physics may lie at the next step towards a more general theory, such as the observed unification of forces that is achieved if a new symmetry, supersymmetry, is added, as well as the possibility that the neutrino masses are generated by the see saw mechanism, which is also straightforwardly implemented in grand unified theories (GUTs). A final problem of the SM is that the scalar particle that appears, the Higgs boson, which has not yet been found, is sensitive to the highest energy scale in the theory, and therefore should have an extremely large mass. This large mass is excluded by electroweak precision tests as well as the requirement that the Higgs should be light enough to unitarize the theory. The introduction of supersymmetry, Large Extra Dimensions or Little Higgs models can ameliorate this problem. Unfortunately, none of these appealing possibilities has been confirmed, but the Large Hadron Collider (LHC) at CERN should reach energies high enough to uncover the signals of most of the proposed extensions of the SM, which would, for example, be manifest in the appearance of the superpartners or Kaluza Klein modes, in the case of extra dimensional theories.

In addition to these direct searches, the effects of physics that lies beyond the SM can be detected in indirect searches, where the heavy particles that are added to the SM are present in loop corrections. In this manner, it was possible to estimate rather precisely the mass of the top quark before it was actually detected. These indirect searches include electroweak precision measurements such as the ρ parameter, which is, roughly speaking, given by the ratio of the W and Z mass, and also flavor changing neutral current (FCNC)

processes, that occur at loop level only in the SM [4]. Therefore, they offer an appealing way to look for new physics, since they are measurable at rather low energies. The first classic application of this idea was the estimate of the charm quark mass [5] by Gaillard and Lee from Δm_K, the mass difference in the neutral kaon system.

However, flavor physics is also interesting for two other reasons: Firstly, it may give some insight into the flavor structure of the SM, which is, so far, just put in by hand and therefore contains a number of free parameters, and secondly, the flavor sector is the dominant source of CP violation in the SM. It arises from a complex phase in the unitary Cabibbo Kobayashi Maskawa (CKM) [6, 7] matrix, which describes the mixing of quark flavors in the SM, and was first discovered in the mixing of the neutral kaon system. Here, the neutral K^0 and its antiparticle can be combined to form approximate CP eigenstates, the long lived K_L and the short lived K_S. The fact that both are only approximate CP eigenstates, as observed by the decay of the (dominantly CP odd) K_L into the (CP even) final state $\pi^+\pi^-$, reflected then the first sign of CP violation [8]. Later, also direct CP violation in the kaon system was observed [9], as well as CP violation in the B meson system, where it has been found in the mixing [10, 11] and very recently also in the decay [12, 13]. In addition, there can be CP violation in the lepton sector if Majorana neutrinos are added, but here the experimental verification is still missing.

Having now established CP violation, it has become the main goal of flavor physics to determine and constrain the elements of the CKM matrix, which is conveniently done in the context of a "unitarity triangle" which follows from the unitarity of the CKM matrix. Here, one makes use of the increasingly precise data concerning, in particular, the B meson system, from the B factories BaBar and Belle, for reviews on the status of quark flavor physics see [14–18]. Unfortunately, the task is complicated by the fact the decaying quarks are not directly accessible, since they are bound into hadrons. The resulting strong interaction effects are described in terms of a weak effective Hamiltonian [19] in which the non-perturbative hadron dynamics are encoded in matrix elements of local operators. While there exist several strategies to tackle the problem of estimating them, these hadronic uncertainties complicate severely the predictions of non-leptonic decays, such as the $B \to \pi\pi$ and $B \to \pi K$ decays, which will be the subject of large parts of this thesis. Still, there are a number of increasingly precise constraints that allow for a construction of the UT, which does not yet show any conclusive sign of unitarity violation.

On the other hand, there are some potential hints for new physics in the flavor sector, as well as a number of interesting decay channels that have not yet been tested at all, such as the theoretically clean decays $K \to \pi\nu\bar{\nu}$ and $B_{s/d} \to \mu^+\mu^-$. Among the potential signals of new physics or, at least, inconsistencies with the SM description, the most important ones are the following:

- The measured values of the $B^0_d \to \pi^0\pi^0$ branching ratios from BaBar and Belle point to rather large values, which may be either a signal of new physics or a failure of the theoretical tools used to describe the decays.

- In the $B \to \pi K$ decay system, the branching ratios of those decays that receive significant contributions from electroweak penguin topologies tend to be described rather poorly. The same is true for the CP symmetries, where also the CP asym-

metry of $B_d^0 \to \pi^+ K^-$ is interesting, in which direct CP violation in the B meson system was finally established. It is not affected by electroweak penguins, but poses a challenge to some of the QCD methods used.

- The mixing induced CP asymmetry in $B \to \phi K_S$ is, in the SM expected to be equal to $\sin 2\beta$, where β is one of the UT angles. There has been an ongoing discussion for quite some time now, since the data, especially from Belle, may favor significantly different values. However, the data from BaBar and Belle have some inconsistencies among themselves and are moving towards the SM prediction, so that no conclusive statement is possible yet. Similar comments apply to other s penguin transitions, such as $B \to \pi^0 K_S$, $B \to \eta K_S$ and others.

Of course, further data are required in all of these cases, before the situation can be clarified. Still, it is interesting already now to explore the potential implications, in order to find, what kind of potential new physics these signals may point to, and to what extent the methods used to control the non-perturbative effects are adequate. Concerning these methods, there has been considerable progress in recent years. First, the notion of factorization for hadronic matrix elements has been put on a QCD based footing within the framework of QCD factorization [20, 21], while, in parallel, perturbative QCD (PQCD) [22, 23] has been developed, where even further perturbative calculations are performed. Subsequently, the idea of QCDF has been extended into an effective theory language [24, 25]. The resulting effective theory, soft collinear effective theory (SCET) allows for all-order proofs of factorization. While the global description of non-leptonic decays has therefore advanced, it remains to be seen whether all or any of these methods have the predictive power to confront extremely precise data, since all rely on some simplifying assumptions.

Therefore, in this thesis, we will study in detail the above mentioned discrepancies within the $B \to \pi\pi$ and $B \to \pi K$ decays. Instead of the theoretical methods mentioned, we will rely on the flavor symmetry of the strong interactions and use input from data to determine the hadronic parameters and weak phases involved. Additional theoretical tools will only be required for an estimate of the symmetry breaking factors. The analysis will consist of several steps [26, 27], introducing additional assumptions in each one, that can always be tested. Explicitly, we proceed as follows:

- Beginning with the $B \to \pi\pi$ decays, we use isospin symmetry to parameterize the decay amplitudes in terms of several hadronic parameters as well as weak phases. Using then the data for the branching ratios as well as the CP asymmetries for $B_d^0 \to \pi^+\pi^-$ allows for a theoretically clean determination of all hadronic parameters if the CKM angle γ is used an input. Under the the assumption of SU(3) flavor symmetry of strong interactions (and including the factorizable breaking effects) one can use data also from $B_d^0 \to \pi^+ K^-$ to additionally fix γ. We find $\gamma = 73.9^{+5.8}_{-6.5}$ [28, 29], which is somewhat higher than the value obtained from UT fits. This low value of γ is driven largely by the new, low value of $\sin 2\beta$ from $\mathcal{A}_{\rm CP}^{\rm mix}(B_d \to J/\psi K_{\rm S})$, which is in some friction with the other input used. Therefore, we consider our value to be the "true" γ and construct a unitarity triangle from it, using also $|V_{ub}/V_{cb}|$ as input. The discrepancy with $\sin 2\beta|_{J/\psi K_{\rm S}}$ can be

attributed to small NP corrections to $B_d^0 - \bar{B}_d^0$ mixing. Finally, we predict the CP asymmetries in $B_d^0 \to \pi^0\pi^0$, where we find agreement with the data, albeit with large uncertainties. The large experimental $B_d^0 \to \pi^0\pi^0$ branching ratio is then a purely hadronic effect induced through large non-factorizable terms.

- For the next step, we move to the $B \to \pi K$ system. In contrast to $B \to \pi\pi$, these decays are loop dominated and therefore much more sensitive to NP. In addition, there are sizeable contributions from electroweak penguin topologies, which are a favored place for new physics to enter. In order to determine all the hadronic parameters involved, we invoke again the SU(3) flavor symmetry and assume also that penguin annihilation and exchange topologies are negligible. The electroweak penguin contribution remains undetermined, but can be calculated from the Wilson coefficients of the effective Hamiltonian, which are calculable in the SM and in any of its extensions. We find satisfactory agreement within the SM for those quantities that are not affected by electroweak penguins, while the description of those where they contribute fails. We find the values of the corresponding parameters that are required to fit the data and obtain an enhancement of the electroweak penguins, which is accompanied by a large CP violating phase with a negative sign.

- In order to further test the scenario of enhanced electroweak penguins and to distinguish it from potential hadronic effects in $B \to \pi K$, we finally study the impact that the corresponding parameters have on several extremely clean (semi-)leptonic rare decays, such as the inclusive $b \to s l^+ l^-$ decay, as well as $K_{\rm L} \to \pi^0 \nu\bar{\nu}$, $K^+ \to \pi^+ \nu\bar{\nu}$ and $B_{s/d} \to \mu^+\mu^-$, among others. In order to obtain a connection to these decays, we specify a simple and predictive scenario, where NP enters only in the C function, that, within the SM, describes the electroweak penguin. The connection required is then established by inverting the renormalization group equations (RGEs) for the corresponding Wilson coefficients, which are given up to next to leading order. With the resulting values for the C function, we find that we overshoot the bound coming from $b \to s l^+ l^-$. Therefore, we maintain that the $B \to \pi K$ data point to NP, but consider several modifications of the present data set, that would satisfy this bound. Calculating then the rare decays in these scenarios shows, that they clearly distinguish and test the scenarios. In particular, we find that the branching ratio of $K_{\rm L} \to \pi^0 \nu\bar{\nu}$ can be enhanced by approximately an order of magnitude with respect to the SM. In combination with a measurement of $K^+ \to \pi^+ \nu\bar{\nu}$, it also allows to fix the NP scenario completely, subject to several ambiguities that can be resolved by considering additional processes. We then reconsider the $B \to \pi K$ observables in these scenarios and find that the CP asymmetries $\mathcal{A}_{\rm CP}^{\rm mix}(B_d \to \pi^0 K_{\rm S})$, $\mathcal{A}_{\rm CP}^{\rm dir}(B_d \to \pi^0 K_{\rm S})$ and $\mathcal{A}_{\rm CP}^{\rm dir}(B^\pm \to \pi^0 K^\pm)$ are very sensitive to magnitude and sign of the electroweak penguin parameters, where we find also that the current data are somewhat better described by a positive sign of the phase. Finally, we comment also on $\mathcal{A}_{\rm CP}^{\rm mix}(B_d \to \phi K_{\rm S})$, where we, however, do not expect a large effect.

The assumption of SU(3) flavor symmetry can be tested with several predictions such as the predictions of the $B \to \pi K$ observables without contributions from electroweak

penguins. We further study the implications of larger SU(3) breaking effects and find that they can not explain the present data. Furthermore, we will show how the size of penguin annihilation and exchange topologies can be tested at LHCb.

Let us point out here that the optimal strategy would be a different one than the one that we are pursuing. If all the data from the rare decays were available, they would by very well suited to constrain and determine the new physics scenario, if any signal is seen. Using the parameters thus obtained, one could then test the hadron dynamics in the non-leptonic decays. Unfortunately, with the data at hand, it is necessary to follow our route of the analysis, which still allows several stringent tests to be performed.

As we have seen, the decays $K_{\rm L} \to \pi^0 \nu\bar{\nu}$ and $K^+ \to \pi^+ \nu\bar{\nu}$ are a sensitive probe of our new physics scenario. In addition, they are theoretically extremely clean, since the operator matrix element required can be extracted from the tree level decay $K^+ \to \pi^0 e^+ \nu$. Additional subleading contributions have been calculated, and by now also the calculation of the NNLO part of the charm component has been completed [30]. Therefore, in the second part of this thesis, we analyze both of these decays with respect to the SM prediction and their potential to determine CKM factors, if they are measured. In the course of this analysis, we begin with the present scenario, where we take the CKM factors from a UT fit and make predictions for both decays. They are [31]

$$\mathrm{BR}(K^+ \to \pi^+ \nu\bar{\nu}) = 7.77 \pm 1.23 \cdot 10^{-11} \tag{1.1}$$

$$\mathrm{BR}(K_{\rm L} \to \pi^0 \nu\bar{\nu}) = 3.05 \pm 0.56 \cdot 10^{-11} \tag{1.2}$$

Here, the largest uncertainties arise from the CKM factors. As a contrast, the present experimental numbers read [32, 33]

$$\mathrm{BR}(K^+ \to \pi^+ \nu\bar{\nu}) = 14.7^{+13.0}_{-8.9} \cdot 10^{-11}\,, \tag{1.3}$$

$$\mathrm{BR}(K_{\rm L} \to \pi^0 \nu\bar{\nu}) < 2.9 \cdot 10^{-7} \qquad (90\%\,\text{confidence})\,. \tag{1.4}$$

The experimental number for $K^+ \to \pi^+ \nu\bar{\nu}$ is then about twice as large as the SM prediction, but still compatible within the uncertainties. On the other hand, the experimental bound for $K_{\rm L} \to \pi^0 \nu\bar{\nu}$ is several orders of magnitude above the corresponding prediction. As a next step, since it will take several years to obtain precise values of the branching ratios, we project into the future, by assuming better known CKM factors and other inputs. This shows, which kind of precision is required to predict the branching ratios at the level of 5 % or less.

Finally, assuming that the branching fractions are measured, we then investigate their potential to determine CKM factors. In particular, a measurement of the purely CP violating decay $K_{\rm L} \to \pi^0 \nu\bar{\nu}$ gives the theoretically cleanest determination of the CP violating UT parameter $\bar{\eta}$. On the other hand, combining measurements of both decays, one obtains a formula for $\sin 2\beta$ that is valid not only in the SM, but in any extension where no new CP violating phases occur. Additionally, it is not afflicted with uncertainties stemming from $|V_{cb}|$. This measurement can therefore easily be used to test the notion of minimal flavor violation (MFV), which means precisely that there are no

new CP violating phases and also that there are no new operators present, as compared to the SM. Finally, we show how the complete unitarity triangle can be constructed from the measurement of both decays.

The remainder of this thesis is organized as follows: In Chapter 2 we give a brief review of the SM and the most important background on flavor physics. In this context, we review also the effective theory description of weak decays and give the renormalization group equations for the Wilson coefficients, that are required later. Chapter 3 then contains our analysis of the $B \to \pi\pi$ decays, where we also briefly compare our results to those obtained from alternative approaches. Next, in Chapters 4 and 5 we turn to our new physics analyses. In Chapter 4 we begin with the $B \to \pi K$ system and study its implications for rare decays in Chapter 5. Finally, we study the $K \to \pi\nu\bar{\nu}$ decays in Chapter 6 and conclude in Chapter 7. In the appendices, we collect the theoretical expressions for all observables and an additional test of flavor symmetry that is provided by the $B_s \to K^+K^-$ system.

Chapter 2

Theoretical Background

2.1 CP Violation and the Unitarity Triangle

2.1.1 Brief Review of the Standard Model

The Standard Model (SM) of Particle Physics is todays accepted theory of electroweak and strong interactions. It is a $SU(2)_L \times U(1) \times SU(3)_C$ gauge theory, in which the weak force and electromagnetism are, in a sense, unified by a mixing of the corresponding $SU(2)_L$ and $U(1)$ gauge bosons[1]. Here, the $U(1)$ of hypercharge is an abelian gauge theory, while the $SU(2)_L$ and $SU(3)_C$ are both non-abelian. The particle content of the SM can then be classified as follows:

- **Fermions:** The SM fermions fall into two classes, leptons and quarks. The leptons are subject only to electroweak interactions, while quarks also carry color and are thus affected by strong interactions. In both classes, there are three left-handed doublets under the $SU(2)_L$, which read as follows:

$$\begin{pmatrix} \nu_e \\ e^- \end{pmatrix}_L \qquad \begin{pmatrix} \nu_\mu \\ \mu^- \end{pmatrix}_L \qquad \begin{pmatrix} \nu_\tau \\ \tau^- \end{pmatrix}_L \tag{2.1}$$

$$\begin{pmatrix} u \\ d' \end{pmatrix}_L \qquad \begin{pmatrix} c \\ s' \end{pmatrix}_L \qquad \begin{pmatrix} t \\ b' \end{pmatrix}_L \tag{2.2}$$

  There are also the corresponding right-handed fields, which transform as singlets. The primes added to down-type quarks correspond to the fact that weak eigenstates and mass eigenstates need not be (and are not) the same. This will be discussed further below.

- **Vector bosons:** There are 12 vector bosons mediating the gauge interactions: 8 gluons for the strong interaction, 3 W bosons for the weak interaction and one B for the U(1) of hypercharge. As mentioned above, the gauge bosons of the weak

[1]This should not be confused with a true unification of forces, since there are still two separate parameters corresponding to the two coupling constants.

and hypercharge gauge groups mix, specifically, the neutral W^3 and the B mix to the physical Z^0 and A gauge bosons

$$\begin{pmatrix} Z^0 \\ A \end{pmatrix} = \begin{pmatrix} \cos\theta_{\mathrm{W}} & -\sin\theta_{\mathrm{W}} \\ \sin\theta_{\mathrm{W}} & \cos\theta_{\mathrm{W}} \end{pmatrix} \begin{pmatrix} W^3 \\ B \end{pmatrix}, \tag{2.3}$$

where $\sin^2\theta_{\mathrm{W}} = 0.23120$ is the sine of the weak mixing angle.

- **Scalar Higgs Particle:** A Lagrangian consisting only of fermion and gauge contents does not allow for fermion masses or for massive W and Z bosons, if invariance under the SM gauge group is required. This problem is circumvented by the introduction of a scalar Higgs particle which gives the corresponding masses through electroweak symmetry breaking. In effect, the Higgs acquires a vacuum expectation value (VEV), which breaks the symmetry $SU(2)_L \times U(1)_Y \to U(1)_{\mathrm{em}}$, so that the photon explicitly remains massless. Additionally, it unitarizes the WW scattering amplitudes, which diverge in a theory without a scalar. This Higgs scalar is the one missing ingredient of the experimental verification of the SM as it stands. So far, there exists a lower bound from LEP of $m_h > 114\mathrm{GeV}$, while the indirect searches from electroweak precision tests seem to point to a potentially light Higgs. This gives some confidence that it should be findable at the LHC. Another question concerning the Higgs is the stability of its mass: Quantum corrections to scalar particles are quadratically divergent and are therefore of order of the cutoff scale. This leads to one important motivation for supersymmetry, since the superpartners can cancel the resulting divergences. On the whole, electroweak symmetry breaking, though a very interesting and hot topic, will not be of much relevance for the rest of our work and we will not discuss it in any further detail.

Another interesting aspect, that will be extremely relevant for what follows, are the interaction vertices of gauge bosons and fermions, concerning, in particular, the possibility of flavor changes. Since the only transformations that keep the Lagrangian invariant are unitary transformations between the flavors, the neutral current will always conserve flavor at tree level, while the charged current vertex can have flavor changing contributions. Concentrating on the quark sector, this vertex is given by

$$\mathcal{L}_{\mathrm{CC}} = \frac{g_2}{2\sqrt{2}}(J^+_\mu W^{+\mu} + J^-_\mu W^{-\mu}), \tag{2.4}$$

where

$$J^+_\mu = (\bar{u}d')_{V-A} + (\bar{c}s')_{V-A} + (\bar{t}b')_{V-A} \tag{2.5}$$

denotes the charged current and g_2 is the $SU(2)_L$ coupling constant. The subscript $V-A$ corresponds to a Dirac structure of $\gamma^\mu(1-\gamma^5)$, reminding us that the weak interactions couple only left-handedly. Here, the primed quarks are weak eigenstates, which can be obtained from the mass eigenstates by a unitary transformation with the Cabibbo Kobayashi Maskawa (CKM) Matrix

$$\begin{pmatrix} d' \\ s' \\ b' \end{pmatrix} = \begin{pmatrix} V_{ud} & V_{us} & V_{ub} \\ V_{cd} & V_{cs} & V_{cb} \\ V_{td} & V_{ts} & V_{tb} \end{pmatrix} \begin{pmatrix} d \\ s \\ b \end{pmatrix} = V_{\mathrm{CKM}} \begin{pmatrix} d \\ s \\ b \end{pmatrix}. \tag{2.6}$$

The CKM Matrix will be the central object in much of the following work.

2.1.2 Wolfenstein Parameterization and the Unitarity Triangle

There are several possible parameterizations of the CKM matrix, such as the Standard Parameterization of the Particle Data Group [34], but the parameterization we will use in the following is the Wolfenstein Parameterization [35], which makes the hierarchy of matrix elements very transparent. The basic observation is that the CKM element $V_{us} \approx 0.22$ is very small and allows for an expansion of the matrix elements in $\lambda = V_{us}$. Then, the leading order form of the CKM matrix is

$$V_{\rm CKM} = \begin{pmatrix} 1-\frac{\lambda^2}{2} & \lambda & A\lambda^3(\varrho - i\eta) \\ -\lambda & 1-\frac{\lambda^2}{2} & A\lambda^2 \\ A\lambda^3(1-\varrho-i\eta) & -A\lambda^2 & 1 \end{pmatrix} + \mathcal{O}(\lambda^4)\,. \tag{2.7}$$

The extension of this definition to higher orders in λ is not unambiguous, but by the now the proposal of [36] has been generally accepted. Here, in particular, the parameters ρ and η are generalized to

$$\bar{\varrho} = \varrho(1-\frac{\lambda^2}{2}), \qquad \bar{\eta} = \eta(1-\frac{\lambda^2}{2})\,, \tag{2.8}$$

while the explicit form of the CKM elements in this parameterization can also be found in [37]. In any case, it is a unique feature that the hierarchy of the CKM matrix is such that the largest elements are the diagonal ones and the off-diagonal elements become increasingly smaller. This pattern is not shown in the sector of leptonic mixing. Another extremely important aspect of the CKM matrix is the fact that it is, in general, imaginary, as represented by the parameter $\bar{\eta}$. An imaginary part of the CKM is responsible for CP violation, and is, in fact, the only source of CP violation in the SM, apart from the analogous mixing terms in the leptonic mixing[2] sector and an additional QCD vacuum term, which is found to be small (this is called the "strong CP problem" and will play no further role in our discussion).

While at least some of the CKM elements can, in principle, be determined from the decay vertices, it is very instructive to consider another quantity, namely the unitarity triangle (UT). This is obtained by writing down the nine unitarity relations for the CKM matrix. All six of the off diagonal relations represent different, but commensurate, triangles. The most interesting of these is the one described by

$$V_{ud}V_{ub}^* + V_{cd}V_{cb}^* + V_{td}V_{tb}^* = 0, \tag{2.9}$$

because all three terms in (2.9) come with the same power of λ. Usually, the triangle is normalized by $V_{cd}V_{cb}^*$ and is then displayed in the $\bar{\rho} - \bar{\eta}$ plane as in Fig. 2.1.

The angles β and γ correspond directly to the phases of the CKM matrix elements V_{td} and V_{ub}, respectively, i.e.

$$V_{td} = |V_{td}|e^{-i\beta}, \quad V_{ub} = |V_{ub}|e^{-i\gamma}, \tag{2.10}$$

while α is then given by the unitarity relation $\alpha + \beta + \gamma = 180°$. On the other hand, the sides of the UT are given by

$$R_b \equiv \frac{|V_{ud}V_{ub}^*|}{|V_{cd}V_{cb}^*|} = \sqrt{\bar{\varrho}^2 + \bar{\eta}^2} = (1-\frac{\lambda^2}{2})\frac{1}{\lambda}\left|\frac{V_{ub}}{V_{cb}}\right|\,, \tag{2.11}$$

[2]These only exist in SM extended by right-handed neutrinos

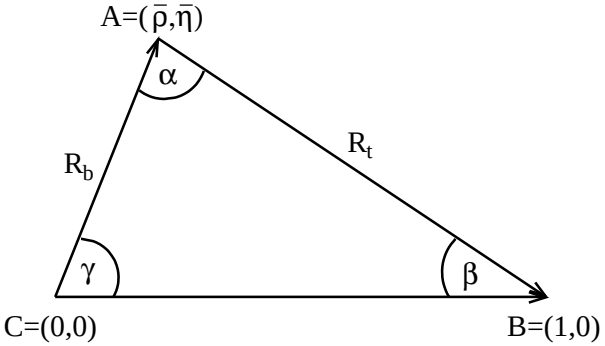

Figure 2.1: Unitarity triangle and the $\bar{\rho} - \bar{\eta}$ plane.

$$R_t \equiv \frac{|V_{td}V_{tb}^*|}{|V_{cd}V_{cb}^*|} = \sqrt{(1-\bar{\varrho})^2 + \bar{\eta}^2} = \frac{1}{\lambda}\left|\frac{V_{td}}{V_{cb}}\right|, \tag{2.12}$$

so that they are directly measurable in terms of CKM elements.

Let us conclude this section with some relations that will be used later in this work. First, for convenience, often quantities $\lambda_i^{(j)}$ as $\lambda_i^{(j)} = V_{id}V_{ij}^*$ are used. Here, j corresponds to a b or s quark, depending on whether B or K mesons are discussed and i is an arbitrary up-type quark. The combinations $\lambda_i^{(j)}$ usually appear when FCNC processes are calculated. Specifically, for K decays, the real and imaginary parts of $\lambda_i^{(s)}$ for $i = c, t$ are given by

$$\mathrm{Im}\lambda_t^{(s)} = -\mathrm{Im}\lambda_c^{(s)} = \eta A^2\lambda^5 = \mid V_{ub} \mid\mid V_{cb} \mid \sin\delta \tag{2.13}$$

$$\mathrm{Re}\lambda_c^{(s)} = -\lambda(1 - \frac{\lambda^2}{2}) \tag{2.14}$$

$$\mathrm{Re}\lambda_t = -(1 - \frac{\lambda^2}{2})A^2\lambda^5(1-\bar{\varrho})\,. \tag{2.15}$$

The corresponding term for $i = u$ can always be replaced using the unitarity relation equivalent to (2.9) that applies to the CKM elements with the strange quark as the down type member.

The parameters $\bar{\varrho}$ and $\bar{\eta}$ can be expressed in terms of the UT parameters as

$$\bar{\varrho} = 1 - R_t\cos\beta, \qquad \bar{\eta} = R_t\sin\beta\,, \tag{2.16}$$

while the side R_t is given in terms of the angles as

$$R_t = \frac{\sin\gamma}{\sin(\beta+\gamma)}\,. \tag{2.17}$$

The corresponding formulae for R_b are

$$\bar{\varrho} = R_b\cos\gamma, \qquad \bar{\eta} = R_b\sin\gamma \tag{2.18}$$

$$R_b = \frac{\sin\beta}{\sin(\beta+\gamma)}\,. \tag{2.19}$$

These formulae allow for the complete construction of the UT, corresponding to the (β,γ), (R_b,γ), (R_t,β) strategies introduced in [38]. In particular, the (β,γ) strategy is even theoretically clean, since β and γ can be measured without hadronic uncertainties, but might be polluted by new physics contributions that enter into $B^0_d-\bar{B}^0_d$ mixing. This point will be discussed further in later sections of this chapter. Also, we will use these formulae to obtain certain CKM factors from the $K\to\pi\bar{\nu}\nu$ decays in Chapter 6.

2.1.3 Phenomenological Status of the Unitarity Triangle

In this section, we shall very briefly review the phenomenological constraints and parameters that are used to determine the values of the UT in the $\bar{\rho}-\bar{\eta}$ plane, in order to show how some of our later results fit in. We will be extremely brief, and refer the reader to the excellent reviews and works [17, 39, 40] for more information. In general, one can proceed as follows in order to construct the UT:

- Use the CKM matrix elements $|V_{us}|$, $|V_{ub}|$ and $|V_{cb}|$ as determined from tree level decays. Here, $|V_{us}|$ can be found from tree level kaon decays, τ decays and hyperon decays, where the best present value is given by $|V_{us}|=0.225\pm0.001$ [41]. Similarly, $|V_{ub}|$ and $|V_{cb}|$ are determined from tree level $b\to u(c)l\nu$ transitions. In both cases there are two competing strategies namely inclusive and exclusive determinations and there are very heated discussions on which of the two strategies to prefer. This is particularly relevant in the case of $|V_{ub}|$, where the two values differ significantly. We use the values of [40], i.e. $|V_{ub}|=(4.22\pm0.20)10^{-3}$ and $|V_{cb}|=0.0415\pm0.0008$. For the interesting quantity $|V_{ub}/V_{cb}|$, this corresponds to $|V_{ub}/V_{cb}|=0.102\pm0.005$.

- At this point, one can decide about which other constraints to use. A clean and pure SM fit is obtained if only the tee level determinations of γ from $B\to DK$ is used. This corresponds to a true tree level determined UT without any pollution from new physics. Additional constraints used are $\sin 2\beta$ from $B\to J/\Psi K_S$ (we will come back to this below), the CP violating parameter ϵ_K, R_t from ΔM_d and $\Delta M_d/\Delta M_s$ as the "classical" constraints, as well as the newer constraints α from $B\to\rho,\pi$ and $B\to\rho\rho$, $\cos 2\beta$ from $B\to J/\Psi K^*_S$, $\sin(2\beta+\gamma)$ from $B\to D\pi$ and $B\to D\rho$ as well as β from $B\to D^0\pi^0$. Again we refer the reader to [39,40], where in particular, the corresponding web page provides references and numerical input for all these constraints.

- The constraints discussed above can be used in different combinations for a fit. We show the situation for a fit with several constraints in Fig. 2.2. The main message from this picture is that the unitarity triangle is rather well constrained and that no significant departures from unitarity have been found yet. One should keep in mind, however, that only very few of the constraints used are actually very precise as of now. Therefore, there is still room for for new physics to appear.

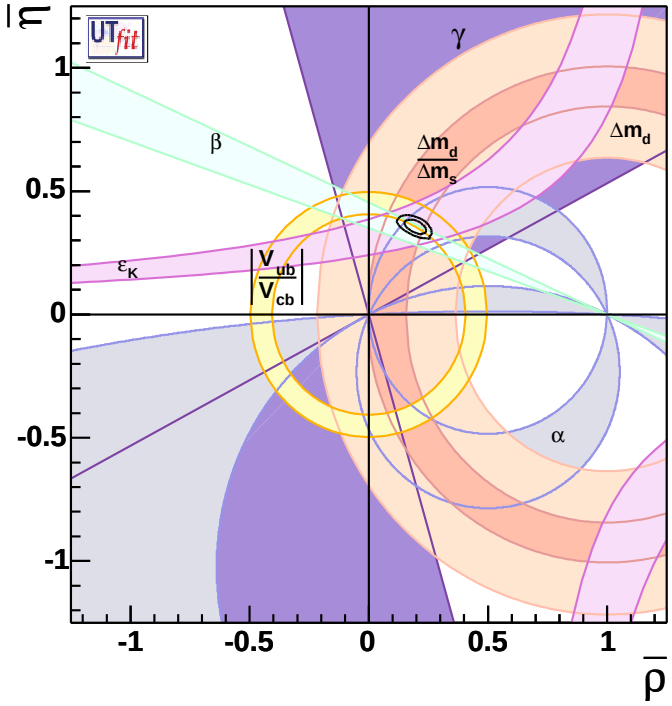

Figure 2.2: Complete fit [40] for the unitarity triangle in the $\bar{\rho} - \bar{\eta}$ plane. The results are shown at 68% and 95% confidence level.

2.1.4 CP violation in the Standard Model

As noted above, the main source of CP violation in the Standard Model is the imaginary part of the CKM matrix. Therefore, an obvious quantity to measure CP violation is the CP asymmetry of flavor violating decays, for example, in the case of B decays

$$a_{\mathrm{CP}}(t) \equiv \frac{\Gamma(B_q^0(t) \to f) - \Gamma(\overline{B_q^0}(t) \to f)}{\Gamma(B_q^0(t) \to f) + \Gamma(\overline{B_q^0}(t) \to f)}, \tag{2.20}$$

where we have assumed the particularly simple and interesting case of the final state being a CP eigenstate. Taking into account the time evolution [15, 42, 43] of the B meson states, the CP asymmetry can be decomposed into a mixing induced and a direct component:

$$a_{\mathrm{CP}}(t) = \mathcal{A}_{\mathrm{CP}}^{\mathrm{dir}}(B_q \to f)\, \cos(\Delta M_q t) + \mathcal{A}_{\mathrm{CP}}^{\mathrm{mix}}(B_q \to f)\, \sin(\Delta M_q t)\,, \tag{2.21}$$

where the mixing induced and direct CP asymmetries can be calculated from the decay amplitudes as

$$\mathcal{A}_{\mathrm{CP}}^{\mathrm{dir}}(B_q \to f) = \frac{1 - \left|\xi_f^{(q)}\right|^2}{1 + \left|\xi_f^{(q)}\right|^2} \quad \text{and} \quad \mathcal{A}_{\mathrm{CP}}^{\mathrm{mix}}(B_q \to f) = \frac{2\,\mathrm{Im}\,\xi_f^{(q)}}{1 + \left|\xi_f^{(q)}\right|^2}\,. \tag{2.22}$$

We are following the notation of [15], so that

$$\xi_f^{(q)} = e^{-i\Theta_{M_{12}}^{(q)}} \frac{A(\overline{B_q^0} \to f)}{A(B_q^0 \to f)}, \quad \xi_{\overline{f}}^{(q)} = e^{-i\Theta_{M_{12}}^{(q)}} \frac{A(\overline{B_q^0} \to \overline{f})}{A(B_q^0 \to \overline{f})}, \tag{2.23}$$

where

$$\Theta_{M_{12}}^{(q)} = \pi + 2\arg\left(V_{tq}^* V_{tb}\right) - \phi_{\rm CP}(B_q)\,, \tag{2.24}$$

and $\phi_{\rm CP}(B_q)$ is the convention dependent CP phase of the B meson. The phase $\Theta_{M_{12}}^{(q)}$ appears naturally as the phase of $B_q^0 - \overline{B}_q^0$ mixing. As V_{tb} is real to a very good approximation, the phase of $B_d^0 - \bar{B}_d^0$ mixing is simply $\phi_d \equiv 2\beta$.

Let us make this formalism a bit more explicit by showing two examples. The first is the above mentioned measurement of $\sin 2\beta$ [44] from $B_d^0 \to J/\psi K_S$: Due to CKM factors, the amplitude for this decay is entirely dominated by the tree amplitude and is given by

$$A(B_d^0 \to J/\psi K_S) = (1 - \frac{\lambda^2}{2})\lambda^2 A\left(A_{CC} + A_{\rm pen}^{ct}\right)\,, \tag{2.25}$$

where we have decomposed the amplitude according to weak phases and therefore included also the $A_{\rm pen}^{ct}$ piece. Since only amplitudes with one single weak phase dominate, the CP asymmetries are very simple and given by

$$a_{\psi K_{\rm S}} \equiv -\mathcal{A}_{\rm CP}^{\rm mix}(B_d \to J/\psi K_{\rm S}) = -\sin[-(\phi_d - 0)] = \sin 2\beta\,, \tag{2.26}$$

making the mixing induced CP asymmetry a very clean measurement of this UT angle, spoiled only by two very small effects: First, there are additional contributions due to the K^0–$\overline{K^0}$ mixing phase, which are given by $\phi_K = 2\arg(V_{us}^* V_{ud})$ and are negligibly small in the Wolfenstein parameterization. The second correction stems from the contributions of the penguin diagrams. It has been estimated recently [45, 46], with the result that these penguin contributions may actually be becoming as important as the current uncertainties of the B factory data. The current experimental status is

$$\sin 2\beta = \begin{cases} 0.722 \pm 0.04_{stat} \pm 0.023_{syst} & \text{BaBar [47]} \\ 0.652 \pm 0.039_{stat} \pm 0.02_{syst} & \text{Belle. [48]} \end{cases} \tag{2.27}$$

resulting in an average of $\sin 2\beta = 0.685 \pm 0.032$ [49].

The next example are the CP asymmetries in the $B_d^0 \to \pi^+\pi^-$ system, which we will discuss in more detail in Chapter 3. This example makes the explicit phase structure and where to conjugate what very transparent. First, the decay amplitude of this decay is

$$A(B_d^0 \to \pi^+\pi^-) = -|\tilde{T}|e^{i\delta_{\tilde{T}}}\left[e^{i\gamma} - de^{i\theta}\right] \tag{2.28}$$

where we have pulled out the leading tree amplitude and d is, roughly speaking, the ratio of penguin to tree amplitudes. It will be defined more precisely, along with the strong phase θ, in (3.9), when we come back to a systematic discussion. Then, ξ is given by

$$\xi_{\pi^+\pi^-}^{(d)} = -e^{-i\phi_d}\left[\frac{e^{-i\gamma} - de^{i\theta}}{e^{+i\gamma} - de^{i\theta}}\right], \tag{2.29}$$

leading to expressions for both asymmetries

$$\mathcal{A}_{\rm CP}^{\rm dir}(B_d \to \pi^+\pi^-) = -\left[\frac{2d\sin\theta\sin\gamma}{1-2d\cos\theta\cos\gamma+d^2}\right] \tag{2.30}$$

$$\mathcal{A}_{\rm CP}^{\rm mix}(B_d \to \pi^+\pi^-) = \frac{\sin(\phi_d+2\gamma)-2d\cos\theta\sin(\phi_d+\gamma)+d^2\sin\phi_d}{1-2d\cos\theta\cos\gamma+d^2}. \tag{2.31}$$

We will come back to these expressions and analyze them numerically in the course of our detailed discussion of the $B \to \pi\pi$ system.

Finally, let us very briefly comment on the corresponding quantities for neutral kaons. The CP asymmetries analogous to (2.20) are extremely small here and are therefore not very suitable to study. Instead, one defines quantities ε_K and ε'/ε, describing indirect and direct CP violation, respectively. For more information on CP violation in the kaon system, we refer the reader to [37, 50]. Both quantities are, in principle very well suited to constrain the UT and look for new physics, but are afflicted with large hadronic uncertainties. This is, especially true for ε'/ε, see for example [51].

2.2 Description of Weak Decays in the SM

2.2.1 Effective Theory for Weak Decays

In this section we will describe the theoretical tools required to calculate weak decays in the SM. In doing so, we will follow rather closely [37], in particular concerning the notation. Using the same example of a charm decay $c \to su\bar{d}$, one begins by realizing that the amplitude for the decay at leading order in QCD is given by

$$\begin{aligned} A &= -\frac{G_F}{\sqrt{2}}V_{cs}^*V_{ud}\frac{M_W^2}{k^2-M_W^2}(\bar{s}c)_{V-A}(\bar{u}d)_{V-A} \\ &= \frac{G_F}{\sqrt{2}}V_{cs}^*V_{ud}(\bar{s}c)_{V-A}(\bar{u}d)_{V-A} + \mathcal{O}\left(\frac{k^2}{M_W^2}\right), \end{aligned} \tag{2.32}$$

corresponding to a tree level W exchange. In the second line we have expanded the intermediate W propagator for small momenta k. This is justified, since weak decays take place at momentum scales of the bound state mesons, which are much smaller than the W mass. One can therefore safely neglect the $\mathcal{O}(\frac{k^2}{M_W^2})$ terms and calculate the decay width with only the leading term. Physically, this corresponds to integrating out the heavy W for low energies and then studying an effective low energy theory for weak decays, as is shown pictorially in Fig 2.3. The idea of such an effective interaction was originally introduced by Fermi who, before the advent of gauge theories for weak interactions, described nuclear β decay by a four-particle vertex analogous to the one introduced for quarks above. As is expected for an effective field theory, the corresponding Fermi theory of β decays is non-renormalizable, and it was therefore obvious that this model could not be the full story. Also, the corresponding four fermion vertex violates unitarity of the theory. The notion of renormalizability will be elaborated on in the next subsection.

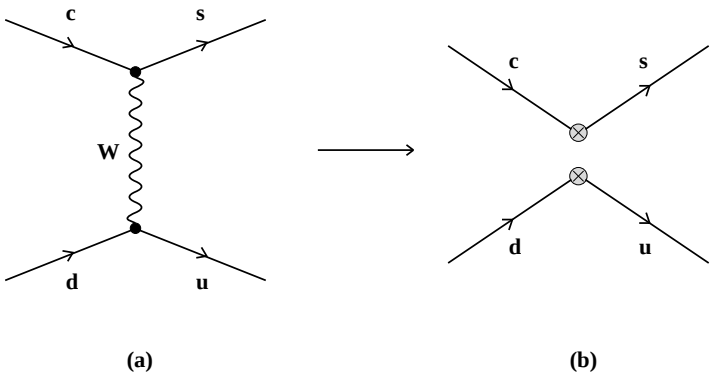

Figure 2.3: $c \to su\bar{d}$ at the tree level.

A similar procedure can also be used for flavor changing neutral current processes. These can occur only at loop level in the SM and are mediated by the so called penguin and box type diagrams. Examples for these are shown in Fig 2.4. When there are heavy particles in the loops, they can be expanded (or integrated) out just like the W boson above. This is, in particular, the case for a top quark running in the loops. Actually, the same holds for for very energetic massless particles, such as a gluon, since in the formal language of the effective theories one has to not only integrate out heavy particles, but any mode that resonates above the characteristic scale of the problem. The result of this exercise is that the penguin and box diagrams are also replaced by effective vertices, only that these are more complicated than the simple one for tree level W exchange.

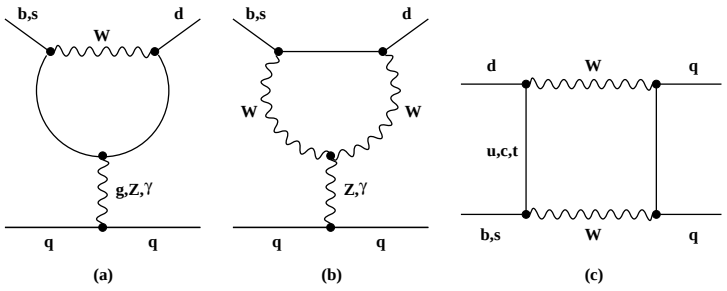

Figure 2.4: One loop penguin and box diagrams in the full theory.

These vertices are found by calculating all possible diagrams that contribute to a particular effective vertex. This statement is a gauge dependent one: For example, to find the effective vertex for a $(\bar{b}d)_{V-A}(\bar{q}q)_{V-A}$ box in Feynman gauge requires the calculation of the third diagram in Fig. 2.4 as well as three other diagrams that replace various internal W bosons by Goldstone bosons. These Goldstone boson diagrams are absent if the calculation is performed in unitary gauge. In any case, if one looks for all possible effective vertices, on finds a $(\bar{q}q)_{V-A}(\bar{q}q)_{V-A}$ one, as well as $(\bar{q}q)_{V-A}(\bar{l}l)_{V-A}$ (the leptonic box), sdZ (a Z penguin), sdG and $sd\gamma$, which correspond to the QCD and photon penguin, respectively. In the latter two cases one must distinguish whether the

massless particle is on mass shell or not, while the Z boson of the Z penguin is integrated out along with the W. These vertices are governed by characteristic functions, the Inami Lim functions [52]. They read, in Feynman gauge:

$$B_0(x_t) = \frac{1}{4}\left[\frac{x_t}{1-x_t} + \frac{x_t \ln x_t}{(x_t-1)^2}\right] \tag{2.33}$$

$$C_0(x_t) = \frac{x_t}{8}\left[\frac{x_t-6}{x_t-1} + \frac{3x_t+2}{(x_t-1)^2}\ \ln x_t\right] \tag{2.34}$$

$$D_0(x_t) = -\frac{4}{9}\ln x_t + \frac{-19x_t^3+25x_t^2}{36(x_t-1)^3} + \frac{x_t^2(5x_t^2-2x_t-6)}{18(x_t-1)^4}\ln x_t \tag{2.35}$$

$$E_0(x_t) = -\frac{2}{3}\ln x_t + \frac{x_t^2(15-16x_t+4x_t^2)}{6(1-x_t)^4}\ln x_t + \frac{x_t(18-11x_t-x_t^2)}{12(1-x_t)^3} \tag{2.36}$$

$$D_0'(x_t) = -\frac{(8x_t^3+5x_t^2-7x_t)}{12(1-x_t)^3} + \frac{x_t^2(2-3x_t)}{2(1-x_t)^4}\ln x_t \tag{2.37}$$

$$E_0'(x_t) = -\frac{x_t(x_t^2-5x_t-2)}{4(1-x_t)^3} + \frac{3}{2}\frac{x_t^2}{(1-x_t)^4}\ln x_t \tag{2.38}$$

$$S_0(x_t) = \frac{4x_t-11x_t^2+x_t^3}{4(1-x_t)^2} - \frac{3x_t^3\ln x_t}{2(1-x_t)^3} \tag{2.39}$$

$$S_0(x_c) = x_c \tag{2.40}$$

$$S_0(x_c,x_t) = x_c\left[\ln\frac{x_t}{x_c} - \frac{3x_t}{4(1-x_t)} - \frac{3x_t^2\ln x_t}{4(1-x_t)^2}\right]. \tag{2.41}$$

Here, $x_i = m_i^2/m_W^2$ and the functions are associated with the effective vertices as follows: B_0 belongs to the leptonic box diagram, C_0 to the Z penguin, D_0 to the photon penguin, E_0 to the QCD penguin and S_0 to the four-quark box diagrams. Above, we have expanded to leading order in x_c and generalized $S_0(x_c,x_t)$ to include simultaneous charm and top exchanges. Also, the primed function are those for the processes where the photon or gluon are kept on shell. Finally, constant, i.e. mass independent, terms, that may arise in the calculation, can be dropped due to the Glashow Iliopoulos Maiani (GIM) cancellation explicitly shown in Eq. (2.9) and the analogous relations for the other rows and columns of the CKM matrix.

As mentioned above, the effective vertices are, in general, gauge dependent. That is, the expressions above look different in gauges other than the Feynman gauge (a peculiarity of Feynman gauge is, for example, that the box diagrams are actually finite, this is lost if the calculation is performed in other gauges). Obviously, if a physical process is calculated, this gauge dependence has to cancel out. Therefore, the only combinations that appear are the gauge invariant combinations [53]

$$C_0(x_t,\xi) - 4B_0(x_t,\xi,1/2) = C_0(x_t) - 4B_0(x_t) = X_0(x_t) \tag{2.42}$$

$$C_0(x_t,\xi) - B_0(x_t,\xi,-1/2) = C_0(x_t) - B_0(x_t) = Y_0(x_t) \tag{2.43}$$

$$C_0(x_t,\xi) + \frac{1}{4}D_0(x_t,\xi) = C_0(x_t) + \frac{1}{4}D_0(x_t) = Z_0(x_t). \tag{2.44}$$

$X_0(x_t)$ and $Y_0(x_t)$ are linear combinations of the $V-A$ components of Z^0–penguin and box–diagrams containing final quarks or leptons with weak isospin T_3 equal to 1/2 and -1/2, respectively. $Z_0(x_t)$ is a linear combination of the vector component of the Z^0–penguin and the γ–penguin. Explicitly, these functions are given by

$$X_0(x_t) = \frac{x_t}{8}\left[\frac{x_t+2}{x_t-1} + \frac{3x_t-6}{(x_t-1)^2}\ \ln x_t\right] \tag{2.45}$$

$$Y_0(x_t) = \frac{x_t}{8}\left[\frac{x_t-4}{x_t-1} + \frac{3x_t}{(x_t-1)^2}\ln x_t\right] \tag{2.46}$$

$$\begin{aligned} Z_0(x_t) = &-\frac{1}{9}\ln x_t + \frac{18x_t^4-163x_t^3+259x_t^2-108x_t}{144(x_t-1)^3} + \\ &+\frac{32x_t^4-38x_t^3-15x_t^2+18x_t}{72(x_t-1)^4}\ln x_t. \end{aligned} \tag{2.47}$$

They will appear frequently later, when we analyze certain specific decay modes. An interesting feature is that all these functions grow with increasing top mass. This effect, referred to as non-decoupling, is counterintuitive, since a heavy particle that is integrated out should "decouple", i.e. appear only as a power suppression just like the mass of the W boson in our first example. In the case of FCNCs, non-decoupling arises, because the Goldstone bosons couple to fermions proportional to the mass of the fermion. As a result, one naively expects that the top diagrams should dominate over the charm and up ones, which would then only be needed for GIM cancellation. However, this hierarchy can be spoiled by CKM factors, as we will see explictly.

In the examples so far, we have entirely neglected any QCD effects. As a first step to include them, we should sandwich the amplitudes obtained between the physical initial and final states, the hadrons. As a result, all the vertex factors can be pulled out, and one is left with matrix elements of the type $\langle i|qqqq|f\rangle$, where i and f denote the initial and final states. These non-perturbative matrix elements need to be calculated, but still this step makes the advantage of the approach introduced in this section rather clear: It would be entirely hopeless to calculate the matrix elements of the complete amplitude, while the simpler, and universal, matrix elements of the four quark operators may be more easily tractable. Unfortunately, it turns out that uncertainties due to these matrix elements still constitute one of the main problems of flavor physics today. This is, in particular, true since the four-quark-operator matrix element can not be calculated on the lattice.

The entire procedure so far is a practical example of a concept widely used in QCD, the operator product expansion (OPE). The general idea is that the matrix element of a non-local operator product can be written as a sum over local operators, while the non-locality resides in calculable Wilson coefficients, as long as the non-locality is small or, equivalently, the energy scale, in our case the W mass, is high enough:

$$A(x)B(0) \overset{x\to 0}{\sim} \sum_n C_n(x)O_n(0)\,, \tag{2.48}$$

This relation holds, as long as the operators are sandwiched between initial and final states. The advantage of this method is precisely the one mentioned earlier: While the process dependent Wilson coefficients can be calculated, the universal matrix elements of the operators are easier to determine than the matrix element of the entire operator product. On a formal level, this corresponds to a separation of energy scales, where the high energy contributions are left in the Wilson coefficients, while the matrix elements describe low energy scales. The meaning of this will become more apparent when we include higher order QCD effects in the next section.

2.2.2 Weak Decays at NLO: Renormalization and the OPE

In the last section, we gave an introduction to the effective theory of weak decays, concentrating on the leading effects and neglecting QCD entirely. Also, we have only spoken about finite contributions, we have not explicitely stated which operators appear in the operator product expansion (2.48) and have neglected their scale dependence. We will clarify all these extremely important aspects in this more technical section. Since it will be quite a lot of ground to cover, let us state our main goal already at this point: The main goal and final result of this subsection will be the renormalization group equations and matching conditions for the Wilson coefficients of the effective Hamiltonian of $\Delta F = 1$ transitions, where $F = S, B$, including electroweak effects. These are, in particular, the Wilson coefficients of the electroweak penguin operators to be introduced below and the $\mathcal{O}(\alpha_s \alpha)$ terms of the anomalous dimensions that govern the running of the Wilson coefficients. The corresponding formulae have been given first in [54], and will be of central importance in later stages of our analysis.

When, for example, QCD processes are calculated beyond the tree level approximation, the corresponding loop diagrams are not finite, but instead have some divergent behavior for large loop momenta. To show this more clearly, consider the calculation of the QCD correction to the quark propagator, as shown in Fig. 2.5. The calculation can be performed with the standard field theory methods, if performed in $d = 4 - 2\varepsilon$ dimensions (the reason for this will become apparent in a moment). The results is given by

$$i\Sigma_{\alpha\beta} = i \not{p} \frac{4}{3} \delta_{\alpha\beta} g_s^2 [2(1-\varepsilon)] \frac{\Gamma(\varepsilon)}{(4\pi)^{2-\varepsilon}} \left(\frac{\mu^2}{-p^2} \right)^{\varepsilon} B(2-\varepsilon, 1-\varepsilon) \tag{2.49}$$

Here, $\Gamma(a)$ and $B(a,b)$ are the well known Euler-functions and we have set the quark mass in the loop to zero but kept the incoming momentum arbitrary. The energy scale μ is arbitrary and is introduced in order to keep the coupling constant dimensionless. Note that the divergent behavior mentioned above now shows up in the pole of the Γ function at $\varepsilon = 0$. Therefore, the entire expression is expanded for small ε to obtain

$$i\Sigma_{\alpha\beta} = i \not{p} \frac{4}{3} \delta_{\alpha\beta} \frac{\alpha_s}{4\pi} [\frac{1}{\varepsilon} + \ln 4\pi - \gamma_E + \ln \frac{\mu^2}{-p^2} + 1] \tag{2.50}$$

so that we have extracted the singularity into a well defined divergence.

On the level of the Lagrangian, this singularity is treated by introducing renormalization constants and counter-terms. In particular, the fields and couplings of the QCD

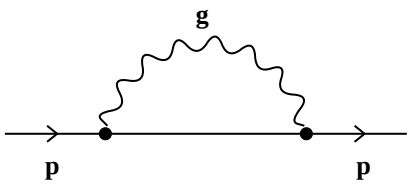

Figure 2.5: Quark-Self-Energy Diagram

Lagrangian are rescaled as

$$\begin{aligned} A^a_{0\mu} &= Z_3^{1/2} A^a_\mu \qquad & q_0 &= Z_q^{1/2} q \\ g_{0,s} &= Z_g g_s \mu^\varepsilon \qquad & m_0 &= Z_m m \,, \end{aligned} \tag{2.51}$$

where the index 0 denotes a bare, i.e. unrenormalized quantity. The renormalization constants Z_i are divergent objects, which are chosen such, that the renormalized parameters are finite. A theory is called renormalizable, if a finite number of renormalization constants only is required to render the prediction for all observable quantities finite up to all orders. Of course, the precise manner in which the divergences are canceled is arbitrary and is referred to as a "renormalization scheme dependence". The most obvious choice is to define the renormalization constants such, that they cancel precisely the divergence of the quantity they renormalize, i.e.

$$Z_l = 1 + \sum_{i,j} \left(\frac{\alpha_s}{4\pi}\right)^i \frac{1}{\varepsilon^j} Z_l^{ij} \,, \tag{2.52}$$

where the Z_{ij} are just mass and μ independent constants. This convention defines a class of minimally subtracted renormalization schemes, which can be transformed within this class by the replacement $\mu \to c\mu$, with c an arbitrary constant. Taking this constant to be $c = e^{\gamma_E/2}(4\pi)^{-1/2}$ defines the $\overline{MS}$ scheme, which is most often used in QCD loop calculations. On the level of Greens function such as the quark propagator introduced earlier, this corresponds to subtracting not only the divergence, but also the constant terms $\ln 4\pi - \gamma_E$, which often appear in this combination.

When the Lagrangian is written in terms of the renormalized fields, it can be split up into a finite part, that looks just like the old QCD Lagrangian but is composed of the renormalized fields, and the counter-terms which contain the divergences and are treated just like new interactions that cancel the divergences arising from calculations with the finite piece. Explicitly, for the QED Lagrangian, which is simpler than the QCD one but shows all the features important for renormalization, this looks a follows:

$$\begin{aligned} \mathcal{L}_{\text{QED}} = &-\frac{1}{4}(F_{\mu\nu})^2 + \bar\psi(i\ \partial\!\!\!/ - m)\psi - e\bar\psi\gamma^\mu\psi A_\mu \\ &-\frac{1}{4}(Z_3 - 1)(F_{\mu\nu})^2 + \bar\psi((Z_\psi - 1)i\ \partial\!\!\!/ - (Z_\psi Z_m - 1)m)\psi - e(Z_g - 1)\bar\psi\gamma^\mu\psi A_\mu. \end{aligned} \tag{2.53}$$

For simplicity, we have set the gauge parameter $\xi = \infty$. The first line contains the finite pieces, while the second contains the counter-terms. For example, the counter-terms

required to renormalize the massless self energy in (2.50) are then immediately seen to be

$$(Z_\psi - 1) i \not{p} \quad \Rightarrow \quad Z_\psi = 1 - \frac{\alpha_s}{4\pi}\frac{4}{3}\frac{1}{\varepsilon}\,. \tag{2.54}$$

For the final step, we just compared the finite pieces of the counter-term and the result from calculating the diagram to obtain the first coefficient of the renormalization constant. The other renormalization constants can be found analogously by keeping the masses in the quark self energy and calculating the one loop corrections to the gluon propagator and the $A\bar{q}q$ vertex. They are

$$Z_m^{11} = -4 \qquad Z_3^{11} = -\left[\frac{2}{3}f - \frac{5}{3}N\right] \qquad Z_g^{11} = -\left[-\frac{2}{6}f + \frac{11}{6}N\right]\,, \tag{2.55}$$

where N and f are the number of colors and flavors, respectively.

The next important point is the appearance of the scale μ. In general, renormalized quantities depend on this scale, in particular this is true for coupling constants and masses, where the dependence on this scale, or the "running", is described by the corresponding renormalization group equations. These can be found from (2.51) by differentiating if one keeps in mind that the bare quantities should obviously not depend on the scale. One finds:

$$\frac{dg(\mu)}{d\ln\mu} = \beta(g(\mu),\varepsilon)\,, \tag{2.56}$$

$$\frac{dm(\mu)}{d\ln\mu} = -\gamma_m(g(\mu))m(\mu)\,, \tag{2.57}$$

where

$$\beta(g,\varepsilon) = -\varepsilon g + \beta(g), \tag{2.58}$$

$$\beta(g) = -g\frac{1}{Z_g}\frac{dZ_g}{d\ln\mu}, \qquad \gamma_m(g) = \frac{1}{Z_m}\frac{dZ_m}{d\ln\mu}. \tag{2.59}$$

$\beta(g)$ and $\gamma_m(g)$ are usually referred to as the anomalous dimensions of the coupling and mass and can be obtained from the $\frac{1}{\varepsilon}$ pole of the renormalization constants:

$$\beta(g) = 2g^3\sum_i \frac{dZ_{i1}^g(g)}{dg^2}, \tag{2.60}$$

$$\gamma_m(g) = -2g^2\sum_i \frac{dZ_{j1}^m(g)}{dg^2}\,, \tag{2.61}$$

which can be proven using (2.58) and (2.59) as well as the parameterization (2.52). The corresponding proof can be found in [37]. When we discuss the running of α_s and the quark masses in the numerical sections of this work, we will usually work to two loop order, i.e. we will use the following expressions for the renormalization group equations:

$$\beta(g) = -\beta_0\frac{g^3}{16\pi^2} - \beta_1\frac{g^5}{(16\pi^2)^2}\,, \tag{2.62}$$

$$\gamma_m(\alpha_s) = \gamma_m^{(0)} \frac{\alpha_s}{4\pi} + \gamma_m^{(1)} \left(\frac{\alpha_s}{4\pi}\right)^2 , \tag{2.63}$$

where

$$\beta_0 = \frac{11N - 2f}{3} , \qquad \beta_1 = \frac{34}{3}N^2 - \frac{10}{3}Nf - 2C_F f , \tag{2.64}$$

$$\gamma_m^{(0)} = 6C_F , \qquad \gamma_m^{(1)} = C_F \left(3C_F + \frac{97}{3}N - \frac{10}{3}f\right) , \tag{2.65}$$

$$C_F = \frac{N^2 - 1}{2N}. \tag{2.66}$$

The leading coefficients of the β and γ function can be easily read off from (2.55).

We are now ready to return to the operator product expansion. Within the OPE, both the Wilson coefficients as well as the matrix elements also depend on μ. The renormalization of the operators proceeds just like for the quark masses:

$$\vec{C}^{(0)} = \hat{Z}_c \vec{C} \qquad \vec{Q}^{(0)} = \hat{Z} \vec{Q} , \tag{2.67}$$

with $\hat{Z}_c^T = \hat{Z}^{-1}$, as the scale dependence of Wilson coefficients and operators has to cancel. Defining next the anomalous dimension matrix $\hat{\gamma}$ by

$$\hat{\gamma} = \hat{Z}^{-1} \frac{d\hat{Z}}{d \ln \mu}, \tag{2.68}$$

the μ-independence of $\vec{C}^{(0)}$ implies

$$\frac{d\vec{C}(\mu)}{d \ln \mu} = \hat{\gamma}^T(\alpha_s) \vec{C}(\mu). \tag{2.69}$$

This equation can easily be solved to leading order, in particular if the operators do not mix, i.e. if the anomalous dimension is diagonal. First, one writes the evolution as

$$C_i(\mu) = U_i(\mu, \mu_W) C_i(\mu_W) . \tag{2.70}$$

where the form of the evolution matrix $U_i(\mu, \mu_W)$ is just as in the well known case of the running of quark masses

$$U_i(\mu, \mu_W) = \exp\left[\int_{g(\mu_W)}^{g(\mu)} dg' \frac{\gamma_i(g')}{\beta(g')}\right] \quad . \tag{2.71}$$

This immediately gives the leading order running for the Wilson coefficients

$$C_i(\mu) = \left[\frac{\alpha_s(M_W)}{\alpha_s(\mu)}\right]^{\frac{\gamma_i^{(0)}}{2\beta_0}} C_i(M_W) . \tag{2.72}$$

Since we have at his point included the possibility of there being several operators, we should pause and consider which operators will be contributing to weak decays. We will

refrain from actually giving them explicitly and refer the reader to [19] for a complete list. However, it is important to have an overview of at least the different types of operators here. In Subsection 2.2.1, we have only considered the single four quark operator that is created by integrating out the W boson at tree level. One finds that a second current-current operator with a different color structure is created if QCD effects are included. Similarly, one has 4 QCD penguin operators and another 4 electroweak penguin operators that arise. Therefore, whenever an anomalous dimension appears in this subsection, it can be considered as a 10×10 matrix. Again, we do not give the matrices explicitely, but refer to [55, 56], where they were first calculated to NLO. Eq. (2.72) can now easily be generalized to the case of operator mixing by going into a basis in which the anomalous dimension is, in fact, diagonal. This generalization reads as

$$\hat{U}^{(0)}(m_1, m_2) = \hat{V} \left[\left(\frac{\alpha_s(m_2)}{\alpha_s(m_1)} \right)^{\vec{a}} \right]_D \hat{V}^{-1} \qquad \text{with} \qquad \vec{a} = \frac{\vec{\gamma}_{\rm i}^{(0)}}{2\beta_0} \,, \tag{2.73}$$

where $(\gamma_i^{(0)})_D$ denotes a diagonal matrix whose diagonal elements are the components of the vector $\vec{\gamma}_{\rm i}^{(0)}$, and $\hat{V}$ is the matrix that diagonalizes $\gamma^{(0)}$:

$$(\gamma^{(0)})_D \equiv \hat{V}^{-1} \gamma^{(0)T} \hat{V} \,. \tag{2.74}$$

Going to two loop order the pure QCD evolution is written as [57]

$$\begin{aligned} \hat{U}(m_1, m_2) &= \left(\hat{1} + \frac{\alpha_s(m_1)}{4\pi} \hat{J} \right) \hat{U}^{(0)}(m_1, m_2) \left(\hat{1} - \frac{\alpha_s(m_2)}{4\pi} \hat{J} \right) \\ &= \hat{U}^{(0)}(m_1, m_2) + \frac{\alpha_s(m_1)}{4\pi} \hat{J} \hat{U}^{(0)}(m_1, m_2) + \frac{\alpha_s(m_1)}{4\pi} \hat{U}^{(0)}(m_1, m_2) \hat{J} \,, \end{aligned} \tag{2.75}$$

where $\hat{U}^{(0)}(m_1, m_2)$ denotes the evolution matrix in the leading logarithmic approximation and $\hat{J}$ summarizes the next-to-leading correction to this evolution. In the second line, we have dropped $\mathcal{O}(\alpha_s^2)$ terms for consistency.

The matrix $\hat{J}$ is given by

$$\hat{J} = \hat{V} \, \hat{S} \, \hat{V}^{-1} \,, \tag{2.76}$$

where the elements of $\hat{S}$ are

$$S_{ij} = \delta_{ij} \, \gamma_i^{(0)} \, \frac{\beta_1}{2\beta_0^2} - \frac{G_{ij}}{2\beta_0 + \gamma_i^{(0)} - \gamma_j^{(0)}} \,, \quad \text{whith} \quad \hat{G} \equiv \hat{V}^{-1} \gamma^{(1)T} \hat{V} \,, \tag{2.77}$$

and $\gamma_i^{(0)}$ denoting the components of $\vec{\gamma}^{(0)}$ and G_{ij} the elements of $\hat{G}$. Although Eq. (2.77) can develop singularities for certain combinations of the $\gamma_i^{(0)}$, the physically relevant evolution matrix (2.76) is always finite after all terms have been combined.

So far, we have included only the QCD running effects. The generalization for electroweak effects was performed in [54], which we follow closely in our notation. In this case, the anomalous dimension is generalized as

$$\hat{\gamma}(g^2, \alpha_{em}) = \hat{\gamma}_{\rm s}(g^2) + \frac{\alpha_{em}}{4\pi} \hat{\Gamma}(g^2) \,, \tag{2.78}$$

where

$$\hat{\gamma}_{\rm s}(g^2) = \frac{\alpha_s}{4\pi}\hat{\gamma}_{\rm s}^{(0)} + \frac{\alpha_s^2}{(4\pi)^2}\hat{\gamma}_{\rm s}^{(1)}\,, \tag{2.79}$$

and

$$\hat{\Gamma}(g^2) = \hat{\gamma}_{\rm e}^{(0)} + \frac{\alpha_s}{4\pi}\hat{\gamma}_{\rm se}^{(1)}\,. \tag{2.80}$$

Here, the $\hat{\gamma}_{\rm s}^{(1)}$ corresponds to the two loop QCD effects, while $\hat{\gamma}_{\rm e}^{(0)}$ and $\hat{\gamma}_{\rm se}^{(1)}$ include the effects of $\mathcal{O}(\alpha_{em})$ and $\mathcal{O}(\alpha_s\alpha_{em})$, respectively. This implies a generalization of the Wilson coefficient evolution as

$$\hat{U}(m_1, m_2, \alpha_{em}) = \hat{U}(m_1, m_2) + \frac{\alpha_{em}}{4\pi}\hat{R}(m_1, m_2)\,. \tag{2.81}$$

$\hat{U}(m_1, m_2)$, which describes pure QCD evolution, is given by (2.76), while $\hat{R}(m_1, m_2)$ describes the additional evolution in the presence of electromagnetic interactions and is parameterized by

$$\hat{R}(m_1, m_2) = -\frac{2\pi}{\beta_0}\,\hat{V}\,\hat{K}(m_1, m_2)\hat{V}^{-1} \equiv \hat{R}^{(0)}(m_1, m_2) + \hat{R}^{(1)}(m_1, m_2)\,. \tag{2.82}$$

To next-to-leading order, $\hat{K}(m_1, m_2)$ can be written as

$$\hat{K}(m_1, m_2) = \hat{K}^{(0)}(m_1, m_2) + \frac{1}{4\pi}\sum_{i=1}^{3}\hat{K}_i^{(1)}(m_1, m_2)\,, \tag{2.83}$$

where the matrix $\hat{K}^{(0)}(m_1, m_2)$ is given by

$$(\hat{K}^{(0)}(m_1, m_2))_{ij} = \frac{\hat{M}_{ij}^{(0)}}{a_i - a_j - 1}\left[\left(\frac{\alpha_s(m_2)}{\alpha_s(m_1)}\right)^{a_j}\frac{1}{\alpha_s(m_1)} - \left(\frac{\alpha_s(m_2)}{\alpha_s(m_1)}\right)^{a_i}\frac{1}{\alpha_s(m_2)}\right]. \tag{2.84}$$

Again, we observe a potential singularity in this expression, but it turns out that, in the case where this happens, the terms in the parenthesis also vanish and the singularity is therefore not a problem in the numerical implementation of these terms.

The $\hat{K}_i^{(1)}(m_1, m_2)$ encompass the different sources of next-to-leading order effects. To introduce them, we first define

$$\hat{\Gamma}^{(1)} = \hat{\gamma}_{\rm se}^{(1)T} - \frac{\beta_1}{\beta_0}\hat{\gamma}_{\rm e}^{(0)T} \tag{2.85}$$

and

$$\hat{M}^{(1)} = \hat{V}^{-1}\left(\hat{\Gamma}^{(1)} + \left[\hat{\gamma}_{\rm e}^{(0)T}, \hat{J}\right]\right)\hat{V}\,. \tag{2.86}$$

The matrices $\hat{K}_i^{(1)}(m_1, m_2)$ are then given as follows

$$\left(\hat{K}_1^{(1)}(m_1, m_2)\right)_{ij} = \begin{cases} \frac{M_{ij}^{(1)}}{a_i - a_j}\left[\left(\frac{\alpha_s(m_2)}{\alpha_s(m_1)}\right)^{a_j} - \left(\frac{\alpha_s(m_2)}{\alpha_s(m_1)}\right)^{a_i}\right] & i \neq j \\ M_{ii}^{(1)}\left(\frac{\alpha_s(m_2)}{\alpha_s(m_1)}\right)^{a_i}\ln\frac{\alpha_s(m_1)}{\alpha_s(m_2)} & i = j \end{cases}, \tag{2.87}$$

$$\hat{K}_2^{(1)}(m_1, m_2) = -\,\alpha_s(m_2)\;\hat{K}^{(0)}(m_1, m_2)\;\hat{S}\,, \tag{2.88}$$

$$\hat{K}_3^{(1)}(m_1, m_2) = \quad \alpha_s(m_1)\;\hat{S}\;\hat{K}^{(0)}(m_1, m_2)\,. \tag{2.89}$$

We have now collected all the expressions that contribute to the running of the Wilson coefficients between the high scale, where the W is integrated out and the low scale of the B meson decay. Finally, we also need the initial conditions for the Wilson coefficients. These are obtained at M_W by integrating out all the heavy particles and matching the corresponding operator expression onto the same one in the full theory with all particles present, just as we have done in the case of the tree level W exchange. Including all NLO QCD and electroweak effects, these coefficients are given by:

$$C_1(Mw) = \frac{\alpha_s(M_W)}{4\pi}\frac{11}{2}\,, \tag{2.90}$$

$$C_2(M_W) = 1 - \frac{\alpha_s(M_W)}{4\pi}\frac{11}{6} - \frac{\alpha_{am}}{4\pi}\frac{35}{18}\,, \tag{2.91}$$

$$C_3(M_W) = -\frac{\alpha_s(M_W)}{24\pi}\widetilde{E}(x_t) + \frac{\alpha_{em}}{6\pi}\frac{1}{\sin^2\theta_W}\left[2B(x_t) + C(x_t)\right]\,, \tag{2.92}$$

$$C_4(M_W) = \frac{\alpha_s(M_W)}{8\pi}\widetilde{E}(x_t)\,, \tag{2.93}$$

$$C_5(M_W) = -\frac{\alpha_s(M_W)}{24\pi}\widetilde{E}(x_t)\,, \tag{2.94}$$

$$C_6(M_W) = \frac{\alpha_s(M_W)}{8\pi}\widetilde{E}(x_t)\,, \tag{2.95}$$

$$C_7(M_W) = \frac{\alpha_{em}}{6\pi}\left[4C(x_t) + \widetilde{D}(x_t)\right]\,, \tag{2.96}$$

$$C_8(M_W) = 0\,, \tag{2.97}$$

$$C_9(M_W) = \frac{\alpha_{em}}{6\pi}\left[4C(x_t) + \widetilde{D}(x_t) + \frac{1}{\sin^2\theta_W}(10B(x_t) - 4C(x_t))\right]\,, \tag{2.98}$$

$$C_{10}(M_W) = 0\,, \tag{2.99}$$

With these initial conditions we have all the ingredients needed to calculate the Wilson coefficients of the electroweak penguin operators as we will do later on.

2.2.3 Minimal Flavor Violation (MFV)

As a final step of the description of weak decays, it is important to consider, what the precise influence of some new physics may be. In this context, the notion of minimal flavor violation (MFV) [58–63] will be of quite some relevance for the rest of this thesis. In brief, it just states that flavor changing and CP violating processes are governed entirely by the CKM matrix, i.e. there are no additional sources of flavor changing and no new

operators. The concept was originally motivated in the context of supersymmetry, where large flavor violating effects could be present in a general scenario, but are not measured. To see its implications more clearly, let us recall from the last section that the general effective Hamiltonian would have a structure like

$$H_{\text{eff}} = \sum \lambda_i F_i O_i \,, \tag{2.100}$$

where the λ_i are the CKM factors, the F_i are the loop functions corresponding to the Inami Lim functions in the SM and the O_i are from the basis of relevant operators. In a general NP model, all of these can be modified with respect to the SM. On the other hand, in MFV, following the definition of [60, 63] the only new contributions appear in the loop functions, while there are no new operators and no new sources of flavor change and, in particular, no further source of CP violation. Also, QCD evolution is not strongly affected by the new physics, especially since there are no new operators. The goal of this definition is that the observable effects in this kind of models are very clearly defined and that one can therefore easily exclude an entire class of models with the appropriate experimental data. There are, for example, rather stringent bounds [64] on several rare K and B decays within the class of MFV. Additionally, the strong constraints on the structure of the effective Hamiltonian can lead to strong correlations between several observables. For example, decays that are governed by the same high energy functions will behave in a correlated way in MFV, but this correlation can be lost if the assumption of MFV is dropped. Finally, a discrepancy in the measurement of any UT angle would immediately signal new sources of flavor or CP violation. Models of MFV type are, for example, the two Higgs doublet models I and II, the MSSM at low $\tan\beta$, the SM with one universal extra dimension as well as the Littlest Higgs model. On the other hand, supersymmetry at large $\tan\beta$ introduces new scalar operators from Higgs diagrams and is therefore not MFV in the definition of [60].

Concerning the construction of the unitarity triangle as described above, one must of course remember that not all the constraints available can be used for a UT fit within the class of MFV. For instance, the constraint from ΔM_d need not necessarily remain valid when there are new contributions to $B_d^0 - \bar{B}_d^0$ mixing, even if these are flavor universal. Fortunately, there exists a universal unitarity triangle (UUT) [60] that remains true in any extension of the SM with MFV. In the construction of this triangle one includes all those constraints that do not depend on new physics apart from the flavor structure. In practice this means that only the constraints where the Inami Lim function don't appear explicitely are taken into account. In the classic construction of [60] the UT is obtained with the constraints from $|V_{ub}/V_{cb}|$, $\sin 2\beta$.

Chapter 3

The $B \to \pi\pi$ Decays

3.1 Basics

In this chapter we analyze in detail the decays of the type $B \to \pi\pi$. These decays have received quite a lot of attention over the last decade (see [15] for a review) in the context of a determination of the CKM angle α. First, we would like to remind the reader that there are three decay channels of this kind:

$$B^+ \to \pi^+\pi^0 \qquad B_d^0 \to \pi^0\pi^0 \qquad B_d^0 \to \pi^+\pi^- \,.$$

This leads to eight observable quantities: Three branching ratios and 5 CP asymmetries, according to the discussion in Section 2.1.4, as $\pi^0\pi^0$ and $\pi^+\pi^-$ are CP eigenstates, while $\pi^+\pi^0$ is not. The current experimental numbers from Belle and BaBar for these quantities are compiled in Table 3.1, where the averages are taken from the Heavy Flavor Averaging Group (HFAG) [49]. Note, that the mixing induced asymmetry in $\pi^0\pi^0$ can not be measured at present. We do not include in this table several experimental results from CLEO and CDF, since the averages are, in fact, dominated by the results from Belle and BaBar. The corresponding numbers can be found in [49].

An interesting situation arises in these decays, since their theoretical description seems a bit unsatisfactory. For example, the predictions of QCD factorization [65] for $B_d^0 \to \pi^0\pi^0$ are smaller than the experimental value, while the calculation of $B_d^0 \to \pi^+\pi^-$ tends to be on the high side. It is then interesting to check whether this can be accommodated in the standard model or if we are already seeing hints of new physics.

If we look at the separate processes, we find that all of these decays are dominated by tree diagrams. To illustrate this, we show in Fig. 3.1 the leading diagrams[1] for $B \to \pi^+\pi^-$. Counting up CKM factors shows that they do not lift the expected loop suppression of the penguin diagrams. Similar reasoning applies for the other decays, so that the discrepancies mentioned above come more likely from difficulties in describing the hadronic effects, instead of from new physics.

[1] To be precise, one should be discussing these contributions in terms of the effective Hamiltonian, where these diagrams don't exist as such. The intuitive picture remains the same, however. For further discussion of the relation between the effective Hamiltonian and the Feynman diagrams, see [74].

Quantity	BaBar	Belle	Average
$\mathrm{BR}(B^\pm \to \pi^\pm\pi^0)/10^{-6}$	$5.8 \pm 0.6 \pm 0.4$ [66]	$5.0 \pm 1.2 \pm 0.5$ [67]	5.5 ± 0.6
$\mathrm{BR}(B_d \to \pi^+\pi^-)/10^{-6}$	$5.5 \pm 0.4 \pm 0.3$ [68]	$4.4 \pm 0.6 \pm 0.3$ [67]	5.0 ± 0.4
$\mathrm{BR}(B_d \to \pi^0\pi^0)/10^{-6}$	$1.17 \pm 0.32 \pm 0.10$ [66]	$2.3^{+0.4+0.2}_{-0.5-0.3}$ [69]	1.45 ± 0.29
$\mathcal{A}_{\mathrm{CP}}^{\mathrm{dir}}(B_d \to \pi^+\pi^-)$	$-0.09 \pm 0.15 \pm 0.04$ [70]	$-0.56 \pm 0.12 \pm 0.06$ [71]	-0.37 ± 0.10
$\mathcal{A}_{\mathrm{CP}}^{\mathrm{mix}}(B_d \to \pi^+\pi^-)$	$0.30 \pm 0.17 \pm 0.03$ [70]	$0.67 \pm 0.16 \pm 0.06$ [71]	0.50 ± 0.12
$\mathcal{A}_{\mathrm{CP}}^{\mathrm{dir}}(B_d \to \pi^0\pi^0)$	$-0.12 \pm 0.56 \pm 0.06$ [72]	$-(0.44^{+0.53}_{-0.52} \pm 0.17)$ [69]	$-(0.28^{+0.40}_{-0.39})$
$\mathcal{A}_{\mathrm{CP}}^{\mathrm{mix}}(B_d \to \pi^0\pi^0)$	-	-	-
$\mathcal{A}_{\mathrm{CP}}^{\mathrm{dir}}(B_d \to \pi^+\pi^0)$	$0.01 \pm 0.10 \pm 0.02$ [66]	$-0.02 \pm 0.08 \pm 0.01$ [73]	-0.01 ± 0.06

Table 3.1: The current status of the $B \to \pi\pi$ experimental data. The uncertainties are statistical and systematic.

In order to make this statement more quantitative, one can, using isospin symmetry and eliminating $\lambda_t^{(b)}$ by GIM, write down the relevant decay amplitudes as:

$$\sqrt{2}A(B^+ \to \pi^+\pi^0) = -[\tilde{T} + \tilde{C} + P_{\mathrm{EW}}] = -[T + C + P_{\mathrm{EW}}] \tag{3.1}$$

$$A(B_d^0 \to \pi^+\pi^-) = -[\tilde{T} + P] \tag{3.2}$$

$$\sqrt{2}A(B_d^0 \to \pi^0\pi^0) = -[\tilde{C} - P + P_{\mathrm{EW}}], \tag{3.3}$$

with

$$P = \lambda^3 A(\mathcal{P}_t - \mathcal{P}_c) \equiv \lambda^3 A \mathcal{P}_{tc} \tag{3.4}$$

$$\tilde{T} = \lambda^3 A R_b e^{i\gamma} \left[\mathcal{T} - (\mathcal{P}_{tu} - \mathcal{E})\right] \tag{3.5}$$

$$\tilde{C} = \lambda^3 A R_b e^{i\gamma} \left[\mathcal{C} + (\mathcal{P}_{tu} - \mathcal{E})\right], \tag{3.6}$$

and P_{EW} being an electroweak penguin amplitude that is numerically extremely small and was neglected in the corresponding equation of [27] (but has been restored in [75] and is included in all numerical results below). Note, that the additional QCD penguin and exchange contributions in $\tilde{T}$ and $\tilde{C}$ cancel when the amplitudes are added, and one finds the isospin relation [76]:

$$\sqrt{2}A(B^+ \to \pi^+\pi^0) = A(B_d^0 \to \pi^+\pi^-) + \sqrt{2}A(B_d^0 \to \pi^0\pi^0). \tag{3.7}$$

Below, we will find it convenient to define ratios of CP averaged branching ratios, since this allows to reduce the number of hadronic parameters by cancellation. As a first step, we define amplitude ratios:

$$x e^{i\Delta} \equiv \frac{\tilde{C}}{\tilde{T}} = \left|\frac{\tilde{C}}{\tilde{T}}\right| e^{i(\delta_{\tilde{C}} - \delta_{\tilde{T}})} = \frac{\mathcal{C} + (\mathcal{P}_{tu} - \mathcal{E})}{\mathcal{T} - (\mathcal{P}_{tu} - \mathcal{E})}. \tag{3.8}$$

$$d e^{i\theta} \equiv -\frac{P}{\tilde{T}} e^{i\gamma} = -\left|\frac{P}{\tilde{T}}\right| e^{i(\delta_P - \delta_{\tilde{T}})} = -\frac{1}{R_b}\left[\frac{\mathcal{P}_{tc}}{\mathcal{T} - (\mathcal{P}_{tu} - \mathcal{E})}\right], \tag{3.9}$$

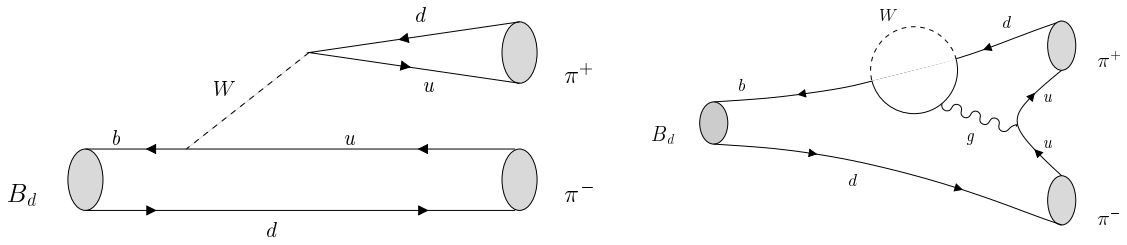

Figure 3.1: Feynman diagrams contributing to $B_d \to \pi^+\pi^-$

$$\tilde{q} \equiv \left|\frac{P_{\rm EW}}{T+C}\right| \approx 1.3\times 10^{-2} \times \left|\frac{V_{td}}{V_{ub}}\right| = 1.3\times 10^{-2} \times \left(1-\frac{\lambda^2}{2}\right)\left|\frac{\sin\gamma}{\sin\beta}\right| \approx 3\times 10^{-2}. \quad (3.10)$$

In the last line, we have estimated the electroweak penguin contributions from the $B \to \pi K$ ones using flavor symmetry following [27, 77, 78]. With these parameters, we can write the decay amplitudes the in following form:

$$\sqrt{2}A(B^+ \to \pi^+\pi^0) = -|\tilde{T}|e^{i\delta_{\tilde{T}}}\left[1+xe^{i\Delta}\right]\left[e^{i\gamma}+\tilde{q}e^{-i\beta}\right] \quad (3.11)$$

$$A(B_d^0 \to \pi^+\pi^-) = -|\tilde{T}|e^{i\delta_{\tilde{T}}}\left[e^{i\gamma}-de^{i\theta}\right] \quad (3.12)$$

$$\sqrt{2}A(B_d^0 \to \pi^0\pi^0) = |P|e^{i\delta_P}\left[1+\frac{x}{d}e^{i\gamma}e^{i(\Delta-\theta)}+\tilde{q}\left(\frac{1+xe^{i\Delta}}{d}\right)e^{-i\theta}e^{-i\beta}\right], \quad (3.13)$$

which allows to express several observables in a transparent way. Our next step will be to determine the hadronic parameters appearing in these expressions.

3.2 Determination of the Hadronic Parameters

In order to determine the hadronic parameters, the first bit of input to use are the branching ratios. To cancel the prefactors in the amplitudes, we define two observables:

$$R_{+-}^{\pi\pi} \equiv 2\left[\frac{\mathrm{BR}(B^+\to\pi^+\pi^0)+\mathrm{BR}(B^-\to\pi^-\pi^0)}{\mathrm{BR}(B_d^0\to\pi^+\pi^-)+\mathrm{BR}(\bar{B}_d^0\to\pi^+\pi^-)}\right]\frac{\tau_{B_d^0}}{\tau_{B^+}} = 2.04\pm 0.28 \quad (3.14)$$

$$R_{00}^{\pi\pi} \equiv 2\left[\frac{\mathrm{BR}(B_d^0\to\pi^0\pi^0)+\mathrm{BR}(\bar{B}_d^0\to\pi^0\pi^0)}{\mathrm{BR}(B_d^0\to\pi^+\pi^-)+\mathrm{BR}(\bar{B}_d^0\to\pi^+\pi^-)}\right] = 0.58\pm 0.13, \quad (3.15)$$

which can be expressed entirely in terms of the hadronic parameters introduced above as well as the weak phase γ:

$$R_{+-}^{\pi\pi} = \frac{1+2x\cos\Delta+x^2}{1-2d\cos\theta\cos\gamma+d^2} \quad (3.16)$$

$$R_{00}^{\pi\pi} = \frac{d^2+2dx\cos(\Delta-\theta)\cos\gamma+x^2}{1-2d\cos\theta\cos\gamma+d^2}. \quad (3.17)$$

Here, we have, for transparency, neglected the electroweak penguin contributions. In order to determine the parameters appearing, we also need to take into account the CP asymmetries. First, we can use the mixing induced and direct CP asymmetries in $B_d^0 \to \pi^+\pi^-$, which are measured to be sizeable:

$$\mathcal{A}_{\rm CP}^{\rm dir}(B_d \to \pi^+\pi^-) = -0.37 \pm 0.10\,, \quad \mathcal{A}_{\rm CP}^{\rm mix}(B_d \to \pi^+\pi^-) = +0.50 \pm 0.12. \tag{3.18}$$

On the other hand, their expressions in terms of the hadronic parameters introduced above are

$$\mathcal{A}_{\rm CP}^{\rm dir}(B_d \to \pi^+\pi^-) = -\left[\frac{2d\sin\theta\sin\gamma}{1-2d\cos\theta\cos\gamma+d^2}\right] \tag{3.19}$$

$$\mathcal{A}_{\rm CP}^{\rm mix}(B_d \to \pi^+\pi^-) = \frac{\sin(\phi_d+2\gamma)-2d\cos\theta\sin(\phi_d+\gamma)+d^2\sin\phi_d}{1-2d\cos\theta\cos\gamma+d^2}. \tag{3.20}$$

Here, $\phi_d = 2\beta$ as in (2.26). In the limit of vanishing penguin contributions $d = 0$, $\mathcal{A}_{\rm CP}^{\rm mix}(B_d \to \pi^+\pi^-)$ simply measures the CKM angle α [76]. Unfortunately, the penguin contributions seem to be sizeable, as indicated by the large direct CP asymmetry, leading only to a measurement of α_{eff}, where

$$\mathcal{A}_{\rm CP}^{\rm mix}(B_d \to \pi^+\pi^-) = \sin 2\alpha_{eff} \tag{3.21}$$

The corrections between α and α_{eff} have been analyzed by several authors over the last years [79–85], where one can also use $B \to \rho\rho$ transitions to determine α, and the corresponding values are actually being used in UT fits nowadays, as discussed in Section 2.1.3. In order to determine all parameters in the expressions (3.1)-(3.3), one more input is required. The three remaining quantities of the $B \to \pi\pi$ decay system are not very suitable, since the CP asymmetry of $B^+ \to \pi^+\pi^0$ is small, as it vanishes in limit of $\tilde{q} = 0$ and the CP asymmetries in $\pi^0\pi^0$ are still affected by large experimental uncertainties. This leaves us with two possibilities: Either we take the angle γ as input, use the four observables mentioned above and determine the four hadronic parameters appearing, or we must include an additional observable if we would also like to determine γ. While the former approach was pursued in [26, 27], here we will follow [28] and attempt to find also γ. This can be done by invoking the SU(3) flavor symmetry of strong interactions and defining [86]:

$$H_{\rm BR} \equiv \underbrace{\frac{1}{\epsilon}\left(\frac{f_K}{f_\pi}\right)^2\left[\frac{\mathrm{BR}(B_d \to \pi^+\pi^-)}{\mathrm{BR}(B_d \to \pi^\mp K^\pm)}\right]}_{7.5 \pm 0.7} \overset{\rm SU(3)}{=} \underbrace{-\frac{1}{\epsilon}\left[\frac{\mathcal{A}_{\rm CP}^{\rm dir}(B_d \to \pi^\mp K^\pm)}{\mathcal{A}_{\rm CP}^{\rm dir}(B_d \to \pi^+\pi^-)}\right]}_{6.7 \pm 2.0} \equiv H_{\mathcal{A}_{\rm CP}^{\rm dir}}, \tag{3.22}$$

where the numbers given use $\epsilon \equiv \lambda^2/(1-\lambda^2) = 0.053$ and $f_K/f_\pi = 160/131$ for the ratio of the kaon and pion decay constants, which correspond to factorizable SU(3) breaking effects. As denoted, the definition of $H_{\rm BR}$ and $H_{\mathcal{A}_{\rm CP}^{\rm dir}}$ are only equal in the strict SU(3) limit, using also additional assumptions that shall be specified in the next section. There we shall also explain in more detail how to obtain the hadronic parameters for the $B \to \pi K$ quantities appearing in (3.22). On the other hand, as we will see, the factorizable SU(3) breaking effects in the hadronic parameters in this relation drop out.

For the moment, however, we will be content with the theoretical expression that arises for H_i,

$$H_{\rm BR/\mathcal{A}_{CP}^{dir}} = \frac{1 - 2d\cos\theta\cos\gamma + d^2}{\epsilon^2 + 2\epsilon d\cos\theta\cos\gamma + d^2}, \tag{3.23}$$

and explore its numerical consequences. The most interesting of these is the determination of γ alluded to earlier. Using the experimental values of $H_{\rm BR}$ and $H_{\mathcal{A}_{\rm CP}^{\rm dir}}$, respectively, we obtain:

$$\gamma|_{\rm BR} = (44.0^{+4.3}_{-3.7})^\circ \quad \vee \quad (70.1^{+5.6}_{-7.2})^\circ, \tag{3.24}$$

$$\gamma|_{\mathcal{A}_{\rm CP}^{\rm dir}} = (42.1^{+3.4}_{-3.6})^\circ \quad \vee \quad (73.9^{+5.8}_{-6.5})^\circ. \tag{3.25}$$

The agreement between the values of γ obtained (which reflects of course the agreement between the experimental numbers of (3.22)) is an encouraging confirmation of the assumptions we use. Nevertheless, we have to decide whether to use the experimental numbers of $H_{\rm BR}$ or $H_{\mathcal{A}_{\rm CP}^{\rm dir}}$ in the following. The cleaner avenue is from $H_{\mathcal{A}_{\rm CP}^{\rm dir}}$, which also leads to smaller uncertainties, and we will use it in what follows. The numerical values of all other parameters can then easily be found, and are given by:

$$d = 0.52^{+0.09}_{-0.09}, \quad \theta = (146^{+7.0}_{-7.2})^\circ \quad , \tag{3.26}$$

$$x = 0.96^{+0.13}_{-0.14} \quad , \quad \Delta = -(53^{+18}_{-26})^\circ. \tag{3.27}$$

In general, there are multiple solutions for all variables, as demonstrated on Figs. 3.2 and 3.3, where we show the situation in the parameter planes for fixed $\gamma = 73.9^\circ$. The contours can be found by solving the theoretical expressions for the mixing and direct asymmetries, as well as for $R^{\pi\pi}_{+-}$ and $R^{\pi\pi}_{00}$. From the direct CP asymmetry, we find

$$d = \frac{1}{\mathcal{A}_{\rm CP}^{\rm dir}(B_d \to \pi^+\pi^-)}\Bigg[\mathcal{A}_{\rm CP}^{\rm dir}(B_d \to \pi^+\pi^-)\cos\theta\cos\gamma - \sin\theta\sin\gamma$$
$$\pm\sqrt{\left[\mathcal{A}_{\rm CP}^{\rm dir}(B_d \to \pi^+\pi^-)\cos\theta\cos\gamma - \sin\theta\sin\gamma\right]^2 - \mathcal{A}_{\rm CP}^{\rm dir}(B_d \to \pi^+\pi^-)^2}\Bigg], \tag{3.28}$$

whereas the mixing induced one gives

$$d = k \pm \sqrt{k^2 - l}, \tag{3.29}$$

with

$$k = \left[\frac{\sin(\phi_d + \gamma) - \mathcal{A}_{\rm CP}^{\rm mix}(B_d \to \pi^+\pi^-)\cos\gamma}{\sin\phi_d - \mathcal{A}_{\rm CP}^{\rm mix}(B_d \to \pi^+\pi^-)}\right]\cos\theta \tag{3.30}$$

$$l = \frac{\sin(\phi_d + 2\gamma) - \mathcal{A}_{\rm CP}^{\rm mix}(B_d \to \pi^+\pi^-)}{\sin\phi_d - \mathcal{A}_{\rm CP}^{\rm mix}(B_d \to \pi^+\pi^-)}. \tag{3.31}$$

Correspondingly, $R^{\pi\pi}_{+-}$ and $R^{\pi\pi}_{00}$ imply

$$x = -\cos\Delta \pm \sqrt{\tilde{R}^{\pi\pi}_{+-} - \sin^2\Delta} \tag{3.32}$$

and

$$x = -d\cos\gamma\cos(\Delta-\theta) \pm \sqrt{\tilde{R}^{\pi\pi}_{00} - [1-\cos^2\gamma\cos^2(\Delta-\theta)]\,d^2}, \tag{3.33}$$

where we have introduced, as in [27]

$$\tilde{R}^{\pi\pi}_{+-} \equiv DR^{\pi\pi}_{+-} \tag{3.34}$$

$$\tilde{R}^{\pi\pi}_{00} \equiv DR^{\pi\pi}_{00}, \tag{3.35}$$

with

$$D \equiv 1 - 2d\cos\theta\cos\gamma + d^2. \tag{3.36}$$

As can be seen, the requirement of γ being within reasonable agreement with standard UT fits (we will comment on this below) chooses both one solution for γ and one for the pair (d,θ). Also, we see that the second solution for d is both in conflict with the naive estimate that the penguin amplitudes should be smaller than the tree, as well as with the predictions of QCD methods which typically predict $d \approx 0.3$ [80]. The second solution for (x,Δ), on the other hand, is only excluded *a posteriori* by studying the implications for CP asymmetries in the $B \to \pi K$ system, and we will come back to this point later.

The uncertainties in the numerical values given above and in the rest of our analysis, unless explicitely stated otherwise, were estimated as follows: All hadronic parameters obtained in the analysis depend on some experimental input as well as on other hadronic parameters used as input (this will be more relevant when we continue to use the parameters obtained above for further calculations in the $B \to \pi K$ system), which in turn depend also on the experimental input. To take into account all the possible cancellations that can occur if several parameters depend on the same input, we find all parameters in terms of the experimental observables and vary then individually the experimental numbers in the 1σ range for the error estimate, while keeping the other input fixed. Then, these errors are added in quadrature. The errors taken into account, apart from the obvious $B \to \pi\pi$ (and later $B \to \pi K$) data, are also the uncertainties in ϕ_d, the CKM factors and some SU(3) breaking factors, that we will discuss in the context of the $B \to \pi K$ system.

3.3 CP Violation in $B_d \to \pi^0\pi^0$

Finally, using the hadronic parameters obtained above, we can now also make predictions for the CP asymmetries in $B \to \pi^0\pi^0$. The appropriate formulae are, setting again $\tilde{q} = 0$ for transparency:

$$\mathcal{A}^{\rm dir}_{\rm CP}(B_d \to \pi^0\pi^0) = \frac{2dx\sin(\theta-\Delta)\sin\gamma}{d^2 + 2dx\cos(\theta-\Delta)\cos\gamma + x^2} \tag{3.37}$$

$$\mathcal{A}^{\rm mix}_{\rm CP}(B_d \to \pi^0\pi^0) = \frac{d^2\sin\phi_d + 2dx\cos(\theta-\Delta)\sin(\phi_d+\gamma) + x^2\sin(\phi_d+2\gamma)}{d^2 + 2dx\cos(\theta-\Delta)\cos\gamma + x^2}. \tag{3.38}$$

We then predict:

$$\mathcal{A}^{\rm dir}_{\rm CP}(B_d \to \pi^0\pi^0) = -0.30^{+0.48}_{-0.26}, \quad \mathcal{A}^{\rm mix}_{\rm CP}(B_d \to \pi^0\pi^0) = -0.87^{+0.29}_{-0.19}. \tag{3.39}$$

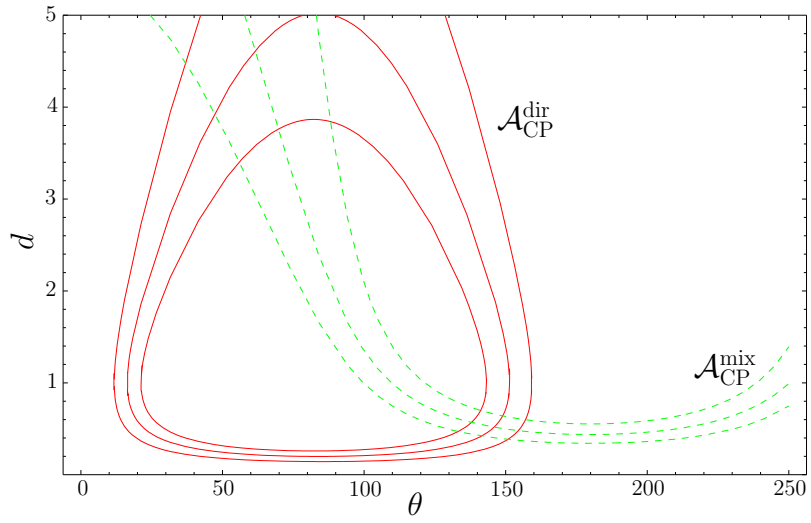

Figure 3.2: The contours in the θ–d plane for $\gamma = 73.9°$ and $\phi_d = 43.4°$. The solid lines correspond to the central value and 1σ upper and lower ranges of $\mathcal{A}_{\rm CP}^{\rm dir}(B_d \to \pi^+\pi^-) = -0.37 \pm 0.10$ and the dashed lines represent $\mathcal{A}_{\rm CP}^{\rm mix}(B_d \to \pi^+\pi^-) = +0.50 \pm 0.12$.

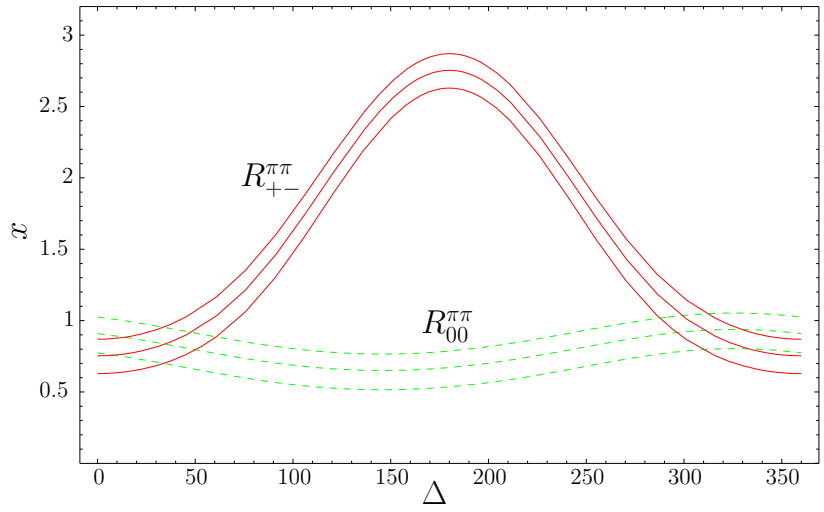

Figure 3.3: The contours in the Δ–x plane. Using $d = 0.52$ and $\theta = 146°$ following from the central values of Fig. 3.2, we obtain the solid set of contours for $R_{+-}^{\pi\pi} = 2.04 \pm 0.28$ and the dashed set of contours for $R_{00}^{\pi\pi} = 0.58 \pm 0.13$.As discussed in the text, there are two solutions, one of which is is later excluded using $B \to \pi K$ data.

On the other hand, the current experimental value for the direct CP asymmetry is [49]:

$$\mathcal{A}_{\rm CP}^{\rm dir}(B_d \to \pi^0\pi^0) = -0.28^{+0.40}_{-0.39}, \tag{3.40}$$

while no experimental value for the mixing-induced asymmetry exists. Needless to say, the uncertainties are rather large but the prediction is still encouragingly good. This gives us some confidence in the assumptions leading to (3.22), as well as the fact that the data will likely not shift significantly. Also, an agreement at this point would lend support to the assumption that the $B \to \pi\pi$ transitions are indeed described very well within the standard model and that new physics contributions are are not required. On the other hand, a precise measurement of one of the asymmetries would make a determination of γ from $B \to \pi\pi$ alone possible.

3.4 Interpretation of the Results

3.4.1 Our Value of γ

After having obtained some quantitative information about the $B \to \pi\pi$ parameters in the last section, these should now be interpreted with respect to their physical meaning.

We begin with some comments on the angle γ: In comparison to the standard UT fits [39, 40], our value for γ is on the high side. This is, on the one hand, in agreement with a recent SCET analysis [87], where an even higher value is favored. On the other hand, one should remember that the CKM fits take into account the angle β as obtained from $B \to J/\psi K_S$, which may be affected by new physics contributions to $B_d^0 - \bar{B}_d^0$ mixing [28, 88]. In particular, there is some tension between the new values of $\sin 2\beta$ and $|V_{ub}/V_{cb}|$, since $\sin 2\beta|_{\rm exp}$ has decreased, while $|V_{ub}/V_{cb}|$ has increased. On the whole, the UT fit values of $\sin 2\beta$ tend to be higher than the experimental number.

In view of this situation, we will consider our value of γ to be the true UT angle and construct our UT from this value and from the value of $|V_{ub}/V_{cb}|$ introduced in Section 2.1.3, i.e. $|V_{ub}/V_{cb}| = 0.102 \pm 0.005$. The NP contributions to $B_d^0 - \bar{B}_d^0$ mixing are parameterized by incorporating a new phase as

$$\phi_d = 2\beta_{\rm true} + \phi_d^{\rm NP}\,. \tag{3.41}$$

The corresponding results are given table 3.2, where we show for comparison also the results of a complete UT fit, a fit to the Reference UT (RUT) with only the tree level γ and $|V_{ub}/V_{cb}| = 0.102 \pm 0.005$ used as input as well as a fit the universal unitarity triangle (UUT) [60], which remains valid in any model with MFV.

3.4.2 Interpretation of the Hadronic Parameters

Let us next analyze the physical content of values for the hadronic parameters that we obtained. The first obvious point is the very large value of x. Since, in the naive limit of top dominated penguins and vanishing exchange topologies, this parameter measures the ratio of color-suppressed over color-allowed tree topologies, the expected value would be closer to 0.3 than $x \approx 1$ which we find. However, as has been first pointed out

Quantity	Our Value	UTfit RUT	Full UT	UUT
γ	$(73.9^{+5.8}_{-6.5})^\circ$	$(65 \pm 18)^\circ$	$(57.6 \pm 5.5)^\circ$	$(51 \pm 10)^\circ$
$\bar{\rho}$	0.127 ± 0.046	0.18 ± 0.12	0.216 ± 0.036	0.259 ± 0.068
$\bar{\eta}$	0.422 ± 0.025	0.41 ± 0.05	0.342 ± 0.022	0.320 ± 0.042
R_b	0.44 ± 0.02	0.45 ± 0.07	0.40 ± 0.03	0.42 ± 0.05
R_t	0.97 ± 0.05	0.92 ± 0.11	0.86 ± 0.03	0.81 ± 0.06
β_{true}	$(25.8 \pm 1.3)^\circ$	$(26.1 \pm 3.0)^\circ$	23.8 ± 1.5	23.4 ± 1.3
α	$(80.3^{+6.6}_{-5.9})^\circ$	$(87 \pm 15)^\circ$	$(98.5 \pm 5.7)^\circ$	$(105 \pm 11)^\circ$
$(\sin 2\beta)_{\text{true}}$	0.782 ± 0.029	0.782 ± 0.065	0.735 ± 0.024	0.728 ± 0.031
ϕ_d^{NP}	$-(8.2 \pm 3.5)^\circ$	$-(8.9 \pm 6.0)^\circ$	$-(4.1 \pm 3.9)^\circ$	$-(3.3 \pm 3.6)^\circ$

Table 3.2: Parameters of the reference UT (RUT) determined through $|V_{ub}/V_{cb}|$ and the CP asymmetries of the $B_d \to \pi^+\pi^-$, $B_d \to \pi^\mp K^\pm$ system, yielding the value of γ in (3.25), compared with the results of [40]. We show also the results of the full UT fit and of the universal unitarity triangle obtained there.

in [89] and later also in [90, 91], the charm- and up-type penguin diagrams may be enhanced if the light quarks in the loop form on-shell intermediate states. These enhanced diagrams have been termed "charming penguins" and are generally thought to be non-factorizable (there is some discussion in the SCET and QCDF community about this point, see [92, 93]). An enhancement of these topologies would explain the large value of x, since it interferes constructively with the color suppressed, but destructively with the color allowed tree diagrams. In terms of branching ratios this results in large values of $B_d^0 \to \pi^0\pi^0$, while $B_d^0 \to \pi^+\pi^-$ is suppressed. Both of these shifts are in accordance with the data. Additionally, the parameter d receives also contributions from the charm penguins and is also enhanced. In this context it is interesting that the values from QCDF tend to be smaller than our values obtained here. It seems then that this kind of large non-factorizable effects can explain the pattern of $B \to \pi\pi$ data, including the large asymmetries, since internal on-shell states automatically generate large imaginary parts for the diagrams and thereby strong phases. However, one should keep in mind that we are pursuing an entirely phenomenological approach, which, while being able to *describe* the data does not offer an *explanation* in the sense that the relevant parameters could be calculated from first principles.

3.5 Alternative Approaches

The decays $B \to \pi\pi$ have been discussed using several theoretical frameworks, some of which are based formally on QCD and others, which are more phenomenological. Here, we would like to compare the results of the different approaches with ours.

3.5.1 Dynamical QCD-Based Approaches:

These include QCD factorization [20,21], Soft Collinear Effective Theory (SCET) [24,94] and PQCD [22,23]. In general, the idea that lies behind these attempts to calculate the hadronic matrix elements is to reduce the non-perturbative quantities to perturbative ones by adding some simplifying assumptions or looking at some dynamical limit. In order to show where the differences and similarities lie, we will very briefly sketch the idea behind these treatments, in particular the general idea of factorization. In the context of hadronic matrix elements, factorization can be naively understood as a "separation" of the decay end products. In particular, for the example of a B meson decaying into a heavy meson and a light one, such as $B \to D\pi$, one can decouple the π meson and is left with a form factor describing the $B \to D$ transition and a separate object for the pion, which is then simply given by the decay constant. Thereby, the matrix element has been simplified enormously. The reasoning behind the idea is that the problematic low energy gluons should have a wave length too long to resolve the light final state meson, which would then decouple. Unfortunately, this naive factorization suggested by Bjoerken is obviously unsatisfying in a very important respect, namely its scale dependence, since the scale dependent matrix element is now reduced to scale independent (since observable) quantities. Therefore, they can no longer cancel the scale dependences of the Wilson coefficients. Also, there are no possible contributions to generate strong phases, so that all CP asymmetries vanish. Both these problems where finally fully overcome in QCD factorization. Here, the matrix element is written as a convolution of non-perturbative objects, the light cone distribution amplitudes, and a perturbative scattering kernel:

$$\begin{aligned}\langle M_1 M_2|\mathcal{O}_i|\bar{B}\rangle = \sum_j F_j^{B\to M_1}(m_2^2) \int_0^1 du\, T_{ij}^I(u)\, \Phi_{M_2}(u) \;+\; (M_1 \leftrightarrow M_2) \\ + \int_0^1 d\xi du dv\, T_i^{II}(\xi,u,v)\, \Phi_B(\xi)\, \Phi_{M_1}(v)\, \Phi_{M_2}(u) \\ ,\end{aligned} \tag{3.42}$$

where $F_j^{B\to M_1}(m_2^2)$ is the form factor, $T_{ij}^{I,II}(u)$ are the perturbative scattering kernels and the $\Phi_i(u)$ are the light cone distribution amplitudes (LCDA) of the mesons. This formula, as it is given, is valid for a decay of a B meson into two light mesons, such as $B \to \pi\pi$. In the case of the heavy meson in the final state, only the first term remains. Additionally, the factorization formula is valid only up to leading order in Λ_{QCD}/m_b, which is formally a small number, but may well be enhanced by large coefficients. In this context, the term factorization acquires a somewhat different meaning, though the intuitive picture of a light meson decoupling remains: Factorization is now considered as a separation of energy scales, just as it is done in the OPE for weak decays. The higher energetic contributions of the matrix element are separated into the scattering kernel, while the true low energy scales are now residing in the LCDAs. On the whole, QCDF provides a theoretical foundation to calculate weak decays, but it as has the potential limitation of the unknown $\mathcal{O}(\Lambda_{QCD}/m_b)$ terms. Finally, we point out that very recently [95], the predictions for the tree level matrix elements have been completely

calculated to NNLO, while the corresponding prediction for the penguin operators are still missing.

Within QCDF, one can prove factorization for non-leptonic decays up to a certain order. An improvement became possible with the advent of the effective theory appropriate for these kind of decays, namely SCET. The general ideas and results are rather similar, in particular one arrives at the analogous factorization formula, but this is achieved in the language of an effective field theory. In this field theory, only soft and collinear gluons are considered, since those are the ones relevant for factorization. In particular, the SCET Lagrangian is constructed from QCD by taking the scaling behavior of the QCD fields and expanding them accordingly. Since the Lagrangian now contains directly the relevant fields, factorization can be proven to all orders.

Finally, the third competing dynamical approach to the non-perturbative dynamics of non-leptonic decays is PQCD. Again, the main goal is to achieve a separation of scales in the decay amplitude and the result is a factorization formula similar to the one obtained in QCD factorization. However, the $B \to \pi$ and $B \to K$ form factors are assumed to be perturbatively calculable. In order to justify this, one invokes Sudakov effects to regulate the soft gluon exchange. Again, there are uncalculable non-factorizable terms, since PQCD also makes use of the large m_b limit. A main difference between QCDF and PQCD is further that in the later case the naive factorization formula is not obtained in the limit $\alpha_s \to 0$ and $m_b \to \infty$.

Concerning now the phenomenology, the prediction of QCD factorization, for example [65] tend to produce branching ratios for $B_d^0 \to \pi^0\pi^0$ as well as CP asymmetries that are too small. Predictions for all branching ratios can be found in table 4.3, where we show also those for the $B \to \pi K$ branching ratios. Looking more explicitly at the corresponding predictions, we find that our hadronic parameters are related to the (r, ϕ) introduced in [65] by

$$d = \frac{r}{R_b}, \quad \theta = \phi - \pi \,, \tag{3.43}$$

where the default QCDF predictions are $r = 0.107 \pm 0.031$ and $\phi = (8.6 \pm 14.3)^\circ$. These lead, together with $R_b = 0.44 \pm 0.02$, to

$$d|_{\rm QCDF} = 0.24 \pm 0.07, \quad \theta|_{\rm QCDF} = -\,(171.4 \pm 14.3)^\circ \,. \tag{3.44}$$

On the other hand, CP asymmetries in the QCDF approach are generally small, since strong phases are either suppressed by α_s or $1/m_b$. For example, the best prediction of [65], labeled S4 for the direct asymmetry of $B_d^0 \to \pi^+\pi^-$ is

$$\mathcal{A}_{\rm CP}^{\rm dir}(B_d \to \pi^+\pi^-)|_{QCDF} = -0.1 \,, \tag{3.45}$$

while the central values of the scenarios given in [65] range from $\sim +0.1$ to -0.1. The large experimental value is quite hard to obtain. The additional NNLO correction to QCDF that have recently been calculated [95,96] bring the predictions for the branching ratios somewhat closer to the data [95], but still do not reach the experimental numbers. No further information on the CP asymmetries is obtained, since they are affected also by the NNLO contributions from the penguin topologies, which are not yet calculated.

The corresponding SCET analyses, such as ones in [87, 97] are deliberately more phenomenological, including for example the charming penguin contributions by hand

and fitting them to the data. These SCET approaches also find that color suppression is lifted and obtain x in the same ball park of our results. Of course, this leads to satisfactory predictions but does not offer an explanation from first principles as why the contributions should be enhanced in precisely the way they are.

Very recently [98, 99], the $B \to \pi\pi$ decays have been reanalyzed within PQCD approach. Here, it is tested whether the enhancement of color-suppressed tree over color-allowed tree diagrams as constrained by the $B \to \pi K$ and $B_d^0 \to \rho^0\rho^0$ data can accommodate, in particular, the large values of the $B_d^0 \to \pi^0\pi^0$. Also, NLO vertex corrections, quark loops and magnetic penguins are included in these analyses. It is found that the theoretical prediction remains too low. The same is true again for the prediction of $\mathcal{A}_{\rm CP}^{\rm dir}(B_d \to \pi^+\pi^-)$, which is now

$$\mathcal{A}_{\rm CP}^{\rm dir}(B_d \to \pi^+\pi^-)|_{PQCD} = 0.18^{+21}_{-13}\,. \tag{3.46}$$

It is therefore closer to the data than the prediction from QCDF, but still on the low side, and that the $B \to \pi\pi$-puzzle still persists. Interestingly, large CP violation of about 60% is possible in the $B_d^0 \to \pi^0\pi^0$ sector.

3.5.2 Phenomenological Approaches and Light Cone Sum Rules

There have been several more phenomenological approaches, relying not so much on pure theory, but also on data to fit some quantities. One of these is, for example pursued by the Italian "charming penguin" collaboration, which also fits the corresponding contributions [90, 100] and describes the branching ratios in question by enhancing them. In this sense, they find the same results as we do. In addition, the angle α and, equivalently, $\gamma = \pi - \beta - \alpha$ are fitted. Also, in accordance with our results, the GIM, i.e. up-type penguins are, in fact, even more strongly enhanced than the "charming" charm penguins. Note that the most recent of these analyses, namely [100], uses some input from factorization and adds non-factorizable contributions and is therefore not entirely model independent, but somewhat similar to the SCET analyses mentioned above.

Next, there are other purely phenomenological analyses as well [101–105], very similar to our own, which have confirmed our results, while they do differ in details concerning the assumption used. In particular, one sometimes uses SU(3) flavor symmetry for a more global analysis [101, 105], while [103] also uses some input from QCDF as does [105]. All these analyses find, however that the color suppressed tree amplitude is enhanced with respect to the factorization expectations. One can therefore conclude that there are indeed large non-factorizable effects, unless the data change in a dramatic manner. An attempt to study and quantify these effects can be found in [106].

Finally, there have been attempts to calculate the contributions from charming penguin [107] as well as the annihilation diagrams [108] from light cone sum rules (LCSRs). This approach is a variation of the standard QCD sum rules, only that one does not expand in some large energy scale in the problem, but one performs a twist expansion around a light like momentum vector. These sum rules can be used to calculate some hadronic matrix elements [109]. Interestingly, these estimates show no sign of any anomalous enhancement of either of the topologies. Therefore, there is either a missing contribution not accounted for by the LCSRs or there is another explanation for the

pattern in the $B \to \pi\pi$ data. Another possibility in this respect that has been under investigation is the effect of final state interaction (FIS) [110], which can be included, but are not sufficiently large to account for the large $B_d^0 \to \pi^0\pi^0$ branching ratio, if the constraint from $B \to \pi K$ is considered [99, 110]. We can therefore conclude that an entirely successful dynamical description of these decays is still missing.

Let us also mention that there have also been several recent studies [111–114] of potential new physics in the $B \to \pi\pi$ decays, particular also in supersymmetric models. It is to be expected that new physics that appears at a competitive level in tree dominated process will also show some signals in further decay modes.

3.6 Conclusions of $B \to \pi\pi$

Let us summarize the main results of our $B \to \pi\pi$ analysis, before we move on to the $B \to \pi K$ decays.

- Using isospin symmetry, the decay amplitudes of the $B \to \pi\pi$ decays can be parameterized in terms of a few hadronic parameters. These are most likely SM amplitudes, since $B \to \pi\pi$ are tree dominated decays. This allows the extraction of all hadronic parameters appearing in a theoretically clean manner, if the CKM angle γ is given as further input.

- Using the SU(3) flavor symmetry of strong interactions (and taking into account factorizable SU(3) breaking effects) some input from $B \to \pi K$ also makes a determination of γ possible. We find a value that is somewhat higher than the one obtained from standard CKM fits. Assuming that this is indeed the true value of γ, this could be due to NP in B_d^0–$\bar{B}_d^0$ mixing so that $\phi_d \neq 2\beta_{SM}$. Potential new physics in ϕ_d has also been found from a pure UT analysis [88].

- The hadronic parameters obtained differ significantly from factorization predictions. In particular, the large values of some CP asymmetries imply large strong phases and the high value of the $B_d^0 \to \pi^0\pi^0$ branching ratio implies enhanced color-suppressed tree and u-penguin topologies.

- With all the information obtained in the last steps it is possible to predict the CP asymmetries of $B_d^0 \to \pi^0\pi^0$, which may both be large. On the other hand, measuring one of these quantities allows for a clean determination of γ. Unfortunately, the analytic behavior of the corresponding expression is such that a rather precise experimental input is required [115].

- We have collected and briefly compared several alternative dynamical and phenomenological studies of $B \to \pi\pi$, where the success of the theoretical description can often be seen to be correlated with the amount of phenomenological input used. There is, as yet no real dynamical mechanism that reproduces the $B \to \pi\pi$ data from first principles.

Chapter 4

The $B \to \pi K$ Decays

4.1 Basics

After our discussion of the $B \to \pi\pi$ decays and some aspects of the $B \to \pi K$ system in the last chapter, we will continue with a complete discussion of $B \to \pi K$. The relevant decays in this context are

$$B^+ \to \pi^+ K^0\,, \qquad B^+ \to \pi^0 K^+\,,$$
$$B_d^0 \to \pi^+ K^-\,, \qquad B_d^0 \to \pi^0 K^0\,.$$

There are now more observable quantities than in the $B \to \pi\pi$ system, for which the experimental status is given in Table 4.1. Theoretically, these decays are interesting because they are expected to be more sensitive to new physics contributions than $B \to \pi\pi$. On the one hand this is due to the fact that the tree diagrams are CKM suppressed, so that the leading diagram is a QCD penguin topology. We show these leading diagrams in Fig. 4.1. Additionally, in this class of decays, the electroweak penguin diagrams not shown there are quite significant, which may well be affected by NP [116–120]. On the other hand, these decays have also received a lot of interest [77, 121] in the context of a determination of the UT angle γ.

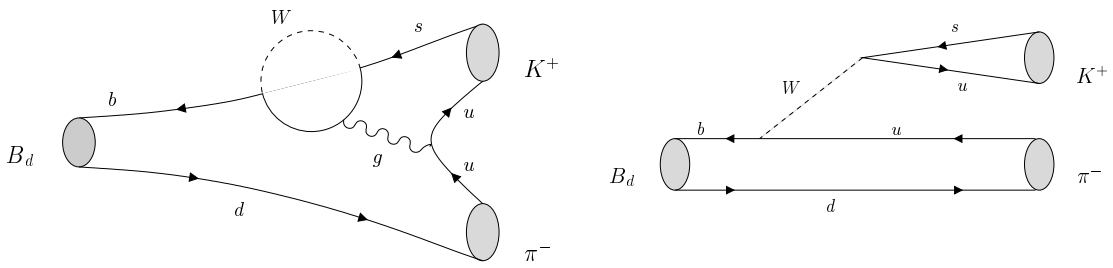

Figure 4.1: Feynman diagrams contributing to $B_d \to \pi^+ K^-$

Quantity	BaBar	Belle	Average
$\mathrm{BR}(B^\pm \to \pi^\pm K^0)/10^{-6}$	$26.0 \pm 1.3 \pm 1.0$ [122]	$22.0 \pm 1.9 \pm 1.1$ [67]	24.1 ± 1.3
$\mathrm{BR}(B^\pm \to \pi^0 K^\pm)/10^{-6}$	$12.0 \pm 0.7 \pm 0.6$ [66]	$12.0 \pm 1.3^{+1.3}_{-0.9}$ [67]	12.1 ± 0.8
$\mathrm{BR}(B_d \to \pi^+ K^-)/10^{-6}$	$19.2 \pm 0.6 \pm 0.6$ [68]	$18.5 \pm 1.0 \pm 0.7$ [67]	18.9 ± 0.7
$\mathrm{BR}(B_d \to \pi^0 K^0)/10^{-6}$	$11.4 \pm 0.9 \pm 0.6$ [123]	$11.7 \pm 2.3^{+1.2}_{-1.3}$ [67]	11.5 ± 1.0
$\mathcal{A}_{\mathrm{CP}}^{\mathrm{dir}}(B_d \to \pi^\mp K^\pm)$	$0.133 \pm 0.030 \pm 0.009$ [12]	$0.113 \pm 0.022 \pm 0.008$ [13]	0.115 ± 0.018
$\mathcal{A}_{\mathrm{CP}}^{\mathrm{dir}}(B_d \to \pi^0 K^0)$	$0.06 \pm 0.18 \pm 0.03$ [123]	$-0.11 \pm 0.18 \pm 0.08$ [48]	-0.02 ± 0.13
$\mathcal{A}_{\mathrm{CP}}^{\mathrm{mix}}(B_d \to \pi^0 K^0)$	$0.35^{+0.30}_{-0.33} \pm 0.04$ [123]	$0.22 \pm 0.47 \pm 0.08$ [48]	0.31 ± 0.26
$\mathcal{A}_{\mathrm{CP}}^{\mathrm{dir}}(B^\pm \to \pi^\pm K)$	$0.09 \pm 0.05 \pm 0.01$ [122]	$-0.05 \pm 0.05 \pm 0.01$ [124]	0.02 ± 0.04
$\mathcal{A}_{\mathrm{CP}}^{\mathrm{dir}}(B^\pm \to \pi^0 K^\pm)$	$-0.06 \pm 0.06 \pm 0.01$ [66]	$-0.04 \pm 0.04 \pm 0.02$ [73]	-0.04 ± 0.04

Table 4.1: The current status of the $B \to \pi K$ input data.

Due to the more complicated amplitude structure and because there are more topologies, there will also be more hadronic parameters in this decay system. It is therefore very important to control hadronic uncertainties if a potential signal of new physics is expected. These decays have been studied in QCDF [65] as well as in SCET [87] as well as PQCD [98], while a third possible route is to use flavor symmetry and to determine all appearing parameters from the $B \to \pi\pi$ parameters. This is what we will do in the following. Thereby, we will be using an approach which is in some ways rather close to [125, 126].

Let us begin by writing down again the amplitude decomposition of the $B \to \pi K$ decays. Using isospin symmetry, we find[1]

$$A(B^+ \to \pi^+ K^0) = -P' \left[1 + \rho_{\mathrm{c}} e^{i\theta_{\mathrm{c}}} e^{i\gamma}\right] \tag{4.1}$$

$$\sqrt{2} A(B^+ \to \pi^0 K^+) = P' \left[1 + \rho_{\mathrm{c}} e^{i\theta_{\mathrm{c}}} e^{i\gamma} - \left(e^{i\gamma} - q e^{i\phi} e^{i\omega}\right) r_{\mathrm{c}} e^{i\delta_{\mathrm{c}}}\right] \tag{4.2}$$

$$A(B_d^0 \to \pi^- K^+) = P' \left[1 - r e^{i\delta} e^{i\gamma}\right] \tag{4.3}$$

$$\sqrt{2} A(B_d^0 \to \pi^0 K^0) = -P' \left[1 + \rho_{\mathrm{n}} e^{i\theta_{\mathrm{n}}} e^{i\gamma} - q e^{i\phi} e^{i\omega} r_{\mathrm{c}} e^{i\delta_{\mathrm{c}}}\right]. \tag{4.4}$$

Here the CP-conserving strong amplitude

$$P' \equiv \left(1 - \frac{\lambda^2}{2}\right) A\lambda^2 (\mathcal{P}'_t - \mathcal{P}'_c) \tag{4.5}$$

is the $B \to \pi K$ counterpart of (3.4), describing the difference of the QCD penguins with internal top and charm quark exchanges,

$$\rho_{\mathrm{c}} e^{i\theta_{\mathrm{c}}} \equiv \left(\frac{\lambda^2 R_b}{1 - \lambda^2}\right) \left[\frac{\mathcal{P}'_t - \tilde{\mathcal{P}}'_u - \mathcal{A}'}{\mathcal{P}'_t - \mathcal{P}'_c}\right], \tag{4.6}$$

[1] We have added primes to the amplitudes to distinguish the $B \to \pi\pi$ from the $B \to \pi K$ topologies

where $\tilde{\mathcal{P}}'_u$ is the strong amplitude of QCD penguins with internal up quark exchanges contributing to the charged $B \to \pi K$ decays and $\mathcal{A}'$ denotes an annihilation amplitude,

$$r_{\rm c} e^{i\delta_{\rm c}} \equiv \left(\frac{\lambda^2 R_b}{1-\lambda^2}\right)\left[\frac{\mathcal{T}'+\mathcal{C}'}{\mathcal{P}'_t-\mathcal{P}'_c}\right], \tag{4.7}$$

where $\mathcal{T}'$ and $\mathcal{C}'$ are the color-allowed and color-suppressed tree-diagram-like topologies corresponding to their $B \to \pi\pi$ counterparts $\mathcal{T}$ and $\mathcal{C}$ in (3.5) and (3.6), respectively,

$$re^{i\delta} \equiv \left(\frac{\lambda^2 R_b}{1-\lambda^2}\right)\left[\frac{\mathcal{T}'-(\mathcal{P}'_t-\mathcal{P}'_u)}{\mathcal{P}'_t-\mathcal{P}'_c}\right], \tag{4.8}$$

where $\mathcal{P}'_u$ is the strong amplitude of QCD penguins with internal up quark exchanges contributing to the neutral $B \to \pi K$ decays,

$$\rho_{\rm n} e^{i\theta_{\rm n}} \equiv \left(\frac{\lambda^2 R_b}{1-\lambda^2}\right)\left[\frac{\mathcal{C}'+(\mathcal{P}'_t-\mathcal{P}'_u)}{\mathcal{P}'_t-\mathcal{P}'_c}\right], \tag{4.9}$$

and the electroweak penguin parameter $qe^{i\phi}e^{i\omega}$ is given by

$$qe^{i\phi}e^{i\omega} = \left|\frac{P'_{\rm EW}}{T'+C'}\right| e^{i(\delta'_{\rm EW}-\delta_{T'+C'})}. \tag{4.10}$$

The weak phase ϕ of the electroweak penguins vanishes in the SM, but we have included it here, anticipating that we will want to discuss the implications of new physics. In (4.1)–(4.4), the contributions from color-suppressed electroweak penguins have been neglected, since they only have a minor impact on our analysis. A more detailed discussed has been given in [27]. We will see that the description of those observables that have only color-suppressed electroweak penguin is rather satisfactory, which gives us more confidence in this assumption. Finally, let us point out the sum rule analogous to (3.7) [127]:

$$\begin{aligned} A(B^+ \to \pi^+ K^0) + \sqrt{2}A(B^+ \to \pi^0 K^+) &= A(B_d^0 \to \pi^- K^+) + \sqrt{2}A(B_d^0 \to \pi^0 K^0) \\ &= -\left[e^{i\gamma} - qe^{i\phi}e^{i\omega}\right]|T'+C'|e^{i\delta_{T'+C'}}. \end{aligned} \tag{4.11}$$

4.2 Determination of the Hadronic Parameters

Let us begin with $r_{\rm c}e^{i\delta_{\rm c}}$, $re^{i\delta}$ and $\rho_{\rm n}e^{i\theta_{\rm n}}$ appearing in (4.1)–(4.4). These are not all independent and obey the relation:

$$r_{\rm c}e^{i\delta_{\rm c}} = re^{i\delta} + \rho_{\rm n}e^{i\theta_{\rm n}} \tag{4.12}$$

$$\rho_{\rm n}e^{i\theta_{\rm n}} = re^{i\delta}x'e^{i\Delta'}, \tag{4.13}$$

with

$$x'e^{i\Delta'} \equiv \frac{\mathcal{C}'+\mathcal{P}'_{tu}}{\mathcal{T}'-\mathcal{P}'_{tu}}, \tag{4.14}$$

which can be derived just from the definition of the parameters. The parameter $x'e^{i\Delta'}$ is very similar to the corresponding parameter $xe^{i\Delta}$ up to the contributions of penguin

annihilation and exchange topologies. Neglecting these and using SU(3) flavor symmetry of strong interactions (we will be concerned with flavor breaking effects later) we find

$$x' e^{i\Delta'} = x e^{i\Delta}. \tag{4.15}$$

Additionally, in the limit of SU(3) symmetry, on can also find

$$r e^{i\delta} = \frac{\epsilon}{d} e^{i(\pi-\theta)} \tag{4.16}$$

with ϵ defined as.

$$\epsilon \equiv \frac{\lambda^2}{1-\lambda^2} = 0.053. \tag{4.17}$$

Therefore, these six parameters can be determined using input from the $B \to \pi\pi$ system. Following these lines, the numerical values we find are:

$$r = 0.11^{+0.07}_{-0.05}, \quad \delta = +(42^{+23}_{-19})^\circ \tag{4.18}$$

$$\rho_{\rm n} = 0.13^{+0.07}_{-0.05}, \quad \theta_{\rm n} = -(29^{+21}_{-26})^\circ \tag{4.19}$$

$$r_{\rm c} = 0.20^{+0.09}_{-0.07}, \quad \delta_{\rm c} = +(2^{+23}_{-18})^\circ. \tag{4.20}$$

The parameter r_c can also be determined alternatively from [128]

$$r_{\rm c} = \sqrt{2}\left|\frac{V_{us}}{V_{ud}}\right| \frac{f_K}{f_\pi} \sqrt{\frac{\mathrm{BR}(B^\pm \to \pi^\pm \pi^0)}{\mathrm{BR}(B^\pm \to \pi^\pm K^0)}} = 0.196 \pm 0.016, \tag{4.21}$$

which relies on the $SU(3)$ flavour symmetry and the neglect of the $\rho_{\rm c}$ term in (4.1). The agreement between the two numbers is a first reassuring test of our assumptions. We will discuss further tests in Sect. 4.5. Concerning the numerical values of the parameters obtained above, it is interesting to see that r_c and δ_c are rather close to the values predicted from QCD factorization [65], while (4.18) and (4.19) are significantly different from the corresponding numbers. Note, finally, that $r_{\rm c}$ can also be found more easily from

$$r_{\rm c} = \frac{\epsilon}{d}\sqrt{[1 - 2d\cos\theta\cos\gamma + d^2]\, R^{\pi\pi}_{+-}}, \tag{4.22}$$

which shows also that both solutions for (x, Δ) lead to the same results. This is not true for the other hadronic parameters determined above.

The parameters $\rho_c e^{i\theta_c}$ can not be found from $B \to \pi\pi$ data and must be estimated [77, 121, 129]. In particular, the CP asymmetry of $B^\pm \to \pi^\pm K$ can be parameterized as

$$\mathcal{A}^{\rm dir}_{\rm CP}(B^\pm \to \pi^\pm K) = -\left[\frac{2\rho_{\rm c}\sin\theta_{\rm c}\sin\gamma}{1 + 2\rho_{\rm c}\cos\theta_{\rm c}\cos\gamma + \rho_{\rm c}^2}\right]. \tag{4.23}$$

The small experimental number of this quantity suggests that either ρ_c or θ_c is small. Also, the upcoming signals of $B^\pm \to K^\pm K$ point towards [130, 131] a small but non-vanishing value of ρ_c. Therefore, we will begin by neglecting this parameter and explore the implications of a non-vanishing ρ_c at the appropriate place in the numerical discussion.

Finally, we would like to determine the electroweak penguin parameter $qe^{i(\omega+\phi)}$ in the SM, which can, again, not be found from the $B \to \pi\pi$ decays. Fortunately, it has been shown [132, 133] that one can calculate it using Fierz identities and SU(3) symmetry:

$$qe^{i(\omega+\phi)} = -\frac{3}{2}\frac{1}{\lambda|V_{ub}/V_{cb}|}\left[\frac{C_9(\mu_b)+C_{10}(\mu_b)\tilde{\xi}}{C_1'(\mu_b)+C_2'(\mu_b)\tilde{\xi}}\right], \tag{4.24}$$

where $\tilde{\xi}$ corresponds to SU(3) breaking effects and the $C_i(\mu_b)$ are the corresponding Wilson coefficients. In the SM, we have therefore $q = 0.69 \cdot 0.086/|V_{ub}/V_{cb}| = 0.58$. The precise value of m_t and the strong coupling have only minor impact and do not introduce significant uncertainties. An important feature of this expression is that the strong phase difference ω between electroweak penguin and tree topologies vanishes in the SU(3) limit.

4.3 Predictions in the Standard Model and Beyond

Having all hadronic parameters at hand, we can make prediction for any observable quantity of interest. In analogy to the $B \to \pi\pi$ system, we introduce several ratios of branching ratios

$$R \equiv \left[\frac{\mathrm{BR}(B_d^0 \to \pi^- K^+) + \mathrm{BR}(\bar{B}_d^0 \to \pi^+ K^-)}{\mathrm{BR}(B^+ \to \pi^+ K^0) + \mathrm{BR}(B^- \to \pi^- \bar{K}^0)}\right]\frac{\tau_{B^+}}{\tau_{B_d^0}} \stackrel{\text{exp}}{=} 0.86 \pm 0.06; \tag{4.25}$$

$$R_{\mathrm{c}} \equiv 2\left[\frac{\mathrm{BR}(B^+ \to \pi^0 K^+) + \mathrm{BR}(B^- \to \pi^0 K^-)}{\mathrm{BR}(B^+ \to \pi^+ K^0) + \mathrm{BR}(B^- \to \pi^- \bar{K}^0)}\right] \stackrel{\text{exp}}{=} 1.01 \pm 0.09 \tag{4.26}$$

$$R_{\mathrm{n}} \equiv \frac{1}{2}\left[\frac{\mathrm{BR}(B_d^0 \to \pi^- K^+) + \mathrm{BR}(\bar{B}_d^0 \to \pi^+ K^-)}{\mathrm{BR}(B_d^0 \to \pi^0 K^0) + \mathrm{BR}(\bar{B}_d^0 \to \pi^0 \bar{K}^0)}\right] \stackrel{\text{exp}}{=} 0.83 \pm 0.08. \tag{4.27}$$

The numerical values correspond to the HFAG averages as given also in Table 4.1.

4.3.1 The Decays $B_d \to \pi^\mp K^\pm$ and $B^\pm \to \pi^\pm K$

We begin our analysis with those decays that are only affected by electroweak penguins in a color-suppressed way. We have then, apart from the direct CP asymmetry of $B_d^0 \to \pi^\pm K^\mp$, two observables, namely $\mathcal{A}_{\mathrm{CP}}^{\mathrm{dir}}(B^\pm \to \pi^\pm K)$ and R. Assuming that ρ_c vanishes, $\mathcal{A}_{\mathrm{CP}}^{\mathrm{dir}}(B^\pm \to \pi^\pm K) = 0$ and

$$R = 1 - 2r\cos\delta\cos\gamma + r^2. \tag{4.28}$$

This expression has also received quite a lot of interest, since it allows for a bound on the CKM angle γ, if the measured value of R is significantly smaller than 1 [134]. From this,

$$R|_{\mathrm{SM}} = 0.963^{+0.019}_{-0.022} \tag{4.29}$$

can be found from the $B \to \pi\pi$ data, subject to the assumptions listed above. This number is about 1.6σ larger than the experimental value given above. However, it turns out that this observable is rather sensitive to a non-vanishing parameter ρ_c.

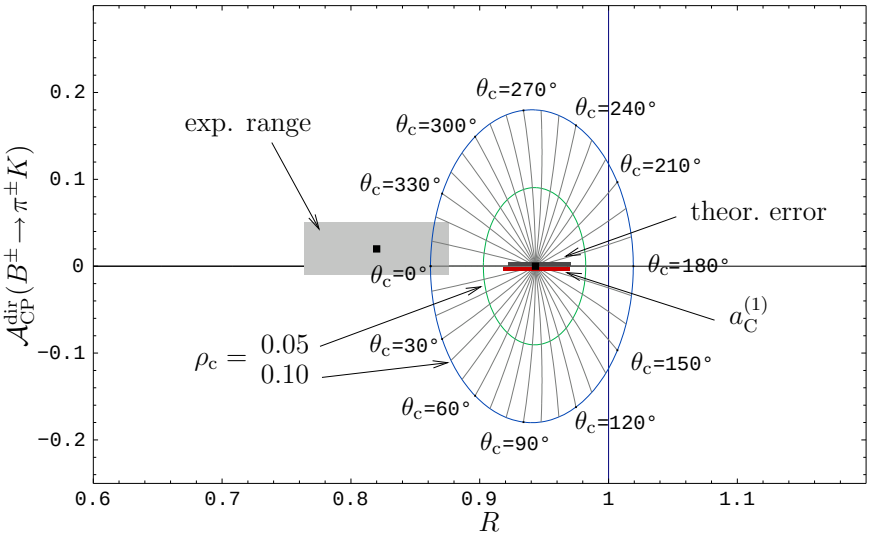

Figure 4.2: The situation in the R–$\mathcal{A}_{\rm CP}^{\rm dir}(B^\pm \to \pi^\pm K)$ plane. We show contours for $\rho_{\rm c} = 0.05$ and $\rho_{\rm c} = 0.10$, with $\theta_{\rm c} \in [0°, 360°]$. The experimental ranges for R and $\mathcal{A}_{\rm CP}^{\rm dir}(B^\pm \to \pi^\pm K)$ and our theoretical prediction are indicated in grey. The second error bar beneath the theoretical prediction (almost identical in size to the first one) indicates the variation of R if color-suppressed EW penguins are taken into account.

To illustrate this situation, we show the predictions for R and $\mathcal{A}_{\rm CP}^{\rm dir}(B^\pm \to \pi^\pm K)$ in the corresponding observable plane for different values of ρ_c in Fig 4.2. Here, we have also added the effect of including color-suppressed electroweak penguins with a suppression factor of $a_C^{(1)}$ as in [27,75]. We observe that values of $\rho_c \sim 0.05$ and $\theta_c \sim 0$ would bring the prediction very close to the experimental values, while the effect of the color-suppressed electroweak penguins is not very significant. As we will see, also the inclusion of large SU(3) breaking effects would not change this situation significantly, so that it would not at all be surprising to see the experimental number increase with future data. In this respect, one should note that radiative corrections to the $B_d^0 \to \pi^- K^+$ branching ratio, which are expected to increase its value, have not yet been included.

Also, we would like to summarize by stating that the decays without significant electroweak penguin contribution seem to be described reasonably well within the SM.

4.3.2 The Decays $B^\pm \to \pi^0 K^\pm$ and $B_d \to \pi^0 K$

Now we turn to those decays that actually have a significant contribution from electroweak penguin topologies. The most important observables in this context are the two observables $R_{\rm n}$ and $R_{\rm c}$ introduced above. Their theoretical expression read

$$\begin{aligned} R_{\rm c} &= 1 - 2r_{\rm c}\cos\delta_{\rm c}\cos\gamma + r_{\rm c}^2 \\ &\quad + qr_{\rm c}\left[2\left\{\cos(\delta_{\rm c}+\omega)\cos\phi - r_{\rm c}\cos\omega\cos(\gamma-\phi)\right\} + qr_{\rm c}\right], \end{aligned} \tag{4.30}$$

whereas

$$R_{\rm n} = \frac{1}{b}\left[1 - 2r\cos\delta\cos\gamma + r^2\right], \tag{4.31}$$

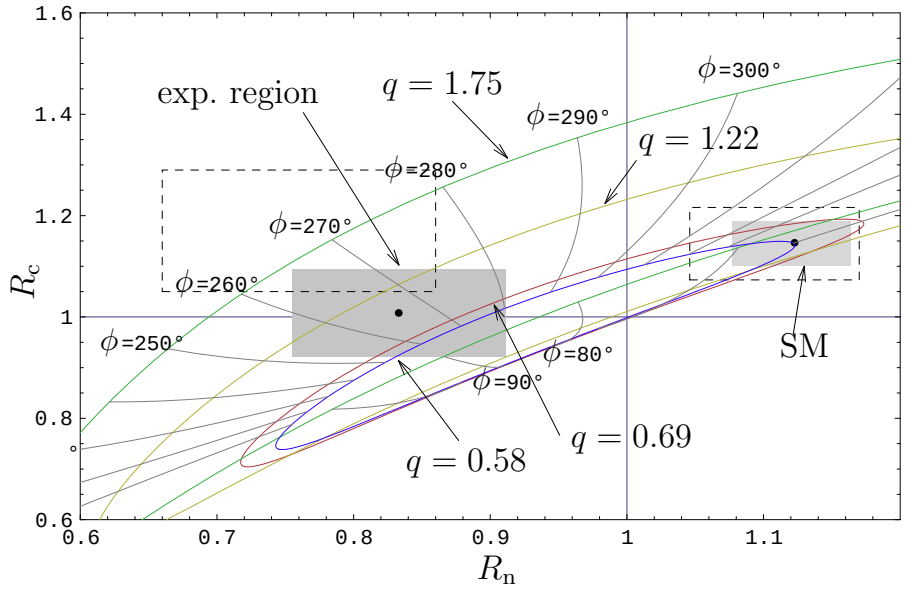

Figure 4.3: The current situation in the R_n–R_c plane: the shaded areas indicate the experimental and SM 1σ ranges, the lines show the theory predictions for the central values of the hadronic parameters and various values of q with $\phi \in [0°, 360°]$.

with

$$b = 1 - 2qr_c \cos(\delta_c + \omega)\cos\phi + q^2 r_c^2 \\ +2\rho_n \left[\cos\theta_n \cos\gamma - qr_c \cos(\theta_n - \delta_c - \omega)\cos(\gamma - \phi)\right] + \rho_n^2. \tag{4.32}$$

The quantity b can also be defined through observables as

$$b \equiv \frac{R}{R_n} = 2\left[\frac{\mathrm{BR}(B_d^0 \to \pi^0 K^0) + \mathrm{BR}(\bar{B}_d^0 \to \pi^0 \bar{K}^0)}{\mathrm{BR}(B^+ \to \pi^+ K^0) + \mathrm{BR}(B^- \to \pi^- \bar{K}^0)}\right]\frac{\tau_{B^+}}{\tau_{B_d^0}} \tag{4.33}$$

With these expressions, the hadronic parameters obtained from $B \to \pi\pi$ earlier and the SM value of q, one can make SM predictions for both:

$$R_c|_{\mathrm{SM}} = 1.15 \pm 0.05, \quad R_n|_{\mathrm{SM}} = 1.12 \pm 0.05. \tag{4.34}$$

While the prediction for R_c is reasonable good, it is obvious that the prediction for R_n is much too high. This pattern of R_n^{exp} being significantly smaller than 1 has been present since the first CLEO data and has been pointed out as a potential signal of physics since the first subsequent analysis [120]. This result follows also from the "Lipkin Sum Rule" [135]:

Since then, the data have become more precise and we are now interested in a more quantitative statement. To this end, we show the predictions for R_n and R_c in the corresponding observable plane for different values of q and its weak phase ϕ. We notice that the experimental region can be reached without an actual enhancement of q, but a large negative weak phase is required. We find that the central values of the data are obtained with

$$q = 0.99\,^{+0.66}_{-0.70}, \quad \phi = -(94\,^{+16}_{-17})°. \tag{4.35}$$

In addition to the observables provided by the branching ratios, there are several CP asymmetries that are affected by electroweak penguins. In particular, the CP asymmetry of $B^+ \to \pi^0 K^+$ is already rather precisely measured. The theoretical expression is

$$\mathcal{A}_{\rm CP}^{\rm dir}(B^\pm \to \pi^0 K^\pm) = \frac{2}{R_{\rm c}} \left[r_{\rm c} \sin\delta_{\rm c} \sin\gamma - q r_{\rm c} \left\{ \sin(\delta_{\rm c}+\omega) \sin\phi + r_{\rm c} \sin\omega \sin(\gamma-\phi) \right\} \right], \tag{4.36}$$

where the expression for $R_{\rm c}$ is given in (4.30) and we have set $\rho_c = 0$. The influence of ρ_c on this asymmetry is also significantly smaller than on $\mathcal{A}_{\rm CP}^{\rm dir}(B^\pm \to \pi^\pm K)$. Calculating this asymmetry from (4.36) in the SM and our new physics model, we find

$$\mathcal{A}_{\rm CP}^{\rm dir}(B^\pm \to \pi^0 K^\pm)|_{\rm SM} = 0.04\,^{+0.09}_{-0.07}, \quad \mathcal{A}_{\rm CP}^{\rm dir}(B^\pm \to \pi^0 K^\pm)|_{\rm NP} = 0.09\,^{+0.20}_{-0.16}. \tag{4.37}$$

Due to rather large uncertainties, one can not make any statements concerning any NP model, but it is interesting to note that both predictions are positive, while the experimental number is negative. We will come back to this CP asymmetry and its explicit sensitivity to electroweak penguins in Sect. 5.4.

Finally, the decay $B_d \to \pi^0 K_{\rm S}$ provides a mixing induced and a direct CP asymmetry, that are also affected by electroweak penguins. Their theoretical expressions are

$$\begin{aligned} \mathcal{A}_{\rm CP}^{\rm dir}(B_d \to \pi^0 K_{\rm S}) = \frac{2}{b} \Big[& q r_{\rm c} \sin(\delta_{\rm c}+\omega) \sin\phi \\ & - \rho_{\rm n} \left\{ \sin\theta_{\rm n} \sin\gamma - q r_{\rm c} \sin(\theta_{\rm n} - \delta_{\rm c} - \omega) \sin(\gamma-\phi) \right\} \Big], \end{aligned} \tag{4.38}$$

$$\begin{aligned} \mathcal{A}_{\rm CP}^{\rm mix}(B_d \to \pi^0 K_{\rm S}) = -\frac{1}{b} \Big[& \sin\phi_d - 2 q r_{\rm c} \cos(\delta_{\rm c}+\omega) \sin(\phi_d+\phi) + q^2 r_{\rm c}^2 \sin(\phi_d+2\phi) \\ & + 2\rho_{\rm n} \left\{ \cos\theta_{\rm n} \sin(\phi_d+\gamma) - q r_{\rm c} \cos(\theta_{\rm n} - \delta_{\rm c} - \omega) \sin(\phi_d+\gamma+\phi) \right\} + \rho_{\rm n}^2 \sin(\phi_d+2\gamma) \Big]. \end{aligned} \tag{4.39}$$

The corresponding SM predictions are

$$\mathcal{A}_{\rm CP}^{\rm dir}(B_d \to \pi^0 K_{\rm S})|_{\rm SM} = 0.06^{+0.09}_{-0.10}, \qquad \mathcal{A}_{\rm CP}^{\rm mix}(B_d \to \pi^0 K_{\rm S})|_{\rm SM} = -(0.82^{+0.03}_{-0.04}), \tag{4.40}$$

while in our NP scenario we find

$$\mathcal{A}_{\rm CP}^{\rm dir}(B_d \to \pi^0 K_{\rm S}) = 0.01\,^{+0.14}_{-0.18}, \quad \mathcal{A}_{\rm CP}^{\rm mix}(B_d \to \pi^0 K_{\rm S}) = -(0.96\,^{+0.04}_{-0.08}). \tag{4.41}$$

Again no stringent test of our scenario is provided as of yet, due to the large uncertainties. In the context of the mixing induced asymmetry, it is also interesting to consider

$$\Delta S \equiv (\sin 2\beta)_{\pi^0 K_{\rm S}} - (\sin 2\beta)_{\psi K_{\rm S}} \stackrel{\rm exp}{=} -0.38 \pm 0.26\,, \tag{4.42}$$

i.e. the difference of the effective phase β_{eff} measured in this decay and the mixing phase β measured from $B_d^0 \to J/\Psi K_S$. We will come back to both quantities and their sensitivity to NP in Sect. 5.4 along with the corresponding predictions for $B^\pm \to \pi^0 K^\pm$.

4.4 Elimination of the Second Solution for (x, Δ)

From the $B \to \pi\pi$ system we obtained two possible solutions for (x, Δ) and have continued our calculation with the pair (3.27). The second solution is

$$x = 0.85^{+0.10}_{-0.09}\,, \quad \Delta = (37^{+21}_{-29})^\circ\,, \tag{4.43}$$

which in turn lead to

$$q = 0.99^{+0.66}_{-0.69}\,, \quad \phi = (-106^{+20}_{-30})^\circ\,, \tag{4.44}$$

if ω is assumed to vanish. The resulting prediction for $\mathcal{A}_{\rm CP}^{\rm dir}(B^\pm \to \pi^0 K^\pm)$,

$$\mathcal{A}_{\rm CP}^{\rm dir}(B^\pm \to \pi^0 K^\pm) = 0.55^{+0.13}_{-0.20}\,, \tag{4.45}$$

is basically ruled out by the experimental number. If a non-vanishing strong phase ω is included, the analysis favors rather high values of $q \sim 1.6$. We will see in Chapter 5 that these kind of large $q-$values are excluded by constraints from semileptonic rare decays. In any case, we find it justified to not consider this second solution any further.

4.5 Consistency Checks and Analysis of SU(3) Breaking Effects

In the analysis presented above, several assumptions have been made, which will be the subject of this section. Let us recapitulate that we have assumed:

- The neglect of penguin annihilation and exchange topologies. As we will discuss below, this assumption can be tested at LHCb.
- The SU(3) limit of QCD. We will discuss the impact of SU(3) breaking below by assuming large non-factorizable SU(3) breaking terms.

Concerning the size of penguin annihilation and exchange topologies, it is interesting [27] to study the decay $B_d^0 \to K^+K^-$, which has only contributions from these topologies, i.e. is parameterized as

$$A(B_d^0 \to K^+K^-) = -\lambda^3 A R_b \left[\mathcal{E} - (\mathcal{PA})_{tu}\right]\left[e^{i\gamma} + \varrho_{\mathcal{PA}} e^{i\vartheta_{\mathcal{PA}}}\right], \tag{4.46}$$

with

$$\varrho_{\mathcal{PA}} e^{i\vartheta_{\mathcal{PA}}} \equiv \frac{1}{R_b}\left[\frac{(\mathcal{PA})_{tc}}{\mathcal{E} - (\mathcal{PA})_{tu}}\right], \tag{4.47}$$

where $(\mathcal{PA})_{tu}$ and $(\mathcal{PA})_{tc}$ are the penguin annihilation amplitudes. The present experimental number is given by [49]

$$\mathrm{BR}(B_d \to K^+K^-) = 0.05^{+0.10}_{-0.09}, \tag{4.48}$$

so that the size of the $(\mathcal{PA})_i$ can be quantified using flavor symmetry:

$$\sqrt{\frac{1}{2}\left[\frac{\mathrm{BR}(B_d \to K^+K^-)}{\mathrm{BR}(B^\pm \to \pi^\pm\pi^0)}\right]\frac{\tau_{B^+}}{\tau_{B_d^0}}} \approx \left|\frac{\mathcal{E} - (\mathcal{PA})_{tu}}{\mathcal{T} + \mathcal{C}}\right| \sqrt{1 + 2\varrho_{\mathcal{PA}}\cos\vartheta_{\mathcal{PA}}\cos\gamma + \varrho_{\mathcal{PA}}^2} \approx 0.07,. \tag{4.49}$$

Since the decay $B_d^0 \to K^+K^-$ can be measured at LHCb, this bound will be further improved. Even at the moment, however, the experimental value does not show any signs of unnaturally enhanced topologies of this type. Similarly, one can use the branching ratios of $B_s \to \pi^+\pi^-$ decay together with $B_d \to K^+K^-$, as well as the corresponding CP asymmetries [27, 86, 136] to constrain these parameters with the experimental data from LHC.

Let us next turn to the impact of SU(3) breaking effects. First, we note that flavor symmetry was assumed only in Eqs. (4.15) and (4.16). In principle both relations are afflicted with flavor breaking factors, but the factorizable contributions that can be quantified appear only (4.15). The corresponding pieces drop out of (4.16) and are added in (4.15) through a ratio of form factors

$$x' e^{i\Delta'} = \left[\frac{f_\pi F_{BK}(M_\pi^2; 0^+)}{f_K F_{B\pi}(M_K^2; 0^+)}\right] x e^{i\Delta}. \tag{4.50}$$

The corresponding form factors can be calculated using Light Cone Sum Rules [137] to be

$$\rho_{SU(3)} = \left[\frac{f_\pi F_{BK}(M_\pi^2; 0^+)}{f_K F_{B\pi}(M_K^2; 0^+)}\right] = 1.05 \pm 0.18, \tag{4.51}$$

so that SU(3) breaking seems to be a rather small effect. These reliably calculable flavor-breaking effects have been included in the numerical values given above, as also done in [28, 75, 138]. Unfortunately, any further estimate of SU(3) will have to rely on estimates, but to check the impact of potentially larger uncertainties, we follow [28] in that we allow for a doubly inflated error of $\rho_{SU(3)}$, i.e. $\rho_{SU(3)} = 1.05 \pm 0.36$ as well as an additional strong phase $-15^\circ < \theta_{SU(3)} < 15^\circ$.

The analogous contributions to (4.16) can also be taken into account as

$$d' = \xi d, \quad \theta' = \theta + \Delta\theta. \tag{4.52}$$

In the numerical analysis, we consider then $\xi = 1.0 \pm 0.18$, and allow the strong phase $\Delta\theta$ to vary freely between -15° and $+15^\circ$.

The effect of including this inflated uncertainties into the numerical discussion is summarized in Table 4.2. Quantitatively, the effect is very small and, in any case, it is not significant enough to explain the $B \to \pi K$ puzzle on the basis of SU(3) breaking alone.

After this explicit numerical discussion, there are also several consistency checks inherent in the $B \to \pi\pi$, $B \to \pi K$ systems. Apart from the agreement between (4.21) and (4.20), these are

- The value of the angle γ obtained from $B \to \pi\pi$ and $B \to \pi K$, which is in reasonable agreement with UT fit numbers.
- The strong phase ω is supposed to be vanishing in the SU(3) limit. This can be tested by taking an additional observable, for example $\mathcal{A}_{\rm CP}^{\rm dir}(B^\pm \to \pi^0 K^\pm)$, into account and solving for q, ϕ and ω. One finds:

$$q = 0.99 \pm 0.67 \quad \phi = -(93^{+16}_{-18})^\circ, \quad \omega = -(22^{+34}_{-27})^\circ\,. \tag{4.53}$$

Quantity	Default values	Non-fact. $SU(3)$ breaking
γ	$(73.9^{+5.8}_{-6.5})^\circ$	$(73.9^{+9.4}_{-9.0})^\circ$
R	0.96 ± 0.02	$0.96^{+0.03}_{-0.04}$
$R_{\rm c}$	1.15 ± 0.05	1.15 ± 0.07
$R_{\rm n}$	1.12 ± 0.05	1.12 ± 0.06
$\mathcal{A}_{\rm CP}^{\rm dir}(B^\pm \to \pi^0 K^\pm)$	$0.04^{+0.08}_{-0.07}$	$0.04^{+0.13}_{-0.11}$
$\mathcal{A}_{\rm CP}^{\rm dir}(B_d \to \pi^0 K_{\rm S})$	$0.06^{+0.09}_{-0.10}$	$0.06^{+0.13}_{-0.16}$
ΔS	0.13 ± 0.05	$0.13^{+0.06}_{-0.07}$

Table 4.2: The impact of large non-factorizable $SU(3)$-breaking effects on our SM analysis. The "default" results of our analysis include factorizable $SU(3)$-breaking corrections, as described in the text.

The uncertainties in the value of ω are still very large, but its value is compatible with 0. This a reassuring sign for small flavor breaking, but it would be highly desirable to further reduce the errors.

- Flavor symmetry can also be tested in the decay rates and CP asymmetries of $B_s \to K^+K^-$. First results for the branching fractions have become available from CDF and they should be well-measurable at LHC. These tests are discussed more extensively in App. A.2.

4.6 Alternative Analyses, or: Is it Just QCD in the End?

Understandably there has been a tremendous amount of discussion of the potential new physics in $B \to \pi K$, and we would like to compare the results of the most important ones with ours. We will put special emphasis on how the $B \to \pi K$ data are accommodated in th respective treatments, i.e. whether the conclusion is that new physics is required or whether QCD dynamics can, in fact, describe the data well enough.

Within QCD factorization, the $B \to \pi K$ decays have been analyzed in [65], including their CP asymmetries, and we have collected the corresponding results in Table 4.3. Here, we give only the values for the scenario labeled S4 in [65], since several quantities have been updated (see caption of the table) in scenarios very similar to this one. The updates are given in this scenario only, since it offers the best agreement with the data. We observe that the description indeed seems to have some difficulty in describing the data, and that new physics in the electroweak penguin sector would resolve this puzzle. Also, the authors of [65] find on closer examination that a large phase (strong or weak) is required. This is in agreement with our findings, but the nature of the new phase is not specified, and there is no further examination of the implications or a quantitative statement about the enhancement required. Another interesting point is that the CP asymmetry of $B_d^0 \to \pi^- K^+$ comes out rather small. In addition, if the default scenario of [65] is considered, the prediction has a wrong sign. Since there is no electroweak pen-

guin contribution to this asymmetry, this seems to imply not only potentially enhanced electroweak penguins, but also significant non-factorizable corrections.

The results arising from SCET are surprisingly different. In [87] an analysis, using flavor symmetry in addition to SCET, was performed, with the result that there are indeed some discrepancies in the $B \to \pi K$ system, in particular concerning our observables $R_{\rm c}$ and $R_{\rm n}$, but it seems that these appear in the channels *without* electroweak penguin contributions. These results depend rather strongly on the angle γ, which this analysis favors to be large, as mentioned in Sect 3.4. The present status of SCET and QCDF analyses is compared in Table 4.3, where the SCET results are from [87] and the QCDF results are the default values from [65]. As [87] perform a fit to several observables, we have separated those used in the fit and those that are predicted. For example, the CP asymmetry of $B_d^0 \to \pi^- K^+$ agrees with the experimental value trivially in this case. Also, we show the dependence on γ as it is present in the analysis. As discussed in Section 3.5, this charming penguin terms are added by hand and also obtained in the fit, which results in rather good predictions for the $B \to \pi\pi$ branching ratios.

More recently, an even more extensive analysis in SCET has appeared [139], which also includes isosinglet states. The results differ in some places from those of [87] since the required fit to SCET parameters there is performed to all decay channels. A main discrepancy between the two analyses is that [139] do not determine the angle γ, so that no statement is made about whether a large value such as the one we obtain might be favored. However, the conclusion that the observables $R_{\rm c}$ and $R_{\rm n}$ may signal new physics is also reached.

For the most recent discussion on PQCD, see [98]. Here, additional NLO contributions from vertex corrections, quark loops and magnetic penguins that enhance C/T are calculated and claimed as a "resolution of the $B \to \pi K$ puzzle". In particular, the pattern of the CP asymmetries is in much better agreement with the data. Concerning the branching ratios, the main effect of these new contributions is to enhance the $B \to \pi^0 K^0$ prediction and bring it closer to the data. Still, the observables R and $R_{\rm n}$ are on the low side of the data for realistic values of γ. The predictions for PQCD can also been seen in Table 4.3.

In addition to these dynamical approaches, there has been a large number of more phenomenological analyses, in particular [39, 100, 101, 110, 140, 141], to name just a few. These analyses use, in general, approaches rather similar to ours, while the conclusions may differ somewhat. In all cases, the basis is an amplitude parameterization which is then fitted to data (one should note that, in the end, even the QCD based SCET approach fits some SCET parameters). The main difference is then how the fit is performed and which contributions are added. For example, [141] does not use flavor symmetry between $B \to \pi\pi$ and $B \to \pi K$, but still arrives at the result that, with present data, the electroweak penguin contribution should be modified. On the other hand, [39, 101] use also this symmetry and do indeed arrive at the same conclusion that there may be new physics, but that the effect is not statistically relevant yet. In [100, 110] one begins with the assumption that there are, in fact, problems in the $B \to \pi K$ system and it is attempted to solve them by including final state interaction terms [110] or charming penguin contributions [100]. In both cases the attempt is not entirely successful: [100] finds a too low value of $\mathrm{BR}(B_d \to \pi^0 K^0)$, which would, if confirmed point towards large

	Expt.	SCET ($\gamma = 83°$)	SCET ($\gamma = 59°$)	QCDF	PQCD
Data in Fit					
$\mathcal{A}_{\rm CP}^{\rm mix}(\pi^+\pi^-)$	0.50 ± 0.12	0.50 ± 0.10	0.51 ± 0.10	-	$0.42^{+0.56+0.05}_{-1.00-0.05}$
$\mathcal{A}_{\rm CP}^{\rm dir}(\pi^+\pi^-)$	-0.37 ± 0.10	-0.37 ± 0.07	-0.38 ± 0.07	-0.10	$-0.18^{+0.12+0.06}_{-0.20-0.07}$
$\mathrm{Br}(\pi^+\pi^-)$	5.0 ± 0.4	5.0 ± 2.0	4.6 ± 1.8	$5.0^{+1.3}_{-1.1}$	$6.5^{+6.7+2.7}_{-3.8-1.8}$
$\mathrm{Br}(\pi^+\pi^0)$	5.5 ± 0.6	5.5 ± 2.2	7.3 ± 2.9	$5.5^{+1.1}_{-0.94}$	$4.0^{+3.4+1.7}_{-1.9-1.2}$
$\mathrm{Br}(\pi^0\pi^0)$	1.45 ± 0.29	1.45 ± 0.58	1.32 ± 0.53	$0.73^{+0.68}_{-0.41}$	$0.29^{+0.50+0.13}_{-0.20-0.08}$
$\mathrm{Br}(\bar{K}^0\pi^-)$	24.1 ± 1.3	24.1 ± 1.2	24.1 ± 1.2	20.3	$24.5^{+13.6+12.9}_{-8.1-7.8}$
$\mathcal{A}_{\rm CP}^{\rm dir}(K^-\pi^+)$	0.115 ± 0.018	0.115 ± 0.023	0.115 ± 0.023	0.04	$0.09^{+0.08+0.06}_{-0.06-0.04}$
Predictions					
$\mathcal{A}_{\rm CP}^{\rm dir}(\pi^+\pi^0)$	-0.01 ± 0.06	$\lesssim 0.05$	$\lesssim 0.05$	0.02	$0.0 \pm 0.0 \pm 0.0$
$\mathcal{A}_{\rm CP}^{\rm dir}(\pi^0\pi^0)$	-0.28 ± 0.40	0.48 ± 0.19	0.52 ± 0.27	0.19	$-0.63^{+0.34+0.15}_{-0.35-0.09}$
$\mathcal{A}_{\rm CP}^{\rm mix}(\pi^0\pi^0)$	-	-0.84 ± 0.23	0.14 ± 0.22	-	-
$\mathrm{Br}(\pi^0\bar{K}^0)$	11.5 ± 1.0	10.4 ± 1.1	10.9 ± 1.2	8.0	$9.1^{+5.6+5.1}_{-3.3-2.9}$
$\mathrm{Br}(\pi^+K^-)$	18.9 ± 0.7	24.0 ± 2.1	22.5 ± 2.1	18.4	$20.9^{+15.6+11.0}_{-8.3-6.5}$
$\mathrm{Br}(\pi^0K^-)$	12.1 ± 0.8	14.3 ± 1.5	12.7 ± 1.4	11.7	$13.9^{+10.0+7.0}_{-5.6-4.2}$
$\mathcal{A}_{\rm CP}^{\rm mix}(\pi^0K_S)$	0.31 ± 0.26	0.77 ± 0.16	0.76 ± 0.16	$0.755^{+0.06}_{-0.04}$	$0.74^{+0.02+0.01}_{-0.03-0.01}$
$\mathcal{A}_{\rm CP}^{\rm dir}(\pi^0K^-)$	-0.04 ± 0.04	0.183 ± 0.075	0.184 ± 0.076	0.04	$0.01^{+0.05+0.05}_{-0.03-0.03}$
$\mathcal{A}_{\rm CP}^{\rm dir}(\bar{K}^0\pi^0)$	-0.02 ± 0.13	0.103 ± 0.058	0.083 ± 0.047	-0.008	$+0.07^{+0.03+0.01}_{-0.03-0.01}$
$\mathcal{A}_{\rm CP}^{\rm dir}(\pi^-\bar{K}^0)$	0.02 ± 0.04	< 0.1	< 0.1	-0.003	0.0 ± 0.0

Table 4.3: Comparison of theoretical predictions for $B \to \pi\pi$ as well as $B \to \pi K$ branching ratios and CP asymmetries in QCD factorization, PQCD and SCET with the experimental values. The SCET numbers are taken from [87], the PQCD values from [98] the predictions for QCDF from [65] except for the $B \to \pi\pi$ branching ratios, where we give the more recent numbers of [95]. The corrections of $\mathcal{A}_{\rm CP}^{\rm mix}(\pi^0 K_S)$ to $\sin 2\beta$ are computed with QCDF in [142].

isospin breaking effects, while in [110] the FIS are fitted and therefore in better agreement with the data. The most obvious discrepancy here remains for the $\mathcal{A}_{\rm CP}^{\rm dir}(B_d \to \pi^0 K^-)$, which we largely omitted from the analysis of this chapter, and will be one of the subjects of Section 5.4.

4.7 Conclusion of $B \to \pi K$

Before moving on to the implications of enhanced electroweak penguins for (semi)leptonic rare decays, let us summarize the results we obtained from $B \to \pi K$

- The hadronic parameters relevant for this decay system can be obtained from $B \to \pi\pi$ using flavor symmetry. The remaining electroweak penguin parameter is calculable and sensitive only to short distance physics.

- Predictions for quantities without significant electroweak penguin contributions are in reasonable agreement with the experimental numbers, while those with electroweak penguins contributing in a color-allowed manner partially show a significant deviation from their experimental values.

- The sensitivity to the electroweak penguin parameter can be traced nicely in the observable plane $R_{\rm n} - R_{\rm c}$. Here, one can read off the value of the electroweak penguin parameters required to reach the data. The result is an enhanced electroweak penguin with a large negative CP violating phase

- The CP asymmetries are also sensitive probes of new physics. We will come back to this point in the next chapter.

- There are several assumptions appearing in the calculation. One can perform several consistency checks as well as estimates of the uncertainties of the assumptions. We find that the uncertainties even when the assumptions are badly violated can not be the sole origin of the $B \to \pi K$ puzzle. Therefore, there may really be new physics in the electroweak penguin sector, if the present data are confirmed by future experiments.

Chapter 5

Implications for Rare K and B Decays

As we have seen in the last chapter, the data of the $B \to \pi K$ system may imply a modified electroweak penguin contribution, where the corresponding values for the electroweak penguin parameters are given in (4.35). It is quite obvious, that, in particular, (semi-)leptonic rare decays, i.e. rare decays that have leptons as final states and therefore receive contributions from these topologies, should also be affected by this modification. In addition, these decays are, in general, much more sensitive to the modification, since they are actually dominantly governed by them, due to the absence of QCD penguins. We will make this statement more quantitative in a later section. Due to the fact that only one matrix element is contributing, and that final state leptons do not influence the matrix elements, these decays also tend to be much cleaner than non-leptonic decays. In the decays discussed below, the matrix elements can either be obtained from measuring tree level dominated decays with the same hadronic states or they are reduced to a decay constant that can be calculated on the lattice and/or with QCD sum rules. Unfortunately, most of these decays have not yet been measured, but dedicated experiments are often being planned or are already under way. In this chapter we will analyze these rare decays in a specific scenario of modified electroweak penguins.

In order to do so, we shall first establish a connection between the hadronic low energy parameters introduced in the $B \to \pi K$ system and the high energy functions that govern the behavior of the rare decays. This analysis is also interesting once the question arises as to which concrete model of new physics can show the specific phenomenological signals that the $B \to \pi K$ system might be pointing towards. Next, we collect all the relevant formula for the rare decays in question and give some general background on the specific features and problems of each of the decay channels. We analyze these formulae numerically in the subsequent section, where we will find that the rare decays also have some messages for the non-leptonic decays. Therefore, we end this chapter with a renewed analysis of a somewhat wider set of non-leptonic decays, under consideration of these implications. In particular, we take also the opportunity to comment on the situation in $B \to \phi K_{\rm S}$.

5.1 Connection of $B \to \pi K$ to Short Distance Physics

As a first step in our our studies, it is necessary to establish a correlation between the purely phenomenological parameters of our $B \to \pi K$ analysis and the calculable short distance quantities of the OPE. To attack this question, we remember that q, in the SU(3) limit of the standard model, is given by:

$$q = \left| \frac{P'_{\rm EW}}{T' + C'} \right| e^{i(\delta'_{\rm EW} - \delta_{T'+C'})} = -\frac{3}{2} \frac{1}{\lambda |V_{ub}/V_{cb}|} \left[\frac{C_9(\mu_b) + C_{10}(\mu_b)}{C'_1(\mu_b) + C'_2(\mu_b)} \right] = 0.58\,. \tag{5.1}$$

In any model of new physics this relation is modified by replacing the SM Wilson coefficients with the corresponding ones of the respective model, which can amount to simply replacing the standard model loop functions or to adding entirely new contributions (see the discussion of Sect. 2.2.3).

Therefore, to continue, we have to specify a certain scenario in which we work, and for simplicity and predictive power, we make the following assumptions:

- New physics modifies the C function that describes electroweak penguins, but does not modify box and QCD penguin diagrams. This modification is allowed to be complex, i.e. $C \to C_{NP} e^{i\theta_C}$, as opposed to our first analysis in [143], where no complex phase was introduced.

- There is no new flavor dependence in the couplings. This means that we have a straightforward connection between K and B physics, since we allow for only one *universal*, complex C function.

This kind of scenario, which constitutes the minimal extension of MFV that has a possibility of describing the $B \to \pi K$ data, has been already discussed extensively with respect to (semi-)leptonic K [144–146] and B decays [147] alone, but we will extend it to non-leptonic decays in what follows. The advantage of this scenario is that it makes several stringent predictions, and can thus be easily tested, ruled out or verified.

In contrast to the model independent approach we are following, there have also been several investigations of the implications of supersymmetry on the $B \to \pi K$ decays [113, 148–151], sometimes combined also with $B \to \pi\pi$. Additionally, also the rare decays to be discussed here have been under some investigation [145, 146, 152–154] in SUSY models with similar signatures. However, in supersymmetry the modifications usually show up not only in the electroweak penguins, but also in the chromomagnetic penguin topologies. Another possible scenario, studied in [155–157], is a scenario with a flavor non-universal Z boson that introduces FCNCs at tree level. These can appear either if an additional vector-like quark is introduced, or if there is an additional $U(1)$ gauge symmetry with an associated Z' boson.

Coming back to our scenario, the next step to study the implications for rare decays must then be to find values for the C function that correspond to a given value of q, which means that we need to turn around the numerical analysis of 5.1. The appropriate renormalization group equations to calculate NLO Wilson coefficients with contributions from electroweak penguins have been given in Sect 2.2.2 and the results need only be

inverted to find the value of C for an arbitrary value of q. Numerically, this leads to [27, 143]:

$$|C(v)|e^{i\theta_C} = 2.35\,\bar{q}e^{i\phi} - 0.82, \quad \bar{q} = q\left[\frac{|V_{ub}/V_{cb}|}{0.086}\right], \tag{5.2}$$

where we have explicitly factored out the dependence on $|V_{ub}/V_{cb}|$. The numerical factors correspond to $\alpha_s(M_Z) = 0.119$ and $m_t(m_t) = 167$ GeV, the precise values of which have only a small impact numerically. Therefore, the associated uncertainties can be neglected in what follows. We can now immediately also find the values for the X, Y and Z functions introduced in (2.45)-(2.47):

$$X = |X|e^{i\theta_X}, \quad Y = |Y|e^{i\theta_Y}, \quad Z = |Z|e^{i\theta_Z}, \tag{5.3}$$

with

$$|X| = \sqrt{5.52\,\bar{q}^2 - 0.42\,\bar{q}\cos\phi + 0.01}, \quad \tan\theta_X = \frac{2.35\,\bar{q}\sin\phi}{2.35\,\bar{q}\cos\phi - 0.09} \tag{5.4}$$

$$|Y| = \sqrt{5.52\,\bar{q}^2 - 3.00\,\bar{q}\cos\phi + 0.41}, \quad \tan\theta_Y = \frac{2.35\,\bar{q}\sin\phi}{2.35\,\bar{q}\cos\phi - 0.64} \tag{5.5}$$

$$|Z| = \sqrt{5.52\,\bar{q}^2 - 4.42\,\bar{q}\cos\phi + 0.88}, \quad \tan\theta_Z = \frac{2.35\,\bar{q}\sin\phi}{2.35\,\bar{q}\cos\phi - 0.94}. \tag{5.6}$$

Also, we will find it useful to define the following weak phases

$$\beta_X \equiv \beta - \beta_s - \theta_X, \quad \beta_Y \equiv \beta - \beta_s - \theta_Y, \quad \beta_Z \equiv \beta - \beta_s - \theta_Z, \tag{5.7}$$

where $\beta_s = -1^\circ$ is the $B_s^0 - \bar{B}_s^0$ mixing phase, or, equivalently, the phase of V_{ts}:

$$V_{ts} = -|V_{ts}|e^{-i\beta_s}\,. \tag{5.8}$$

The weak phases β_i replace the phase β whenever it appears in a SM formula for a branching ratio in combination with the corresponding loop function. Using then $|V_{ub}/V_{cb}| = 0.102$ and the values of q and ϕ from (4.35) gives, for the absolute values of these functions:

$$|C| = 3.07 \pm 1.78, \qquad |Y| = 2.97 \pm 1.82, \tag{5.9}$$

$$|X| = 2.76 \pm 1.89, \qquad |Z| = 3.14 \pm 1.76, \tag{5.10}$$

to be compared with $C = 0.79$, $X = 1.53$, $Y = 0.98$ and $Z = 0.68$ in the SM. Taken at face value, it is quite clear that these numbers would imply some spectacular effects in many decays. Unfortunately, an analysis for MFV [64] finds, that the present data, mainly for the inclusive $b \to sl^+l^-$ decay, strongly constrain the allowed values of X and Y and give the following 95% probability upper bounds:

$$X \leq 1.95, \qquad Y \leq 1.43. \tag{5.11}$$

While our scenario of NP, which has new complex phases, goes beyond MFV, the inspection of the known formulae for $b \to sl^+l^-$ shows that the upper bound on Y in (5.11) is difficult to avoid, if the only NP contribution resides in the EW penguins and the

operator basis is the same as in the SM. For our analysis below, we will, therefore, use an only slightly more generous bound and impose $|Y| \leq 1.5$. Taking then those values of (q, ϕ) from (4.35) that also satisfy $|Y| = 1.5$ leaves one with

$$q = 0.48 \pm 0.07, \quad \phi = -(93 \pm 17)^\circ. \tag{5.12}$$

Note that this corresponds to a *suppression* of the magnitude of the EW penguin parameter. Since the $B \to \pi K$ data seem to signal modified electroweak penguins, but require the data to shift slightly within our approach, we will investigate how various modifications of (q, ϕ), that allow to satisfy the bounds in (5.11), influence our results for the observables of the $B \to \pi K$ system presented in Chapter 4 and the predictions for rare decays that we will discuss in detail.

For this purpose, we have introduced three scenarios that represent possible future measurements of $R_{\rm n}$ and $R_{\rm c}$:

- Scenario A: $q = 0.48$, $\phi = -93^\circ$, is compatible with the present $B \to \pi K$ data and the rare decay bounds (see (5.12)).
- Scenario B: We assume that $R_{\rm n}$ goes up, and take $q = 0.66$, $\phi = -50^\circ$, which leads to $R_{\rm n} = 1.03$, $R_{\rm c} = 1.13$ and some interesting effects in rare decays, as we shall see. This would, for example, occur if radiative corrections to the $B^0_d \to \pi^+ K^-$ branching ratio enhance $R_{\rm n}$ [158], though this alone would probably account for only an enhancement of about 5%.
- Scenario C: Assume that both $R_{\rm n}$ and $R_{\rm c}$ move towards 1: Taking $R_{\rm n} = R_{\rm c} = 1$ leads to $q = 0.54$, $\phi = 61^\circ$. The *positive* sign of the phase in this scenario distinguishes it strongly from both others.

In the following section, we will collect all relevant information on the rare decays we discuss, before we then study the implications of these scenarios.

5.2 Basic Formulae for Rare Decays

In this section, we give the necessary generalization of the SM formulas to our scenario for the rare decays we discuss. We have first derived these in [27], but will slightly rewrite some of them using a more convenient description of the CKM factors. The corresponding SM formulae can always be obtained simply by setting all the β_i to $\beta - \beta_s$.

We begin with the decays $K^+ \to \pi^+ \nu\bar{\nu}$ and $K_{\rm L} \to \pi^0 \nu\bar{\nu}$, which proceed in the SM through Z^0 penguin and leptonic box diagrams. In both cases, one has to take into account the diagrams with internal top and charm exchange, since the smallness of $V^*_{ts}V_{td}$ compensates for the quark mass enhancement of the top contributions. This effect is typical for K decays, while B decays, as well as $B^0_i - \bar{B}^0_i$ mixing, are entirely dominated by the top exchange due to the large value, in particular, of $|V_{tb}|$. Both $K \to \pi\bar{\nu}\nu$ decays are remarkably clean, since the required hadronic matrix elements of the leading contributions can be extracted from the well measured tree level decay $K^+ \to \pi^0 e^+ \nu$ and other long distance contributions are well under control. Therefore, these decays

are well suited to test any kind of new physics scenario, and we will have much more to say about them in the next chapter, which is devoted to an in-detail analysis of precisely these decays. Here, we give only the formulae for the branching ratios, which in our scenario are generalized as follows

$$\mathrm{BR}(K^+ \to \pi^+ \nu\bar{\nu}) = \kappa_+ \left[\left| \frac{\lambda_t}{\lambda^5} X \right|^2 + 2 \left| \frac{\lambda_t}{\lambda^5} X \right| \bar{P}_c(X) \cos\beta_X + \bar{P}_c(X)^2 \right], \tag{5.13}$$

$$\mathrm{BR}(K_\mathrm{L} \to \pi^0 \nu\bar{\nu}) = \kappa_L |\frac{\lambda_t}{\lambda} X|^2 \sin^2\beta_X \tag{5.14}$$

where

$$\bar{P}_c(X) = \left(1 - \frac{\lambda^2}{2}\right)(P_c(X) + \delta P_c(X)), \tag{5.15}$$

$$\kappa_+ = r_{K^+} \frac{3\alpha^2 \mathrm{BR}(K^+ \to \pi^0 e^+ \nu)}{2\pi^2 \sin^4\theta_w} \lambda^8 = (5.04 \pm 0.06) \cdot 10^{-11} \left[\frac{\lambda}{0.2248}\right]^8, \tag{5.16}$$

$$\kappa_L = \kappa_+ \frac{r_{K_L}}{r_{K^+}} \frac{\tau(K_L)}{\tau(K^+)} = (2.12 \pm 0.03) \cdot 10^{-10} \left[\frac{\lambda}{0.2248}\right]^8. \tag{5.17}$$

$P_c(X) = 0.38 \pm 0.04$ comes from the NNLO calculation of the charm contribution [30,159] and $\delta P_c(X) = 0.04 \pm 0.02$ results from the calculation of long distance effects in light quark loops [160].

There is quite a lot of CKM phenomenology that can be done when these decays are measured, but let us here concentrate on the well-known minimal flavor violation relation [161]:

$$(\sin 2\beta)_{\pi\nu\bar{\nu}} = (\sin 2\beta)_{\psi K_\mathrm{S}}, \tag{5.18}$$

As is obvious from (5.13), this relation is generalized to determine β_X, which makes it an extremely interesting test of our scenario. The corresponding equations are then:

$$\sin 2\beta_X = \frac{2 r_s}{1 + r_s^2}, \tag{5.19}$$

where

$$r_s = \frac{\varepsilon_1 \sqrt{B_1 - B_2} - \bar{P}_c(X)}{\varepsilon_2 \sqrt{B_2}} = \cot\beta_X \,. \tag{5.20}$$

The parameters ϵ_i are ± 1, and the reduced branching ratios are defined by:

$$B_1 = \frac{\mathrm{BR}(K^+ \to \pi^+ \nu\bar{\nu})}{\kappa_+}, \quad B_2 = \frac{\mathrm{BR}(K_\mathrm{L} \to \pi^0 \nu\bar{\nu})}{\kappa_L}. \tag{5.21}$$

Experimentally, it is obviously extremely difficult to obtain precise values for both decays. Nevertheless, three events of $K^+ \to \pi^+ \nu\bar{\nu}$ have been observed at Brookhaven, resulting in a branching fraction of

$$\mathrm{BR}(K^+ \to \pi^+ \nu\bar{\nu})|_{exp} = (14.7^{+13.0}_{-8.9}) \cdot 10^{-11} \tag{5.22}$$

On the other hand, there is only an upper limit on $\mathrm{BR}(K_\mathrm{L} \to \pi^0 \nu\bar{\nu})$, which reads

$$\mathrm{BR}(K_\mathrm{L} \to \pi^0 \nu\bar{\nu})|_{exp} < 2.9 \cdot 10^{-7} \tag{5.23}$$

at 90% confidence level. More details on the present and future experimental situation will be given in Chapter 6. Anticipating a more detailed numerical discussion, we note that the SM values for the decays are $\sim 8 \cdot 10^{-11}$ and $\sim 3 \cdot 10^{-11}$, so that $K^+ \to \pi^+ \nu\bar{\nu}$ agrees with the SM within the uncertainties, while the bound on $K_\mathrm{L} \to \pi^0 \nu\bar{\nu}$ is still a rather large margin away from the corresponding value.

The next decays we will turn to are the decays $B_{s/d} \to \mu^+\mu^-$. They are governed by the Y function, and the corresponding branching fractions are:

$$\mathrm{BR}(B_s \to \mu^+\mu^-) = 2.42 \times 10^{-6} \times \left[\frac{\tau_{B_s}}{1.46\ \mathrm{ps}}\right] \left[\frac{F_{B_s}}{238\ \mathrm{MeV}}\right]^2 |V_{tb}^* V_{ts}|^2 |Y(v)|^2 \tag{5.24}$$

$$\mathrm{BR}(B_d \to \mu^+\mu^-) = 1.82 \times 10^{-6} \times \left[\frac{\tau_{B_d}}{1.54\ \mathrm{ps}}\right] \left[\frac{F_{B_d}}{203\ \mathrm{MeV}}\right]^2 |V_{tb}^* V_{td}|^2 |Y(v)|^2, \tag{5.25}$$

where $\tau_{B_{d,s}}$ and $F_{B_{d,s}}$ are the lifetime and decay constants. The latter can be obtained in both QCD sum rule and lattice determinations. Nevertheless, these decays are less clean than the $K \to \pi\nu\bar{\nu}$ discussed above due to the uncertainties inherent in these parameters. On the other hand, the one B decay that is similarly clean is the inclusive $B \to X_s \nu\bar{\nu}$ decay, which is, however, experimentally extremely challenging. The branching fraction is given by:

$$\mathrm{BR}(B \to X_q \nu\bar{\nu}) = 1.58 \times 10^{-5} \left[\frac{\mathrm{BR}(B \to X_c e\bar{\nu})}{0.104}\right] \left[\frac{0.54}{f(z)}\right] \frac{|V_{tq}|^2}{|V_{cb}|^2} |X(v)|^2, \tag{5.26}$$

All of these decays provide information only on the magnitude of the electroweak penguin parameter, but are not sensitive to any CP violating phases, at least in our scenario. At present, the best experimental limits on these decays come from CDF, which give

$$\mathrm{BR}(B_s \to \mu^+\mu^-) < 0.8 \cdot 10^{-7} \qquad \mathrm{BR}(B_d \to \mu^+\mu^-) < 2.3 \cdot 10^{-8} \tag{5.27}$$

at 90% confidence level, while the SM predictions are both $\mathcal{O}(10^{-9})$ and will be given explictly in the next section along with the SM predictions for the other decays under discussion. No dedicated experiments for these decays are planned, but they should be well measurable at LHC.

Now, we turn to the decays $K_L \to \pi^0 l^+ l^-$, where the leptons can be muons or electrons. Here, due to the contributions of the photon penguins, long distance effects are important (in contrast to the $K_\mathrm{L} \to \pi^0 \nu\bar{\nu}$ case) and theoretical predictions are therefore much less clean. However, recent analyses [162, 163] have reduced these uncertainties considerably for both decays. They receive CP conserving, as well as CP violating contributions, where the former where estimated from new data for $K_L \to \pi^0\gamma\gamma$ and found to be entirely negligible [162]. The latter consist of terms that arise through direct and mixing induced CP violation as well as interference between both. For example, the

branching ratio in the electron case is, in our scenario, given by

$$\mathrm{BR}(K_\mathrm{L}\to\pi^0e^+e^-)_\mathrm{CPV}=10^{-12}\times\left[C_\mathrm{mix}+\bar{C}_\mathrm{int}\left(\frac{|\lambda_t|}{3\times10^{-4}}\right)+\bar{C}_\mathrm{dir}\left(\frac{|\lambda_t|}{3\times10^{-4}}\right)^2\right], \tag{5.28}$$

where

$$C_\mathrm{mix}=(15.7\pm0.3)|a_s|^2,\qquad |a_s|=1.2\pm0.2, \tag{5.29}$$

$$\bar{C}_\mathrm{int}=1.02\,\hat{y}_{7V}\sqrt{C_\mathrm{mix}},\qquad \bar{C}_\mathrm{dir}=0.56\,(\hat{y}_{7A}^2+\hat{y}_{7V}^2). \tag{5.30}$$

Here, $|a_s|$ is an $\mathcal{O}(p^4)$ chiral coupling, which is estimated from $K_S\to\pi^0e^+e^-$ and

$$\hat{y}_{7V}=[P_0+P_EE(v)]\sin(\beta-\beta_s)+\frac{|Y(v)|}{\sin^2\theta_\mathrm{w}}\sin\beta_Y-4|Z(v)|\sin\beta_Z \tag{5.31}$$

$$\hat{y}_{7A}=-\frac{|Y(v)|}{\sin^2\theta_\mathrm{w}}\sin\beta_Y, \tag{5.32}$$

contain the high energy physics, where $P_0=2.89\pm0.06$ [164] and P_E is $\mathcal{O}(10^{-2})$. The formula for the muonic case has a similar structure, but the following replacements have to be performed [163]:

$$C_\mathrm{mix}=(3.7\pm0.3)|a_s|^2,\quad \bar{C}_\mathrm{int}=1.02\,\hat{y}_{7V}\sqrt{C_\mathrm{mix}} \tag{5.33}$$

$$\bar{C}_\mathrm{dir}=\frac{9}{2\pi^2}(0.63\,(\hat{y}_{7A}^2+\hat{y}_{7V}^2)+0.85y_{7A}^2) \tag{5.34}$$

The experimental limits from KTeV read [165, 166]

$$\mathrm{BR}(K_\mathrm{L}\to\pi^0e^+e^-)<2.8\cdot10^{-10}\quad \mathrm{BR}(K_\mathrm{L}\to\pi^0\mu^+\mu^-)<3.8\cdot10^{-10}\,, \tag{5.35}$$

which are both about an order of magnitude larger than the SM predictions.

Another interesting decay is the decay $K_L\to\mu^+\mu^-$. The short distance contribution of these decays can be rather reliably calculated within the SM and reads:

$$\mathrm{BR}(K_\mathrm{L}\to\mu^+\mu^-)_\mathrm{SD}=1.95\times10^{-9}\times\left[\bar{P}_c(Y)+A^2R_t|Y(v)|\cos\beta_Y\right]^2, \tag{5.36}$$

where β_Y is defined in (5.7), and

$$\bar{P}_c(Y)=\left(1-\frac{\lambda^2}{2}\right)P_c(Y), \tag{5.37}$$

with $P_c(Y)=0.121\pm0.012$ [167]. Unfortunately, the extraction of the short distance contributions from the experimental values is plagued with rather large uncertainties due to long distance contributions. There have been several attempts to extract the short distance amplitudes [168–173], but let us here quote the most recent result of [173], which reads

$$\mathrm{BR}(K_L\to\mu^+\mu^-)_\mathrm{SD}|_{exp}<2.5\cdot10^{-9}\,, \tag{5.38}$$

while the SM prediction is about $8\cdot10^{-10}$.

Finally, one needs to take into account that the parameter ε'/ε is also very strongly affected by electroweak penguins. The calculation has been performed up to NLO [54], and the resulting formula, generalized again to our scenario, is

$$\frac{\varepsilon'}{\varepsilon} = \tilde{r} A^2 R_t \lambda^5 \times \tilde{F}_{\varepsilon'}(v), \tag{5.39}$$

with

$$\tilde{F}_{\varepsilon'}(v) = [P_0 + P_E\, E(v)] \sin(\beta - \beta_s) + P_X\, |X(v)| \sin\beta_X + P_Y\, |Y(v)| \sin\beta_Y + P_Z\, |Z(v)| \sin\beta_Z. \tag{5.40}$$

Here the P_i encode the information about the physics at scales $\mu \leq \mathcal{O}(m_t, M_W)$, and are given in terms of the hadronic parameters

$$R_6 \equiv B_6^{(1/2)} \left[\frac{121\text{MeV}}{m_s(m_c) + m_d(m_c)}\right]^2, \quad R_8 \equiv B_8^{(3/2)} \left[\frac{121\text{MeV}}{m_s(m_c) + m_d(m_c)}\right]^2 \tag{5.41}$$

as follows:

$$P_i = r_i^{(0)} + r_i^{(6)} R_6 + r_i^{(8)} R_8. \tag{5.42}$$

The $r_i^{(j)}$ are the $\Delta S = 1$ Wilson coefficients on which we refer the reader to [19]. Unfortunately, any theoretical prediction for ε'/ε is afflicted with large theoretical uncertainties from hadronic matrix elements, so that we will not go into an extensive numerical analysis of this quantity. We have, however, checked that, with central values of the matrix elements given, e.g. in [51], one tends to find values of ε'/ε that are not in agreement with experiment. Explicitely, we used $R_6 = 1.2$, $R_8 = 1.0$, which leads to

$$\varepsilon'/\varepsilon = 2.2 \times 10^{-4}, \qquad \text{while} \qquad \varepsilon'/\varepsilon|_{exp} = 16.6 \times 10^{-4}\ [174, 175] \tag{5.43}$$

With the values for (q, ϕ) that were found in [27], even a negative value was obtained. Taking a somewhat larger value of B_6 and a smaller one of B_8, such as $R_6 = 2.6$, $R_8 = 0.81$ brings the result back into agreement with the experimental number. We can therefore conclude that the parameter ε'/ε will only become a problem for our scenario if the hadronic uncertainties are substantially decreased.

5.3 Numerical Analysis

In this section we analyze the formulae presented in the previous section for our scenarios A, B, C. Taking the values of the CKM parameter as discussed in Section 3.4, we can predict all decays. The corresponding results are given in Table 5.1. We show also the corresponding SM predictions for comparison as well as the present experimental limits (or values). We observe that, in particular, the interplay of the to $K \to \pi\bar{\nu}\nu$ modes is a very good and clean indication of which kind of NP scenario to look for. Due to the interference of charm and top contributions in $K^+ \to \pi^+\bar{\nu}\nu$, it is also the decay that can most naturally be suppressed (though this is in contrast to the present experimental value). On the other hand, $\text{BR}(K_L \to \pi^0\bar{\nu}\nu)$ is always enhanced due to

the large values of ϕ and the absence of the charm contribution. This can be easily seen, as $\mathrm{BR}(K_L \to \pi^0 \bar{\nu}\nu)$ behaves in our scenario as

$$\frac{\mathrm{BR}^{NP}(K_L)}{\mathrm{BR}^{SM}(K_L)} = \left(\frac{\left|X^{NP}\right|}{|X^{SM}|} \frac{\sin\beta_X}{\sin\left(\beta - \beta_s\right)} \right)^2 . \tag{5.44}$$

Decay	SM	Scen A	Scen B	Scen C	Exp. bound (90% C.L.)
$\mathrm{BR}(K^+ \to \pi^+ \bar{\nu}\nu)/10^{-11}$	9.3	2.7	8.3	8.4	$(14.7^{+13.0}_{-8.9})$ [32]
$\mathrm{BR}(K_L \to \pi^0 \bar{\nu}\nu)/10^{-11}$	4.4	11.6	27.9	7.2	$< 2.9 \cdot 10^4$ [33]
$\mathrm{BR}(K_L \to \pi^0 e^+ e^-)/10^{-11}$	4.2	5.4	8.2	5.6	< 28 [166]
$\mathrm{BR}(K_L \to \pi^0 \mu^+ \mu^-)/10^{-11}$	1.6	2.2	3.7	2.6	< 38 [165]
$\mathrm{BR}(B \to X_s \bar{\nu}\nu)/10^{-5}$	3.6	2.8	4.8	3.3	< 64 [176]
$\mathrm{BR}(B_s \to \mu^+ \mu^-)/10^{-9}$	3.9	9.2	9.1	7.0	80 [177]
$\mathrm{BR}(K_L \to \mu^+ \mu^-)_{\mathrm{SD}}/10^{-9}$	0.9	0.9	0.001	0.6	< 2.5 [173]

Table 5.1: Branching ratios for several rare decays in the three scenarios introduced in the text.

Let us therefore discuss in a bit more detail these two decays in our scenario of modified electroweak penguins. As already mentioned in the previous section, the measurement of both decays allows to determine the CKM angle β in the standard model and in any model with MFV. On the other hand, in our model with additional CP violation, one finds in this way the phase β_X introduced in (5.7). Simultaneously, one can of course determine the magnitude of the X function, so that, in principle, these two decays alone are enough to very cleanly pin down the corresponding scenario. This can be seen in Fig. 5.1, where we show, as in [178], the X dependence of both branching ratios for fixed values of β_X. A remarkable feature is that for phases around $\beta_X \approx 111°$, as obtained specifically in scenarios A and B, the ratio $\mathrm{BR}(K_L)/\mathrm{BR}(K^+)$ is very close to the model independent Grossman Nir bound $\mathrm{BR}(K_L)/\mathrm{BR}(K^+) < 4.4$ [179] that follows from isospin. In general, there are some ambiguities in the determination of β_X in this manner, but these can be resolved by studying also additional quantities.

Alternatively, it interesting to study the ratio of the branching ratio of both decays as function of the angle β_X, as shown in Fig. 5.2. For negative angles, the figure is just mirrored around the y axis, and it is plain that it is precisely the large values of $\beta_X \approx 90°$ that produce the largest enhancement of $K_\mathrm{L} \to \pi^0 \nu\bar{\nu}$ over $K^+ \to \pi^+ \nu\bar{\nu}$. This figure also shows nicely how the modification of the phase can strongly modify the pattern of the decays and can enhance and suppress both decays with respect to each other. In addition to the $K \to \pi\bar{\nu}\nu$ decays, one should note that nearly all of the decays considered here show some prominent signals in the case of new physics in the electroweak penguin sector. They offer therefore an extremely important test of the potential new physics signals from $B \to \pi K$. In particular, they are very well suited to establish these signals more firmly and, in the optimistic case of this confirmation, to distinguish the different models of new physics.

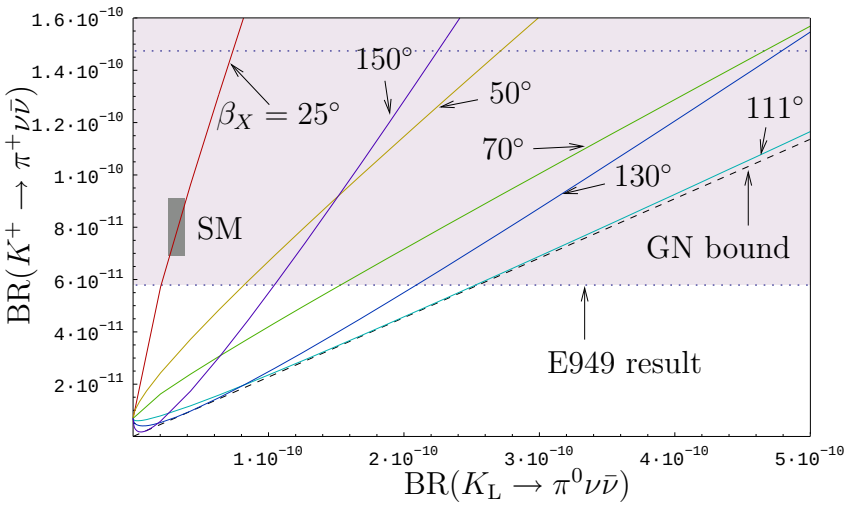

Figure 5.1: Potential to determine the phase and magnitude of the X function from both $K \to \pi\bar{\nu}\nu$ decays: A measurement of both decays allows both parameters of our scenario to be fixed.

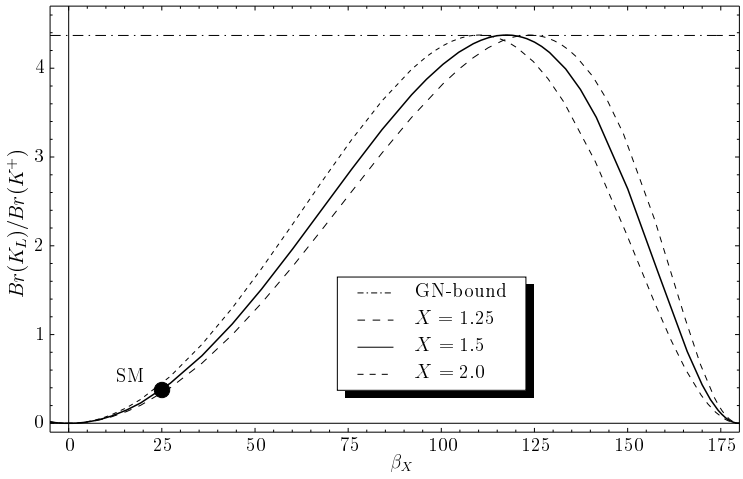

Figure 5.2: The ratio of both $K \to \pi\bar{\nu}\nu$ decays as a function of the phase β_X, where we show also the SM value and the upper bound that follows from isospin.

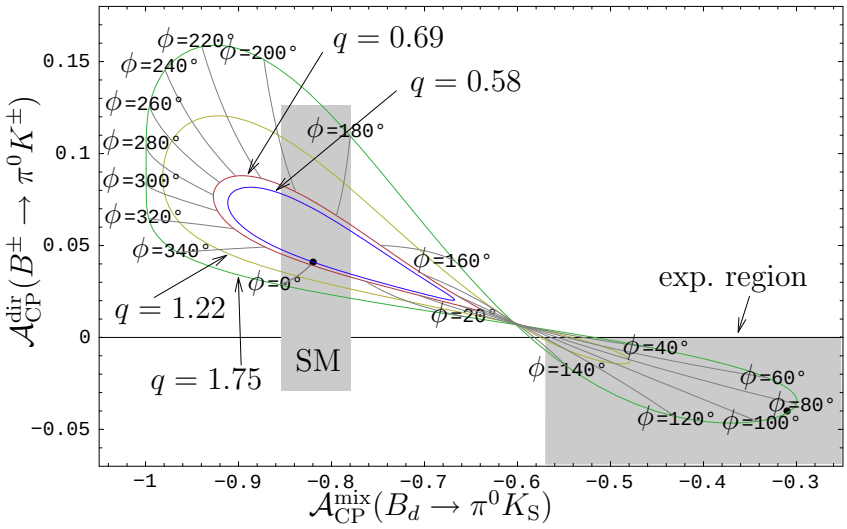

Figure 5.3: The situation in the $\mathcal{A}_{\rm CP}^{\rm mix}(B_d \to \pi^0 K_{\rm S})$–$\mathcal{A}_{\rm CP}^{\rm dir}(B^\pm \to \pi^0 K^\pm)$ plane: we show contours for values of $q = 0.69$ to $q = 1.75$ with $\phi \in [0°, 360°]$. The grey area represents the 1σ experimental range , and the central value is indicated by the black dot.

5.4 Implications for the $B \to \pi K$ System and other Non-Leptonic Decays

So far, in this chapter we have discussed the implications of the Scenarios A,B and C for rare decays. Let us now check, whether the scenarios are compatible with the other observable quantities that exist in the $B \to \pi K$ system. In particular, we will find that the CP asymmetries in this system will be very interesting in this respect. To begin, let us note that a very naive estimate that neglects the color-suppressed tree and electroweak penguin topologies shows that one expects the two asymmetries $\mathcal{A}_{\rm CP}^{\rm mix}(B_d \to \pi^+ K^-)$ and $\mathcal{A}_{\rm CP}^{\rm mix}(B_d \to \pi^0 K^-)$ to be equal. The rather large discrepancy in the experimental values is sometimes considered to be another potential sign of new physics in the $B \to \pi K$ system (see [180] for an early clarification of this matter). On the other hand, we have seen that the color-suppressed tree topologies are of the same order of magnitude as the color-allowed ones, so that the naive argument breaks down. One possibility to clarify this situation is to introduce sum rules that should be satisfied within the standard model [181]. On the other hand, we can use our hadronic parameters to predict both asymmetries for various values of q and ϕ. Therefore, in Figure 5.4, we show both $\mathcal{A}_{\rm CP}^{\rm mix}(B_d \to \pi^0 K_{\rm S})$ and $\mathcal{A}_{\rm CP}^{\rm dir}(B^\pm \to \pi^0 K^\pm)$ for several values of q as functions of ϕ in analogy to the $R_{\rm n} - R_{\rm c}$ plots introduced in Sect 4.3.2. On the other hand, $\mathcal{A}_{\rm CP}^{\rm mix}(B_d \to \pi^+ K^-)$ receives contributions from electroweak penguins only in color-suppressed form and is not affected by NP in our scenario.

We find indeed, that, while hadronic parameters can reduce the difference of the two asymmetries, it is very hard to find the negative value of $\mathcal{A}_{\rm CP}^{\rm dir}(B^\pm \to \pi^0 K^\pm)$ in the standard model, while a scenario with a larger value for q and a positive phase would bring the predictions closer to the data.

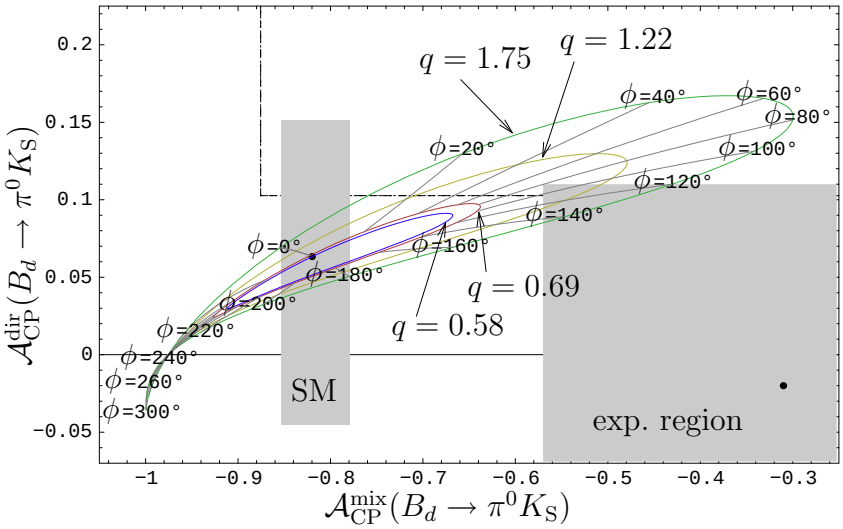

Figure 5.4: The situation in the $\mathcal{A}_{\rm CP}^{\rm mix}(B_d \to \pi^0 K_{\rm S})$–$\mathcal{A}_{\rm CP}^{\rm dir}(B_d \to \pi^0 K_{\rm S})$ plane, in analogy to Fig. 5.4.

Another phenomenon that has received some interest lately, is the experimental value of $\mathcal{A}_{\rm CP}^{\rm mix}(B_d \to \pi^0 K_{\rm S})$. In general, one expects the following relations for the CP asymmetries in $B_d \to \pi^0 K_{\rm S}$:

$$\mathcal{A}_{\rm CP}^{\rm dir}(B_d \to \pi^0 K_{\rm S}) \approx 0, \quad \underbrace{\mathcal{A}_{\rm CP}^{\rm mix}(B_d \to \pi^0 K_{\rm S})}_{\equiv -(\sin 2\beta)_{\pi^0 K_{\rm S}}} \approx \underbrace{\mathcal{A}_{\rm CP}^{\rm mix}(B_d \to \psi K_{\rm S})}_{\equiv -(\sin 2\beta)_{\psi K_{\rm S}}}. \tag{5.45}$$

The corrections to these relations have been calculated within QCD factorization [142] and estimated using SU(3) flavor symmetry [182]. While the first of these equations is rather well satisfied, the absolute value of $\mathcal{A}_{\rm CP}^{\rm mix}(B_d \to \pi^0 K_{\rm S})$ comes out somewhat low. Therefore, in analogy to our discussion before, we study the sensitivity of both asymmetries to the electroweak penguin parameters and show the corresponding analysis in Fig 5.4. Again, we find that a scenario with a positive phase is favored.

Finally, to conclude our discussion of the $B \to \pi K$ system, we show the explicit values of all observables that depend on electroweak penguins in the three scenarios considered earlier, in Table 5.2. In analogy to the statements made above, it seems that scenario C is slightly favored by the CP asymmetries. On the other hand, the uncertainties in this sector are still rather large so that conclusive statements can not yet be made. It will be very interesting to observe, in which direction the data of both branching ratios and CP asymmetries move.

Another non-leptonic decay that receives contributions from electroweak penguins, and has been under some discussion is $B \to \phi K_S$. In particular, the mixing induced CP asymmetry should be approximately equal to $\sin 2\beta$, where corrections within the SM are expected to be small [142, 183]. On the other hand, in contrast to $B \to J/\psi K_S$, here the dominant contribution to the decay is a QCD penguin topology, so that the sensitivity to new physics is increased. Additionally, for quite some time, the data from BaBar and Belle (while showing some disagreement among themselves), seemed to favor

Quantity	Scen A	Scen B	Scen C	Experiment
$R_{\rm n}$	0.88	1.03	1	0.83 ± 0.08
$R_{\rm c}$	0.96	1.13	1	1.01 ± 0.09
$\mathcal{A}_{\rm CP}^{\rm dir}(B^\pm \to \pi^0 K^\pm)$	0.07	0.06	0.02	-0.04 ± 0.04
$\mathcal{A}_{\rm CP}^{\rm dir}(B_d \to \pi^0 K_{\rm S})$	0.04	0.03	0.09	-0.02 ± 0.13
$\mathcal{A}_{\rm CP}^{\rm mix}(B_d \to \pi^0 K_{\rm S})$	-0.89	-0.91	-0.70	-0.31 ± 0.26

Table 5.2: The $B \to \pi K$ observables for the three scenarios introduced in the text.

smaller values for this asymmetry. This has triggered quite some discussion of potential new physics models that would be able to accommodate a discrepancy in this channel (see [184–187] for early discussions). By now, the newest data [49] have moved both together and towards the expected Standard model value:

$$\mathcal{A}_{\rm CP}^{\rm mix}(B_d \to \phi^0 K_{\rm S}) = 0.47 \pm 0.19\,. \tag{5.46}$$

As one can see, some discrepancy still persists. Since electroweak penguins may be sizable in this channel, it is now interesting to see what happens if we introduce our modified electroweak penguin parameters. We would like to analyze some kind of observable plane, and therefore we define [188]:

$$\mathcal{D}^-_{\phi K} \equiv \frac{1}{2}\left[\mathcal{A}_{\rm CP}^{\rm dir}(B_d \to \phi K_{\rm S}) - \mathcal{A}_{\rm CP}^{\rm dir}(B^\pm \to \phi K^\pm)\right] \tag{5.47}$$

$$\mathcal{D}^+_{\phi K} \equiv \frac{1}{2}\left[\mathcal{A}_{\rm CP}^{\rm dir}(B_d \to \phi K_{\rm S}) + \mathcal{A}_{\rm CP}^{\rm dir}(B^\pm \to \phi K^\pm)\right]. \tag{5.48}$$

Next, we will parameterize the decay amplitudes as:

$$A(\bar{B}^0_d \to \phi \bar{K}^0) = A_0\left[1 + v_0 e^{i(\Delta_0 - \phi)}\right] = A(B^- \to \phi K^-) \tag{5.49}$$

$$A(B^0_d \to \phi K^0) = A_0\left[1 + v_0 e^{i(\Delta_0 + \phi)}\right] = A(B^+ \to \phi K^+). \tag{5.50}$$

Here, A_0 is the leading QCD penguin amplitude, while the v_0 describes the the strength of the electroweak penguins compared to the QCD ones and Δ_0 is the corresponding CP conserving strong phase difference. We only include the $I = 0$ isospin component, since a large $I = 1$ part should be accompanied by significantly non-vanishing values of the direct asymmetries [188], in particular of $\mathcal{D}^-_{\phi K}$. Then, the CP asymmetries are given by:

$$\mathcal{A}_{\rm CP}^{\rm dir}(B_d \to \phi K_{\rm S}) = -\left[\frac{2v_0 \sin\Delta_0 \sin\phi}{1 + 2v_0\cos\Delta_0\cos\phi + v_0^2}\right] = \mathcal{A}_{\rm CP}^{\rm dir}(B^\pm \to \phi K^\pm) \tag{5.51}$$

$$\mathcal{A}_{\rm CP}^{\rm mix}(B_d \to \phi K_{\rm S}) = -\left[\frac{\sin\phi_d + 2v_0\cos\Delta_0\sin(\phi_d+\phi) + v_0^2\sin(\phi_d+2\phi)}{1 + 2v_0\cos\Delta_0\cos\phi + v_0^2}\right]. \tag{5.52}$$

The main difficulty is now obviously the determination of the hadronic parameters v_0 and Δ_0. If we are only interested in an order of magnitude estimate, we can use naive factorization and assume top quark dominance in the QCD penguins. Then, this amplitude

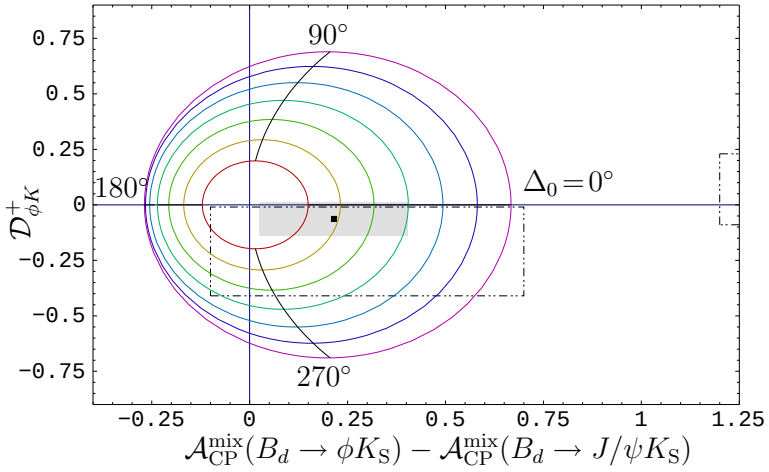

Figure 5.5: The implications of electroweak penguin contributions for $B \to \phi K_s$. The lines correspond to values of $v_0 = 0.1 - 0.4$ in steps of 0.05.

is found to be [27]:

$$v_0 e^{i\Delta_0}\Big|^{\rm SM}_{\rm fact} \approx -\left[\frac{2(C_9(m_b)+C_{10}(m_b))}{4(C_3(m_b)+C_4(m_b))+3C_5(m_b)+C_6(m_b)}\right]$$
$$= -\left[\frac{2\times(-1.280+0.328)}{4\times(0.014-0.030)+3\times 0.009-0.038}\right]\times\frac{1}{128} = -0.20, \qquad (5.53)$$

where we have used only the LO Wilson coefficients [19] and find that $\Delta_0 \approx 180°$. On the other hand, we can discuss the relevant quantities for several values of v_0 and Δ_0, as shown in Fig. 5.4, to account for the large uncertainties in this naive estimate, where we keep $\phi = -85°$ for definiteness. Taking the naive estimate at face value, we would have to conclude that the effect of these topologies is not large and would favor values of $\mathcal{A}^{\rm dir}_{\rm CP}(B_d \to \phi K_{\rm S})$ that are larger than $\mathcal{A}^{\rm dir}_{\rm CP}(B_d \to J/\psi K_{\rm S})$. Flipping the sign of the phase ϕ in this scenario would bring the prediction closer to the data, as one can easily see by expanding the expressions (5.52) for small v_0:

$$\mathcal{D}^+_{\phi K} = -2v_0 \sin\Delta_0 \sin\phi + \mathcal{O}(v_0^2) \qquad (5.54)$$

$$\mathcal{A}^{\rm mix}_{\rm CP}(B_d \to \phi K_{\rm S}) - \mathcal{A}^{\rm mix}_{\rm CP}(B_d \to J/\psi K_{\rm S}) = -2v_0 \cos\Delta_0 \sin\phi \cos\phi_d + \mathcal{O}(v_0^2). \qquad (5.55)$$

On the other hand, this effect can always be compensated by the appropriate choice of the strong phase Δ_0. Therefore, the only safe conclusion we can draw from this analysis is that we do not expect very large modifications of the SM pattern.

Chapter 6

Phenomenology of $K \to \pi\nu\bar{\nu}$

As we have seen in the previous section, the decays $K_L \to \pi^0\nu\bar{\nu}$ and $K^+ \to \pi^+\nu\bar{\nu}$ are very sensitive to new physics in the electroweak penguins. In addition, they have the virtues mentioned before, namely their theoretical cleanness and the resulting high degree of calculability. Therefore, we devote this chapter to an in-detail study of these two decays with a main emphasize on the predictions in the SM and their power to determine CKM parameters within the SM. Thereby, we follow rather closely our own work in [31]. For further reviews of these decays the reader is referred to [18, 189–192] In the following, we first collect all relevant formulae for the predictions of both decays in the SM, as well as for the determination of the CKM factors appearing, followed by a numerical analysis of them.

Before we do so, let us briefly outline the experimental perspectives for the measurements of both decays. The present experimental status has been given already in (1.3),(1.4):

$$\mathrm{BR}(K^+ \to \pi^+\nu\bar{\nu}) = 14.7^{+13.0}_{-8.9} \cdot 10^{-11}\,, \tag{6.1}$$

$$\mathrm{BR}(K_L \to \pi^0\nu\bar{\nu}) < 2.9 \cdot 10^{-7} \qquad (90\%\,\text{confidence})\,. \tag{6.2}$$

The present value for $\mathrm{BR}(K^+ \to \pi^+\nu\bar{\nu})$ includes the first signals of two events from E787 [193, 194], as well as the new signal from E949 [32], both experiments of which were performed at Brookhaven. On the other hand, the present bound on $\mathrm{BR}(K_L \to \pi^0\nu\bar{\nu})$ comes from KTeV [33].

Future improvements for $K_L \to \pi^0\nu\bar{\nu}$ and $K^+ \to \pi^+\nu\bar{\nu}$ are planned at KEK/J-Parc (see [195] for a review of the corresponding K physics program), while future data for $K^+ \to \pi^+\nu\bar{\nu}$ are also expected from the P-326 at CERN SPS [196], which, if approved, hopes to measure $\approx$ 80 events of $K^+ \to \pi^+\nu\bar{\nu}$ in 2 years. Unfortunately, both the CKM/Kplus experiment at Fermilab as well as the KOPIO experiment at Brookhaven have been canceled. A more detailed up-to-date discussion of the experimental prospects for both decays can be found in [197, 198].

6.1 Basics of $K \to \pi\nu\bar{\nu}$ and main Formulae

In the Standard Model, the decay $K^+ \to \pi^+\nu\bar{\nu}$ is described by the Z^0 penguin and box diagrams shown in Fig. 6.1. The relevant contributions to the branching fraction arise

from the charm and top contributions (since the t part is CKM suppressed), while the up component is only necessary for the GIM cancellation. Calculating the corresponding diagrams and their QCD corrections, the branching ratio is given by:

$$\mathrm{BR}(K^+ \to \pi^+ \nu\bar{\nu}) = \kappa_+ \cdot \left[\left(\frac{\mathrm{Im}\lambda_t}{\lambda^5} X(x_t) \right)^2 + \left(\frac{\mathrm{Re}\lambda_c}{\lambda} P_c(X) + \frac{\mathrm{Re}\lambda_t}{\lambda^5} X(x_t) \right)^2 \right], \quad (6.3)$$

$$\kappa_+ = r_{K^+} \frac{3\alpha^2 \mathrm{BR}(K^+ \to \pi^0 e^+ \nu)}{2\pi^2 \sin^4 \theta_w} \lambda^8 = (5.04 \pm 0.06) \cdot 10^{-11} \left[\frac{\lambda}{0.2248} \right]^8. \quad (6.4)$$

The quantities appearing in the formula have been introduced after (5.13).

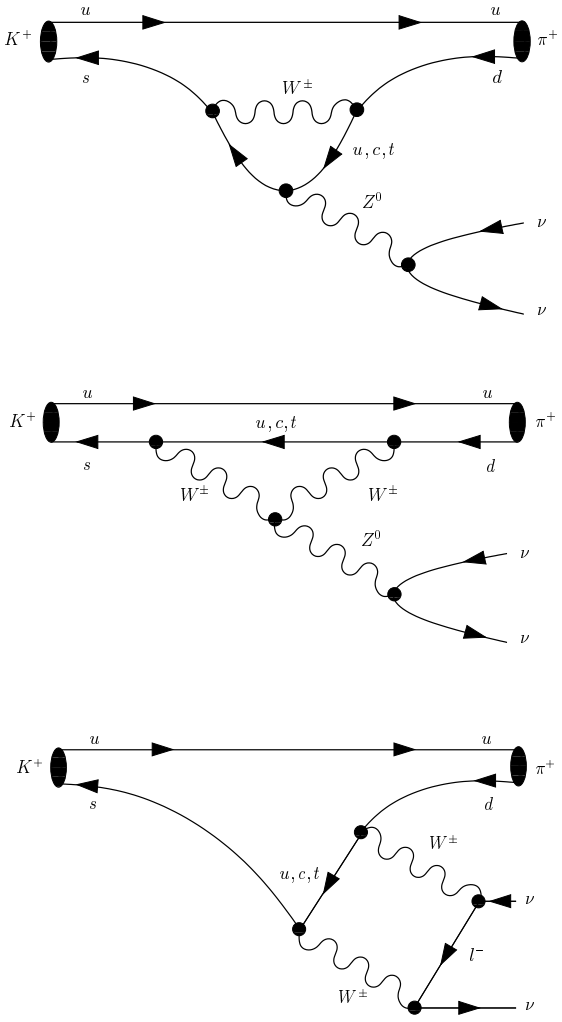

Figure 6.1: The penguin and box diagrams contributing to $K^+ \to \pi^+ \nu\bar{\nu}$. For $K_\mathrm{L} \to \pi^0 \nu\bar{\nu}$ only the spectator quark is changed from u to d.

In particular, the leading long distance QCD effects are governed by the matrix element of a single operator that can be extracted from the precise measurement of

the tree level decay $K^+ \to \pi^0 e^+ \nu$, and further sub leading effects are very well under control [160, 199–206]. A brief summary of long distance contributions can also be found in [31], and the potential improvements from lattice calculations are investigated in [207]. Additionally, higher order electroweak effects have been studied in the large m_t limit and are also found to be negligible [208].

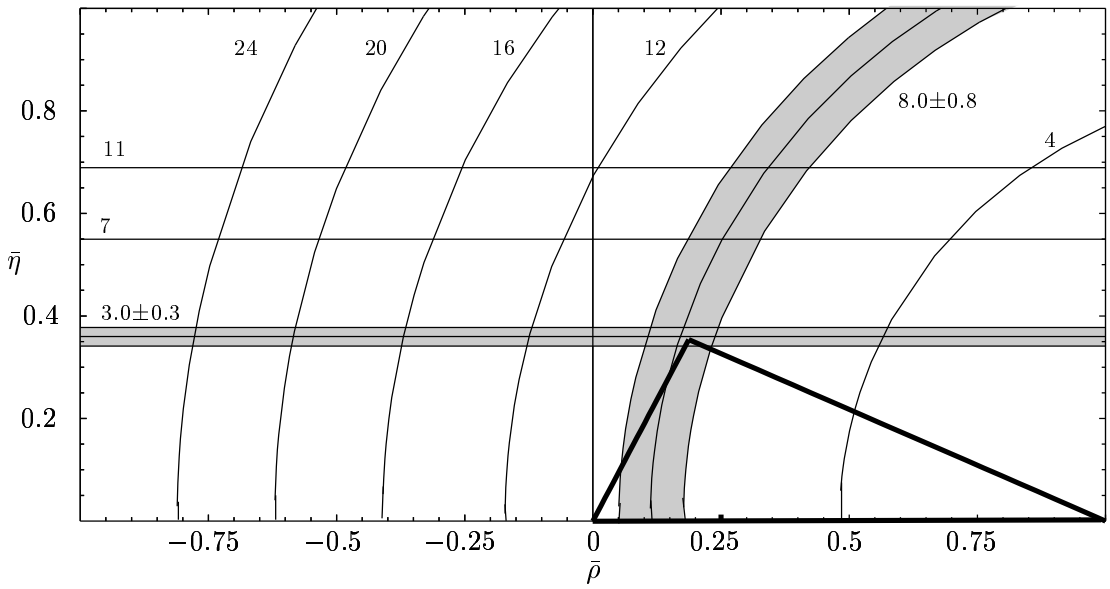

Figure 6.2: Unitarity triangle from $K \to \pi\nu\bar{\nu}$. We show the constraints arising from several hypothetical measurements of $K^+ \to \pi^+\nu\bar{\nu}$ and $K_L \to \pi^0\nu\bar{\nu}$ in units of 10^{-11}. A UT is constructed from a measurement of $\mathrm{BR}(K^+ \to \pi^+\nu\bar{\nu}) = 8.0 \pm 0.8 \cdot 10^{-11}$ and $\mathrm{BR}(K_L \to \pi^0\nu\bar{\nu}) = 3.0 \pm 0.3 \cdot 10^{-11}$

As stated above, there are top as well as charm contributions, denoted by $X(x_t)$ and $P_c(X)$, respectively. The top contribution, described by the X function, is given simply by

$$X(x_t) = X_0(x_t) + \frac{\alpha_s(m_t)}{4\pi} X_1(x_t) = \eta_X \cdot X_0(x_t), \qquad \eta_X = 0.995, \tag{6.5}$$

where

$$X_0(x_t) = \frac{x_t}{8}\left[-\frac{2+x_t}{1-x_t} + \frac{3x_t - 6}{(1-x_t)^2}\ln x_t\right] \tag{6.6}$$

as in (2.45) and the QCD correction is calculated to be [209–211]

$$\begin{aligned} X_1(x_t) = &- \frac{29x_t - x_t^2 - 4x_t^3}{3(1-x_t)^2} - \frac{x_t + 9x_t^2 - x_t^3 - x_t^4}{(1-x_t)^3}\ln x_t \\ &+ \frac{8x_t + 4x_t^2 + x_t^3 - x_t^4}{2(1-x_t)^3}\ln^2 x_t - \frac{4x_t - x_t^3}{(1-x_t)^2} L_2(1-x_t) \\ &+ 8x\frac{\partial X_0(x_t)}{\partial x_t}\ln x_\mu \end{aligned} \tag{6.7}$$

where $x_\mu = \mu_t^2/M_W^2$, $\mu_t = \mathcal{O}(m_t)$ and

$$L_2(1-x_t) = \int_1^{x_t} dt \frac{\ln t}{1-t}. \tag{6.8}$$

The scale involved $\mu \sim m_t$ is rather high, so that an NNLO calculation is not necessary, since the scale uncertainties are already small at the NLO level. Note, that the appearing operator does not renormalize under QCD, which explains the absence of renormalization group effects.

On the other hand, the calculation of the charm contribution is much more involved, since the charm quark is not integrated out simultaneously with the W boson. As a result, intermediate-scale diagrams are generated, in which also additional operators appear. Therefore, an entire renormalization group analysis is required, which has been performed to NLO [167, 212] and to NNLO [30, 159] precision. Summing over leptons (the electron and muon can be treated equivalently), one finds

$$P_c(X) = \frac{1}{\lambda^4}\left[\frac{2}{3}X_{\rm NL}^e + \frac{1}{3}X_{\rm NL}^\tau\right] = (0.38 \pm 0.04)\left(\frac{0.2248}{\lambda}\right)^4, \tag{6.9}$$

where we quote the result from [159]. The NNLO calculation has reduced the scale uncertainties in $P_c(X)$ severely and the main source of uncertainty now has its origin in the value of the charm quark mass. Here, long distance effects can be added and amount to $\delta P_c = 0.04 \pm 0.02$ [160], and are thus, as one can see, very well under control.

This complication of the charm contribution is absent is the decay $K_{\rm L} \to \pi^0\nu\bar{\nu}$, since it is purely CP violating in the SM and any MFV model [213]. The imaginary part of λ_c is nearly vanishing, and one is left with the top contribution only. Then, the branching ratio is:

$$\mathrm{BR}(K_L \to \pi^0\nu\bar{\nu}) = \kappa_L \cdot \left(\frac{\mathrm{Im}\lambda_t}{\lambda^5}X(x_t)\right)^2 \tag{6.10}$$

$$\kappa_L = \kappa_+ \frac{r_{K_L}}{r_{K^+}}\frac{\tau(K_L)}{\tau(K^+)} = (2.12 \pm 0.03)\cdot 10^{-10}\left[\frac{\lambda}{0.2248}\right]^8 \tag{6.11}$$

This decay is even cleaner than its charged counterpart, since perturbative uncertainties are nearly absent, and, again, long distance contributions are estimated to be negligible [206]. Therefore, this decay provides virtually the cleanest possible determination of the CP violating UT parameter $\bar{\eta}$, or, alternatively, an extremely clean test of the SM.

Let us in this context focus on the determination of UT parameters in the SM in the remainder of this section. For this, also the expression following from (6.3) and (2.13)-(2.15) is useful [36]:

$$\mathrm{BR}(K^+ \to \pi^+\nu\bar{\nu}) = \bar{\kappa}_+ |V_{cb}|^4 X^2(x_t)\frac{1}{\sigma}\left[(\sigma\bar{\eta})^2 + (\varrho_c - \bar{\varrho})^2\right], \tag{6.12}$$

where

$$\sigma = \left(\frac{1}{1-\frac{\lambda^2}{2}}\right)^2. \tag{6.13}$$

The measured value of $\mathrm{BR}(K^+ \to \pi^+ \nu\bar{\nu})$ then describes an ellipse in the $(\bar{\varrho}, \bar{\eta})$ plane centered at $(\varrho_c, 0)$ (see Fig. 6.2) with

$$\varrho_c = 1 + \frac{\lambda^4 P_c(X)}{|V_{cb}|^2 X(x_t)} \tag{6.14}$$

and the squared axes

$$\bar{\varrho}_1^2 = r_0^2, \qquad \bar{\eta}_1^2 = \left(\frac{r_0}{\sigma}\right)^2, \tag{6.15}$$

where

$$r_0^2 = \left[\frac{\sigma \cdot \mathrm{BR}(K^+ \to \pi^+ \nu\bar{\nu})}{\bar{\kappa}_+ |V_{cb}|^4 X^2(x_t)}\right]. \tag{6.16}$$

Using then the measured value of $|V_{ub}/V_{cb}|$ allows to determine $\bar{\varrho}$ and $\bar{\eta}$ with

$$\bar{\varrho} = \frac{1}{1-\sigma^2}\left(\varrho_c - \sqrt{\sigma^2 \varrho_c^2 + (1-\sigma^2)(r_0^2 - \sigma^2 R_b^2)}\right), \qquad \bar{\eta} = \sqrt{R_b^2 - \bar{\varrho}^2} \tag{6.17}$$

where $\bar{\eta}$ is assumed to be positive. Then,

$$R_t^2 = 1 + R_b^2 - 2\bar{\varrho}, \qquad V_{td} = A\lambda^3(1 - \bar{\varrho} - i\bar{\eta}), \qquad |V_{td}| = A\lambda^3 R_t, \tag{6.18}$$

can be used to obtain any desired CKM factor. This allows, in principle, a complete determination of the UT in the SM from $K^+ \to \pi^+ \nu\bar{\nu}$ alone.

If one looks at $K_{\mathrm{L}} \to \pi^0 \nu\bar{\nu}$ only, one can immediately find

$$\mathrm{BR}(K_{\mathrm{L}} \to \pi^0 \nu\bar{\nu}) = \bar{\kappa}_L \eta^2 |V_{cb}|^4 X^2(x_t), \qquad \bar{\kappa}_L = \frac{\kappa_L}{\lambda^8} = (3.34 \pm 0.05) \cdot 10^{-5} \tag{6.19}$$

from which $\bar{\eta}$ can be determined, as mentioned above:

$$\bar{\eta} = 0.351 \sqrt{\frac{3.34 \cdot 10^{-5}}{\bar{\kappa}_L}} \left[\frac{1.53}{X(x_t)}\right] \left[\frac{0.0415}{|V_{cb}|}\right]^2 \sqrt{\frac{\mathrm{BR}(K_{\mathrm{L}} \to \pi^0 \nu\bar{\nu})}{3 \cdot 10^{-11}}}. \tag{6.20}$$

Alternatively, one can also find $\mathrm{Im}\lambda_t$:

$$\mathrm{Im}\lambda_t = 1.39 \cdot 10^{-4} \left[\frac{\lambda}{0.2248}\right] \sqrt{\frac{3.34 \cdot 10^{-5}}{\bar{\kappa}_L}} \left[\frac{1.53}{X(x_t)}\right] \sqrt{\frac{\mathrm{BR}(K_{\mathrm{L}} \to \pi^0 \nu\bar{\nu})}{3 \cdot 10^{-11}}}. \tag{6.21}$$

If one is willing to take the angle β from, for example, a UT fit, (2.16) can be used with (2.17) in (6.20) to also obtain a "golden relation" [31] for the UT angle γ:

$$\frac{\sin\beta \sin\gamma}{\sin(\beta+\gamma)} = 0.351 \sqrt{\frac{3.34 \cdot 10^{-5}}{\bar{\kappa}_L}} \left[\frac{1.53}{X(x_t)}\right] \left[\frac{0.0415}{|V_{cb}|}\right]^2 \sqrt{\frac{\mathrm{BR}(K_{\mathrm{L}} \to \pi^0 \nu\bar{\nu})}{3 \cdot 10^{-11}}}. \tag{6.22}$$

This an extremely clean determination of this angle, which is, however, potentially polluted by new physics through the X function. As a consequence of (6.22), one may also invert this relation to determine $|V_{cb}|$ [214]:

$$|V_{cb}|^2 = 6.05 \cdot 10^{-4} \, \frac{\sin(\beta+\gamma)}{\sin\beta \sin\gamma} \sqrt{\frac{3.34 \cdot 10^{-5}}{\bar{\kappa}_L}} \left[\frac{1.53}{X(x_t)}\right] \sqrt{\frac{\mathrm{BR}(K_{\mathrm{L}} \to \pi^0 \nu\bar{\nu})}{3 \cdot 10^{-11}}}. \tag{6.23}$$

The advantage of this relation is the very weak dependence on $\mathrm{BR}(K_\mathrm{L} \to \pi^0 \nu\bar{\nu})$, since it enters only to the power of 1/4. On the other hand, one has again potential pollution effects from new physics that can enter through the X function.

So far, we have discussed the determination of CKM parameters from one of the decays alone. Using, on the other hand, both decays allows for a complete determination of the unitarity triangle, as we will see. First, from Fig. 6.2 it is clear, that the intersections of the ellipse from $K^+ \to \pi^+ \nu\bar{\nu}$ and the line from $K_\mathrm{L} \to \pi^0 \nu\bar{\nu}$ fix the entire triangle (up to ambiguities), without any input from $|V_{ub}|$. The corresponding formulae are:

$$\mathrm{Im}\lambda_t = \lambda^5 \frac{\sqrt{B_2}}{X(x_t)}, \qquad \mathrm{Re}\lambda_t = -\lambda^5 \frac{\frac{\mathrm{Re}\lambda_c}{\lambda} P_c(X) + \sqrt{B_1 - B_2}}{X(x_t)}\,, \tag{6.24}$$

where we have defined the "reduced" branching ratios as in (5.21)

$$B_1 = \frac{\mathrm{BR}(K^+ \to \pi^+ \nu\bar{\nu})}{\kappa_+}, \qquad B_2 = \frac{\mathrm{BR}(K_\mathrm{L} \to \pi^0 \nu\bar{\nu})}{\kappa_L}\,. \tag{6.25}$$

Using next the expressions for $\mathrm{Im}\lambda_t$, $\mathrm{Re}\lambda_t$ and $\mathrm{Re}\lambda_c$ given in (2.13)-(2.15) one finds

$$\bar{\varrho} = 1 + \frac{P_c(X) - \sqrt{\sigma(B_1 - B_2)}}{A^2 X(x_t)}\,, \qquad \bar{\eta} = \frac{\sqrt{B_2}}{\sqrt{\sigma} A^2 X(x_t)} \tag{6.26}$$

with σ defined in (6.13). Then, the contours in the $(\bar{\rho}, \bar{\eta})$ plane are fixed entirely from (6.26), as soon as the value of $X(x_t)$ is given, in any model with MFV. In models that go beyond MFV, such as the one discussed in Section 5, it may be more sensible to determine the weak phases appearing. In this context, the extremely clean determination [161] of the angle β_{eff}, which consists of the SM angle β as well as a potential CP violating NP phase of $X(x_t)$, is very interesting, as discussed already in (5.19). For completeness, we give here again the corresponding equations:

$$\sin 2\beta = \frac{2 r_s}{1 + r_s^2}, \tag{6.27}$$

where

$$r_s = \frac{\varepsilon_1 \sqrt{B_1 - B_2} - \bar{P}_c(X)}{\varepsilon_2 \sqrt{B_2}} = \cot\beta. \tag{6.28}$$

The main feature of these equation is the absence of both $X(x_t)$, which makes it valid not only in the SM but in any model with MFV. Also, there is no dependence on $|V_{cb}|$, which makes it extremely clean, since the only theoretical or parametric uncertainty arises from $P_c(X)$. We have analyzed these equations in the context of new physics models in Fig. 5.1 and will be more concerned with the determination of the SM phase in what follows.

Finally, we point out that one can, alternatively, determine the UT angle γ from [31]

$$\cot\gamma = \sqrt{\frac{\sigma}{B_2}} \left(A^2 X(x_t) - \sqrt{\sigma(B_1 - B_2)} + P_c(X) \right). \tag{6.29}$$

However, this has the disadvantage of being potentially polluted by new physics appearing in $X(x_t)$. Also, in contrast to (6.27), the input parameter $|V_{cb}|$ does not drop out of (6.29).

Another possibility to obtain γ is to first take R_t from

$$R_t = \frac{\sqrt{B_1 - \bar{P}_c^2 \sin^2\beta_{\text{eff}}} - \bar{P}_c \cos\beta_{\text{eff}}}{\tilde{r} A^2 X(x_t)}. \tag{6.30}$$

This (R_t, β) strategy by means of $K \to \pi\nu\bar{\nu}$ decays gives then $(\bar{\varrho}, \bar{\eta})$ as given in (2.16) and in particular

$$\cot\gamma = \frac{1 - R_t \cos\beta}{R_t \sin\beta}. \tag{6.31}$$

Again, this avenue is affected by the uncertainties from $|V_{cb}|$ as well as potential new physics contributions in $X(x_t)$.

6.2 Numerical results

6.2.1 BR($K_{\text{L}} \to \pi^0\nu\bar{\nu}$) and BR($K^+ \to \pi^+\nu\bar{\nu}$) in the Standard Model

Let us now analyze numerically all of the formulae given in the previous section within the SM. From this analysis, the power of both decays becomes very clear. At the same time, it becomes obvious where the largest sources of uncertainties in the analyses lie.

Here, we will not only be concerned with the present situation, but also with potential future scenarios for the CKM factors as well as for possible measurements of $K^+ \to \pi^+\nu\bar{\nu}$ and $K^+ \to \pi^+\nu\bar{\nu}$, which we introduce in Tables 6.1 and 6.2. In Table 6.1, we list the input used to predict $K^+ \to \pi^+\nu\bar{\nu}$ and $K_{\text{L}} \to \pi^0\nu\bar{\nu}$ in the SM, where Scenario A corresponds the UT fit performed in [31], while the Scenarios B and C are projections of 5 - 10 years into the future. In particular, the uncertainties in $P_c(X)$ should be further reducible with more precise values of the charm quark mass, while a precise determination of γ from tree level strategies should be possible at LHCb. Also, the uncertainties in β should be achievable at the B factories and the LHC. They correspond to an error in $\sin 2\beta$ of ± 0.025 and ± 0.012 for scenarios B and C, respectively. At this level, it will become necessary to quantify in more detail the theoretical uncertainties in $\mathcal{A}_{\text{CP}}^{\text{mix}}(B_d \to J/\psi K_{\text{S}})$, as discussed in Section 2.1.3. Finally, we use for Scenario A the NLO value for $P_c(X)$, as in [31], while Scenario B corresponds essentially to the NNLO calculation, and therefore shows the corresponding reduction of the uncertainties.

Next, in Table 6.2, we introduce two scenarios I and II, for future measurements of $K^+ \to \pi^+\nu\bar{\nu}$ and $K_{\text{L}} \to \pi^0\nu\bar{\nu}$ at the 10% and 5% level, respectively. The realization of both scenarios will require some experimental effort, but we will show in the following that this effort should be well worth making. We also use projected values of $|V_{cb}|$, $P_c(X)$, m_t, as they will also be necessary to determine β, γ, R_b and R_t.

Table 6.1: Input for the determination of the branching ratios $\mathrm{BR}(K^+ \to \pi^+\nu\bar{\nu})$ and $\mathrm{BR}(K_\mathrm{L} \to \pi^0\nu\bar{\nu})$ in three scenarios.

	Scenario A	Scenario B	Scenario C
β	$(23.7 \pm 2.1)^\cdot$	$(23.5 \pm 1.0)^\cdot$	$(23.5 \pm 0.5)^\circ$
γ	$(63.0 \pm 6.0)^\cdot$	$(63.0 \pm 5.0)^\cdot$	$(63.0 \pm 2.0)^\circ$
$\lvert V_{cb}\rvert/10^{-3}$	41.5 ± 0.8	41.5 ± 0.6	41.5 ± 0.4
R_b	0.40 ± 0.06	0.40 ± 0.03	0.40 ± 0.01
$m_t[\mathrm{GeV}]$	168 ± 4.1	168 ± 3	168 ± 1
$P_c(X)$	0.39 ± 0.07	0.39 ± 0.03	0.39 ± 0.02
$\bar{\eta}$	0.354 ± 0.027	0.340 ± 0.009	0.358 ± 0.007
$\bar{\varrho}$	0.187 ± 0.059	0.209 ± 0.017	0.182 ± 0.011

Table 6.2: Input for the determination of CKM parameters from $K \to \pi\nu\bar{\nu}$ in two scenarios.

	Scenario I	Scenario II
$\mathrm{BR}(K^+ \to \pi^+\nu\bar{\nu})/10^{-11}$	8.0 ± 0.8	8.0 ± 0.4
$\mathrm{BR}(K_\mathrm{L} \to \pi^0\nu\bar{\nu})/10^{-11}$	3.0 ± 0.3	3.0 ± 0.15
$m_t[\mathrm{GeV}]$	168 ± 3	168 ± 1
$P_c(X)$	0.39 ± 0.03	0.39 ± 0.02
$\lvert V_{cb}\rvert/10^{-3}$	41.5 ± 0.6	41.5 ± 0.4

The first step of our analysis is a prediction of both decays within the SM. Beginning with the Scenario A, we find that the CKM factors given in Table 6.1 correspond to

$$\mathrm{Im}\lambda_t = (1.40 \pm 0.12) \cdot 10^{-4}, \qquad \mathrm{Re}\lambda_t = -(3.06 \pm 0.25) \cdot 10^{-4} \quad (\text{Scenario A}). \quad (6.32)$$

Using these as input, we find for the branching ratios within the SM:

$$\mathrm{BR}(K^+ \to \pi^+\nu\bar{\nu})_\mathrm{SM} = (7.77 \pm 0.82_{P_c} \pm 0.91) \cdot 10^{-11} = (7.8 \pm 1.2) \cdot 10^{-11}, \quad (6.33)$$

$$\mathrm{BR}(K_\mathrm{L} \to \pi^0\nu\bar{\nu})_\mathrm{SM} = (3.0 \pm 0.6) \cdot 10^{-11}. \quad (6.34)$$

Here, we have separated the parametric from the theoretical uncertainties, which arise only from $P_c(X)$. Adding both in quadrature gives the final uncertainty. The theoretical uncertainties are negligible in $K_\mathrm{L} \to \pi^0\nu\bar{\nu}$. Similarly, from the CKM factors given for Scenario B and C, we find:

$$\mathrm{Im}\lambda_t = (1.35 \pm 0.05) \cdot 10^{-4}, \qquad \mathrm{Re}\lambda_t = -(2.97 \pm 0.11) \cdot 10^{-4} \quad (\text{Scenario B}) \quad (6.35)$$

$$\mathrm{Im}\lambda_t = (1.42 \pm \pm 0.04) \cdot 10^{-4}, \qquad \mathrm{Re}\lambda_t = -(3.08 \pm 0.07) \cdot 10^{-4} \quad (\text{Scenario C}). \quad (6.36)$$

We have collected the corresponding values for the branching fractions in Tables 6.3 and 6.4. In these Tables, in the rows labeled with Scenario A, B and C, we use the complete unitarity triangle fit from Table 6.1. On the other hand, it is interesting to investigate

Table 6.3: Values of $\mathrm{BR}(K^+ \to \pi^+\nu\bar{\nu})$ and $\mathrm{BR}(K_\mathrm{L} \to \pi^0\nu\bar{\nu})$ in the SM in units of 10^{-11} obtained through various strategies described in the text.

Strategy	$\mathrm{BR}(K^+ \to \pi^+\nu\bar{\nu})$ $[10^{-11}]$	$\mathrm{BR}(K_\mathrm{L} \to \pi^0\nu\bar{\nu})$ $[10^{-11}]$
Scenario A	7.77 ± 1.23	3.05 ± 0.56
	$7.77 \pm 0.82_{P_c} \pm 0.91$	
Scenario B	7.46 ± 0.55	2.82 ± 0.25
	$7.46 \pm 0.35_{P_c} \pm 0.43$	
Scenario C	7.85 ± 0.35	3.12 ± 0.17
	$7.85 \pm 0.23_{P_c} \pm 0.27$	
(R_b, γ) (B)	7.85 ± 0.69	3.10 ± 0.60
	$7.85 \pm 0.35_{P_c} \pm 0.60$	
(R_b, γ) (C)	7.85 ± 0.38	3.10 ± 0.23
	$7.85 \pm 0.23_{P_c} \pm 0.30$	

Table 6.4: The anatomy of parametric uncertainties in $\mathrm{BR}(K^+ \to \pi^+\nu\bar{\nu})$ and $\mathrm{BR}(K_\mathrm{L} \to \pi^0\nu\bar{\nu})$ corresponding to the results of Table 6.3.

Strategy	$\sigma\mathrm{BR}(K^+ \to \pi^+\nu\bar{\nu})$ $[10^{-11}]$	$\sigma\mathrm{BR}(K_\mathrm{L} \to \pi^0\nu\bar{\nu})$ $[10^{-11}]$
Scenario A	$\pm 0.72_{\bar{\varrho}} \pm 0.11_{\bar{\eta}} \pm 0.44_{\lvert V_{cb}\rvert} \pm 0.31_{m_t}$	$\pm 0.48_{\bar{\eta}} \pm 0.24_{\lvert V_{cb}\rvert} \pm 0.17_{m_t}$
Scenario B	$\pm 0.20_{\bar{\varrho}} \pm 0.03_{\bar{\eta}} \pm 0.31_{\lvert V_{cb}\rvert} \pm 0.21_{m_t}$	$\pm 0.15_{\bar{\eta}} \pm 0.17_{\lvert V_{cb}\rvert} \pm 0.11_{m_t}$
Scenario C	$\pm 0.13_{\bar{\varrho}} \pm 0.03_{\bar{\eta}} \pm 0.22_{\lvert V_{cb}\rvert} \pm 0.08_{m_t}$	$\pm 0.12_{\bar{\eta}} \pm 0.12_{\lvert V_{cb}\rvert} \pm 0.04_{m_t}$
(R_b, γ) (B)	$\pm 0.06_{R_b} \pm 0.44_{\gamma} \pm 0.33_{\lvert V_{cb}\rvert} \pm 0.23_{m_t}$	$\pm 0.48_{R_b} \pm 0.29_{\gamma} \pm 0.18_{\lvert V_{cb}\rvert} \pm 0.13_{m_t}$
(R_b, γ) (C)	$\pm 0.02_{R_b} \pm 0.18_{\gamma} \pm 0.22_{\lvert V_{cb}\rvert} \pm 0.08_{m_t}$	$\pm 0.16_{R_b} \pm 0.11_{\gamma} \pm 0.12_{\lvert V_{cb}\rvert} \pm 0.04_{m_t}$

what happens if only the constraints from R_b and γ are used in the determination of the CKM parameters, since these are the two parameters that can be obtained from tree level decays. The corresponding numbers are also given in the tables and are labeled by (R_b, γ). Obviously, the uncertainties in this strategy are significantly larger than in the situation where one uses the entire fit, but in Scenario C we have assumed a very precise value of R_b, so that both strategies are competitive here. It will, however, take some time until the values of R_b and γ discussed here become realistic.

We also show, in Table 6.4, the composition of the parametric uncertainties, by splitting errors according to their source (The uncertainty due to P_c is already separated from the others in 6.3). These parametric uncertainties are indeed the dominant ones since the completion of the NNLO calculation. We observe then that the single largest source of uncertainties is the value of $|V_{cb}|$. Concerning the strategy using R_b and γ, it is clear that, with our values of R_b, the influence of γ on the uncertainty is significantly larger. In conclusion, we find that a more precise SM prediction of both decays will especially require more precise information on the CKM factors. Finally, let us also note that our predictions are in the same ball-park of other recent ones given in [30, 190].

6.2.2 Impact of $K^+ \to \pi^+\nu\bar{\nu}$ and $K_{\rm L} \to \pi^0\nu\bar{\nu}$ on the Unitarity Triangle

In the previous subsection, we have found that the SM prediction for $K^+ \to \pi^+\nu\bar{\nu}$ and $K_{\rm L} \to \pi^0\nu\bar{\nu}$ depend rather sensitively in the CKM factors used. Now let us use this information to turn the analysis around: In the following, we will investigate the precision with which CKM factors can be determined from both decays. Here, we will find that the value of $|V_{cb}|$ used as input, as well as its precision, are very important.

We begin with the determination of R_t and $|V_{td}|$ from $K^+ \to \pi^+\nu\bar{\nu}$. As discussed in the previous section, one further CKM input is needed, which can be either β or R_b. Using β as input and taking all the numbers at their present value, including the present experimental number for $K^+ \to \pi^+\nu\bar{\nu}$, we find

$$R_t = 1.35 \pm 0.64, \qquad |V_{td}| = (12.5 \pm 5.9) \cdot 10^{-3} \ , \tag{6.37}$$

where the dominant error arises due to the error in the branching ratio. On the other hand, using R_b and taking again all input at its present value gives

$$R_t = 1.34^{+0.12}_{-0.63}, \qquad |V_{td}| = (12.5^{+1.1}_{-5.9}) \cdot 10^{-3}. \tag{6.38}$$

Note that the large values of R_t, that are in principle allowed by (6.37), are eliminated in (6.38), as they are inconsistent with the value of R_b that is used. At the same time, also large values of $\mathrm{BR}(K^+ \to \pi^+\nu\bar{\nu})$ are cut off, and only values that satisfy $\mathrm{BR}(K^+ \to \pi^+\nu\bar{\nu}) < 1.69 \cdot 10^{-10}$ are allowed.

Considering then more future scenarios, we show the values of R_t and $|V_{td}|$ as found in Scenarios I and II and taking β and R_b from Scenario B in Table 6.5. The values thus obtained are not very sensitive to the actual input of R_b and β, so that the uncertainties in both strategies are very similar. Also, the values obtained in Scenario C are the same within the digits shown. Finally, it is interesting to see what the individual sources of the errors are. Therefore, we separate again the uncertainties, and add the contributions of the dominant ones, which scale as

$$\frac{\sigma(|V_{td}|)}{|V_{td}|} = \pm 0.39 \frac{\sigma(P_c)}{P_c} \pm 0.70 \frac{\sigma(\mathrm{BR}(K^+))}{\mathrm{BR}(K^+)} \pm \frac{\sigma(|V_{cb}|)}{|V_{cb}|} \ . \tag{6.39}$$

We find then

$$\frac{\sigma(|V_{td}|)}{|V_{td}|} = \pm 3.0\%_{P_c} \pm 7.0\%_{\mathrm{BR}(K^+)} \pm 1.4\%_{|V_{cb}|}, \qquad \text{(Scenario I)} \tag{6.40}$$

and

$$\frac{\sigma(|V_{td}|)}{|V_{td}|} = \pm 2.0\%_{P_c} \pm 3.5\%_{\mathrm{BR}(K^+)} \pm 1.0\%_{|V_{cb}|}. \qquad \text{(Scenario II)} \tag{6.41}$$

Adding the errors in quadrature, we find that $|V_{td}|$ can be determined with an accuracy of $\pm 7.7\%$ and $\pm 4.1\%$, respectively. These numbers are increased to $\pm 8.2\%$ and $\pm 4.2\%$, once the uncertainties due to m_t, α_s and β (or $|V_{ub}/V_{cb}|$) are taken into account. The dominant source of uncertainties in these cases is the measured value of the branching

Table 6.5: The values for R_t and $|V_{td}|/10^{-3}$ (in parentheses) from $K^+ \to \pi^+\nu\bar{\nu}$ for various cases considered in the text.

	Scenario I	Scenario II
Scenario B (β)	0.903 ± 0.078 (8.39 ± 0.69)	0.903 ± 0.041 (8.39 ± 0.36)
Scenario B (R_b)	0.905 ± 0.078 (8.41 ± 0.69)	0.905 ± 0.041 (8.41 ± 0.36)

fraction. However, as a measurement of $\mathrm{BR}(K^+ \to \pi^+\nu\bar{\nu})$ with a precision of 5% is very challenging, the determination of $|V_{td}|$ with an accuracy better than $\pm 5\%$ from $\mathrm{BR}(K^+ \to \pi^+\nu\bar{\nu})$ seems very difficult from the present perspective.

On the other hand, the UT side R_t can also be determined from $\Delta M_d/\Delta M_s$. Here, the data are expected to be very precise already from the Tevatron, where the first signs of B_s mixing have been observed. On the other hand, the hadronic matrix elements entering in the corresponding expression limit the precision achievable. Still, a determination of R_t at the 5% level in this manner should hopefully be possible within this decade.

Let us next tun to the possible impact of a precise measurement of $\mathrm{BR}(K_\mathrm{L} \to \pi^0\nu\bar{\nu})$. As we have mentioned, this decay allows for the cleanest determination of the CP violating parameter $\bar{\eta}$ or, alternatively, $\mathrm{Im}\lambda_t$, as shown in (6.20) and (6.21), respectively. Using the values for Scenarios I and II, we find

$$\bar{\eta} = 0.351 \pm 0.022, \qquad \mathrm{Im}\lambda_t = (1.39 \pm 0.08) \cdot 10^{-4} \qquad \text{(Scenario I)}. \tag{6.42}$$

$$\bar{\eta} = 0.351 \pm 0.011, \qquad \mathrm{Im}\lambda_t = (1.39 \pm 0.04) \cdot 10^{-4}. \qquad \text{(Scenario II)} \tag{6.43}$$

Due to the absence of any theoretical errors, the uncertainties arise solely from the experimental values of the branching fraction, and the values of $\mathrm{Im}\lambda_t$ are therefore impressively precise.

Having now determined $\bar{\eta}$, we can continue to construct the complete unitarity triangle. In order to do so, we need one further input, which could be β, γ, R_b or R_t. As discussed in [38], the angle is γ is very useful in this respect, but we will also investigate the impact of β. Using the corresponding parameters from Scenarios I and II, we find the values of $\bar{\varrho}$ and $|V_{td}|$ given in Table 6.6. We compare here also the β and γ strategies. Notice that going from Scenario I to II has a significant impact on the precision obtainable only when using β, while both scenarios give similar results if γ is used. Also, a rather precise value of γ is sufficient to obtain a rather precise value of $\bar{\varrho}$, even if the branching fraction is measured to a precision of 10%.

As an alternative, from a measurement of $\mathrm{BR}(K_\mathrm{L} \to \pi^0\nu\bar{\nu})$, one can use Eq. (6.23) to obtain $|V_{cb}|$. The additional input required in this case are β and γ, but in turn one can also determine $|V_{td}|$. The corresponding values from Scenarios I and II for the branching fraction and scenarios A and B for the CKM factors are given in Table 6.7. The uncertainties for $|V_{cb}|$ thus obtained are larger than the ones obtained from semileptonic decays. However, since the determination from $K_\mathrm{L} \to \pi^0\nu\bar{\nu}$ is theoretically clean, it may provide a useful cross check to the standard determinations. The precision of R_t determined in this manner is rather high, a result of the accurate value of R_t that can be found from β and γ [38].

Table 6.6: The values for $\bar{\varrho}$ and $|V_{td}|/10^{-3}$ (in parentheses) from $K_{\rm L} \to \pi^0\nu\bar{\nu}$ for various cases considered in the text.

	Scenario I	Scenario II
Scenario B (β)	0.193 ± 0.063 (8.18 ± 0.57)	0.193 ± 0.048 (8.18 ± 0.41)
Scenario C (β)	0.193 ± 0.053 (8.18 ± 0.49)	0.193 ± 0.033 (8.18 ± 0.28)
Scenario B (γ)	0.179 ± 0.042 (8.30 ± 0.37)	0.179 ± 0.041 (8.30 ± 0.41)
Scenario C (γ)	0.179 ± 0.019 (8.30 ± 0.18)	0.179 ± 0.017 (8.30 ± 0.16)

Table 6.7: The values for $|V_{cb}|$ and $|V_{td}|$ (in parentheses) in units of 10^{-3} from $K_{\rm L} \to \pi^0\nu\bar{\nu}$, β and γ for various cases considered in the text.

	Scenario I	Scenario II
Scenario B	41.2 ± 1.6 (8.24 ± 0.32)	41.2 ± 1.3 (8.24 ± 0.26)
Scenario C	41.2 ± 1.2 (8.24 ± 0.25)	41.2 ± 0.7 (8.24 ± 0.15)

Table 6.8: The determination of CKM parameters from $K \to \pi\nu\bar{\nu}$ for two scenarios of Table 6.2.

	Scenario I	Scenario II
$\bar{\eta}$	0.351 ± 0.022	0.351 ± 0.011
$\bar{\varrho}$	0.167 ± 0.079	0.167 ± 0.042
$\sin 2\beta$	0.716 ± 0.050	0.716 ± 0.027
β	$(22.8 \pm 2.2)^\circ$	$(22.8 \pm 1.1)^\circ$
γ	$(64.2 \pm 10.9)^\circ$	$(64.2 \pm 5.9)^\circ$
R_b	0.389 ± 0.040	0.389 ± 0.020
R_t	0.902 ± 0.072	0.902 ± 0.039
$\lvert V_{td}\rvert/10^{-3}$	8.38 ± 0.65	8.38 ± 0.34
$\mathrm{Im}\lambda_t/10^{-4}$	1.39 ± 0.08	1.39 ± 0.04
$\mathrm{Re}\lambda_t/10^{-4}$	-3.13 ± 0.29	-3.13 ± 0.15

Finally, as a last step, we will now combine the information from a measurement of both decays to construct the complete unitarity triangle without additional input. The resulting analysis is also in many ways an update of [215], where this kind of construction of the UT was first discussed. The resulting values of for all CKM parameters are shown in Table 6.8, where we find, in particular, that $\sin 2\beta$ and $\mathrm{Im}\lambda_t$ can be found very precisely. Also, all parameters can be obtained in a satisfactory manner already in Scenario I. We show the unitarity triangle, as constructed from the measurements of both decays as assumed in Scenario I, in Fig. 6.2. The values of the branching fractions have been chosen here as such, that they represent the SM values if the CKM input from

Table 6.1 are used. Hopefully however, the apex of the unitarity triangle constructed in this way will *not* agree with the expectation and signal some contributions from new physics. This would, for example, be the case in the scenario of enhanced electroweak penguins with a CP violating phase discussed in Chapters 4 and 5. At this point we should mention that also the value of the X function enters into the determination of the UT and would also be modified in the presence of NP. Of course, the main result of such a scenario would be, however, to modify the value of β according to our analysis in Chapter 5.

Therefore, we analyze next the numerical implications of (6.27). The numerical results for $\sin 2\beta$ are already given in Table 6.8, and we will now be interested in the origin of the uncertainties. To clarify this, we investigate the impact of the separate contributions and split the errors according to:

$$\frac{\sigma(\sin 2\beta)}{\sin 2\beta} = \pm 0.31 \frac{\sigma(P_c)}{P_c} \pm 0.55 \frac{\sigma(\mathrm{BR}(K^+))}{\mathrm{BR}(K^+)} \pm 0.39 \frac{\sigma(\mathrm{BR}(K_L))}{\mathrm{BR}(K_L)} \; . \tag{6.44}$$

For the two scenarios introduced above, this leads to

$$\sigma(\sin 2\beta) = 0.017_{P_c} + 0.039_{\mathrm{BR}(K^+)} + 0.028_{\mathrm{BR}(K_L)} = 0.050 \qquad \text{(Scenario I)} \tag{6.45}$$

and

$$\sigma(\sin 2\beta) = 0.011_{P_c} + 0.020_{\mathrm{BR}(K^+)} + 0.014_{\mathrm{BR}(K_L)} = 0.027, \qquad \text{(Scenario II)} \tag{6.46}$$

where the errors have been added in quadrature. From these decompositions, we observe that in Scenario I, corresponding to the NLO calculation, the uncertainties are actually dominated by the errors in $P_c(X)$. On the other hand, in Scenario II, which corresponds basically to the NNLO calculation, we find that the uncertainty is now dominated by the accuracy of the measurements for the branching fractions. Therefore, precise measurements of both branching ratios would be very desirable, in order to compare the corresponding value of $\sin 2\beta$ with the measurement of $\mathcal{A}_{\mathrm{CP}}^{\mathrm{mix}}(B_d \to J/\psi K_{\mathrm{S}})$.

The same decomposition can be performed in an analogous manner for the angle γ, where the relation (6.22) is used. The result is

$$\sigma(\gamma) = 3.7^\circ_{P_c} + 8.5^\circ_{\mathrm{BR}(K^+)} + 0.4^\circ_{\mathrm{BR}(K_L)} + 3.8^\circ_{|V_{cb}|} + 2.6^\circ_{m_t} = 10.4^\circ \tag{6.47}$$

and

$$\sigma(\gamma) = 2.5^\circ_{P_c} + 4.2^\circ_{\mathrm{BR}(K^+)} + 0.2^\circ_{\mathrm{BR}(K_L)} + 2.5^\circ_{|V_{cb}|} + 0.9^\circ_{m_t} = 5.7^\circ \tag{6.48}$$

for Scenario I and II, respectively, where the errors have again been added in quadrature. Our main observations here are that a measurement of $\mathrm{BR}(K_{\mathrm{L}} \to \pi^0 \nu\bar{\nu})$ has a comparatively small impact, whereas the uncertainties of both $P_c(X)$ as well as $\mathrm{BR}(K^+ \to \pi^+ \nu\bar{\nu})$ are significant.

As a last point of this section, we remember that, in several quantities analyzed here, we found the uncertainties to be dominated by those from $P_c(X)$ and $|V_{cb}|$. Therefore, we conclude by showing the uncertainties induced by these two quantities on several observables under investigation. We do so for different values of $\sigma(P_c)$ and $\sigma(|V_{cb}|)$,

corresponding to the scenarios A,B and C, where the results are given in Tables 6.9 and 6.10.

In conclusion, we have investigated the precision with which certain CKM parameters can be constrained from $K^+ \to \pi^+\nu\bar{\nu}$ and $K_{\rm L} \to \pi^0\nu\bar{\nu}$ with future measurements. We have shown that this can be done remarkably well, as summarized in Table 6.8.

Table 6.9: The uncertainties in various quantities due to the error in P_c.

$\sigma(P_c)$	± 0.07	± 0.03	± 0.02
$\mathrm{BR}(K^+ \to \pi^+\nu\bar{\nu})/10^{-11}$	± 0.82	± 0.34	± 0.23
$\bar{\eta}$	–	–	–
$\bar{\varrho}$	± 0.067	± 0.029	± 0.019
$\sin 2\beta$	± 0.042	± 0.018	± 0.012
β	$\pm 1.8^\circ$	$\pm 0.8^\circ$	$\pm 0.5^\circ$
γ	$\pm 9.4^\circ$	$\pm 3.8^\circ$	$\pm 2.5^\circ$
R_b	± 0.033	± 0.019	± 0.009
R_t	± 0.061	± 0.026	± 0.017
$\lvert V_{td}\rvert/10^{-3}$	± 0.57	± 0.24	± 0.16
$\mathrm{Im}\lambda_t/10^{-4}$	–	–	–
$\mathrm{Re}\lambda_t/10^{-4}$	± 0.25	± 0.11	± 0.07

Table 6.10: The uncertainties in various quantities due to the error in $|V_{cb}|$.

$\sigma(\lvert V_{cb}\rvert)/10^{-3}$	± 0.8	± 0.6	± 0.4
$\mathrm{BR}(K^+ \to \pi^+\nu\bar{\nu})/10^{-11}$	± 0.44	± 0.31	± 0.22
$\bar{\eta}$	± 0.013	± 0.010	± 0.007
$\bar{\varrho}$	± 0.033	± 0.025	± 0.016
$\sin 2\beta$	–	–	–
β	–	–	–
γ	$\pm 5.3^\circ$	$\pm 3.9^\circ$	$\pm 2.6^\circ$
R_b	± 0.003	± 0.002	± 0.001
R_t	± 0.036	± 0.027	± 0.018
$\lvert V_{td}\rvert/10^{-3}$	± 0.17	± 0.12	± 0.08
$\mathrm{Im}\lambda_t/10^{-4}$	–	–	–
$\mathrm{Re}\lambda_t/10^{-4}$	–	–	–

Chapter 7

Conclusions and Outlook

In this work we have analyzed several non-leptonic B decays with respect to possible contributions from new physics effects. In this analysis, we have exploited several correlations between different decay channels, which allowed us to overcome the main difficulty inherent in any analysis of non-leptonic decay, namely the calculation of the hadronic matrix elements. These correlations allow, in principle, to disentangle effects of beyond-SM physics from hadronic uncertainties. Specifically, we have investigated the non-leptonic decays $B \to \pi\pi$ and $B \to \pi K$ within a scenario of modified electroweak penguin contributions with a possible CP violating phase. Finally, we have extended the analysis to several rare K and B decays, where the modification of the electroweak penguin parameters should show some prominent signals.

The analysis consisted of several subsequent steps and proceeded in detail as follows:

- We began by investigating the decays $B \to \pi\pi$, which are tree level dominated and therefore expected to be described to a very good approximation within the SM. Using the SU(2) isospin symmetry of strong interactions, the amplitudes were parameterized in terms of several hadronic parameters as well as the weak CKM phase γ. We then used the additional assumption of SU(3) flavor symmetry to determine both γ and the hadronic parameters. In this process, we included numerically the contributions of the electroweak penguins parameters, which have only a very minor impact. From the values of the parameters obtained, the CP violating asymmetries of the $B_d^0 \to \pi^0\pi^0$ decays were predicted, which can also be used to determine γ, once they are more precisely measured.

- Using in the next step the SU(3) flavor symmetry of strong interactions, we determine the hadronic parameters of the $B \to \pi K$ decay system. The electroweak penguin parameters in these decays can be calculated from pure short distance physics using again the assumption of SU(3) flavor symmetry. We then determined the electroweak penguin parameter necessary to describe the $B \to \pi K$ decay data. Additionally, we analyzed the CP asymmetries within this decay system.

- As a last step, we found the correlation between the phenomenological parameters of the $B \to \pi K$ system and the short distance functions that govern the rare semi-leptonic decays in question. This was done in a scenario, where only the C

function, which describes the electroweak penguin topology, is modified and can obtain a non-vanishing CP violating phase. In order to achieve this, we had to use the renormalization group equations that govern the running of the Wilson coefficients in the OPE, including those of the electroweak penguins, which we solved to next-to-leading order. We found that the rare decays already give some constraints on the electroweak penguin parameters, whereupon we reanalyzed the $B \to \pi K$ system and commented on the CP asymmetries in $B_d^0 \to \phi K_S$.

Having now recapitulated the steps of our analysis, let us summarize our main findings:

- The angle γ obtained from our analysis is somewhat higher than the one usually quoted by the standard UT fits. This is in accordance with a recent SCET analysis of $B \to \pi\pi$ and $B \to \pi K$, that finds an even larger value. Since there is some discrepancy in the UT fits between the angle β and the side R_b determined from $|V_{ub}/V_{cb}|$, we attribute this discrepancy to some small NP contribution in $B_d^0 - \bar{B}_d^0$ mixing and take the angle γ we find as the true UT angle, from which we construct a unitarity triangle.

- The hadronic parameters of the $B \to \pi\pi$ system point towards sizeable departures from factorization. In particular, we find that, while the $B \to \pi\pi$ decays are well described within the SM, there seem to be some hadronic interference effects which enhance the contribution from the color-suppressed tree diagram and reduce the corresponding color-allowed one. This enhancement may come from GIM-penguin-type diagrams and leads to an apparent lifting of color suppression. Finally, we used these parameters to predict the CP asymmetries in $B_d^0 \to \pi^0\pi^0$, and find a rather encouraging agreement with the experimental numbers, though the uncertainties are too large to draw any definite conclusions yet. These predictions will allow a test not only of our assumption on the flavor symmetries, but also show whether our value for γ is realistic.

- Within the $B \to \pi K$ system, we find that the observable R, which is not affected by electroweak penguins, is described rather well with the parameters we determine from those of the $B \to \pi\pi$ system with the assumption of flavor symmetry and negligible annihilation and exchange topologies. The remaining discrepancy can be attributed to a sizeable value for the parameter ρ_c, which describes certain rescattering effects. This sizeable value of ρ_c is also favored by recent experimental data for $B^\pm \to K^\pm K$.

- Investigating, on the other hand, the observables that receive significant contributions from color-allowed electroweak penguins, in particular the observable $R_{\rm n}$, which describes the branching ratios of neutral B_d^0 decays, we found that the theoretical description of the corresponding decays is rather bad. This situation could be tracked in the plane of the observables $R_{\rm n}$ and $R_{\rm c}$, which allowed us to determine the value of the electroweak penguin parameters necessary to describe these decays. We found that the electroweak penguin parameter should be enhanced and carry a large negative CP violating phase.

- This modification of the electroweak penguins has severe implications for several (semi-)leptonic rare decays that proceed dominantly through the electroweak penguin topologies. Restricting ourselves to a very simple and predictive scenario, we found striking effects in the $K \to \pi\bar{\nu}\nu$ system, where the large CP violating phase results in a spectacular enhancement of the CP violating decay $K_{\rm L} \to \pi^0\nu\bar{\nu}$. Using, on the other hand, $K_{\rm L} \to \pi^0\nu\bar{\nu}$ and $K^+ \to \pi^+\nu\bar{\nu}$ combined allows an easy test of our scenario, since both the magnitude and phase of the electroweak penguins can be determined. At the same time, we find that the electroweak penguin parameters implied by the $B \to \pi K$ decays violate existing experimental bounds that come, in particular, from the inclusive decay $b \to s l^+ l^-$.

- In view of this situation, we discussed several possible experimental scenarios of future $B \to \pi K$ data and their implications for the rare decays. We found that the pattern of enhancements and suppressions in the rare decays channels under investigation allows to discriminate between the different scenarios rather easily. In this context, we also studied the impact of possible precise measurements of the CP asymmetries in $B^0_d \to \pi^0 K_S$ and $B^+ \to \pi^0 K^+$, which are both rather sensitive to, in particular, the phase of the electroweak penguins, and both tend to favor a *positive* sign instead of the negative one implied by the branching ratios. Unfortunately, the uncertainties are too large to make any clear statements. We have also emphasized that large effects in $\mathcal{A}_{\rm CP}^{\rm mix}(B_d \to \phi K_{\rm S})$ should not be expected, but a quantitative analysis would require better knowledge of the hadronic parameters.

In the course of the analysis, we have used several assumptions, such as the assumption of SU(3) flavor symmetry and that penguin annihilation and exchange topologies can be neglected. We have discussed how well these assumptions are expected to hold and have pointed out possible tests of them. To account for SU(3) flavor breaking, we have included the quantifiable factorizable SU(3) breaking effects, and have estimated the impact of possible larger contributions, where we found that the impact of these effects is moderate and can not explain the $B \to \pi K$ puzzle as the present data point to. Also, we have emphasized that the impact of annihilation and exchange topologies can be tested at the LHC. Finally, we have made very specific assumptions on the model that should describe the $B \to \pi K$ data, which are tested in the rare decay sector, as discussed above. Analogously, any other new physics scenario can be tested in a similar way, though some of the predictive power of our scenario may be lost. One should also keep in mind that the uncertainties are still too large to make any solid claim for new physics and that future data, be it from $B \to \pi K$ or any of the rare decays discussed, will be required before a definite verdict can be reached.

In the final part of this thesis, we have investigated in detail the decays $K_{\rm L} \to \pi^0\nu\bar{\nu}$ and $K^+ \to \pi^+\nu\bar{\nu}$. These are highly interesting, since they are very sensitive to new physics contributions and are theoretically extremely clean. The last point is especially true for $K_{\rm L} \to \pi^0\nu\bar{\nu}$, which has entirely negligible hadronic uncertainties, while $K^+ \to \pi^+\nu\bar{\nu}$ suffers from additional uncertainties in the charm contribution, which have been reduced by a very recent NNLO calculation. We began with an analysis within the SM, using

the present situation as well as some future projections, where we found that, at present, $K^+ \to \pi^+\nu\bar{\nu}$ can be predicted to an accuracy of approximately 10%, while the corresponding uncertainty of $K_{\rm L} \to \pi^0\nu\bar{\nu}$ is about 20%. In both cases, the main uncertainties have their origin in the CKM factors present in the decays. Therefore, we continued with an in detail analysis of the determination of several CKM parameters from either $K_{\rm L} \to \pi^0\nu\bar{\nu}$, $K^+ \to \pi^+\nu\bar{\nu}$ or both decays combined. Our results can be summarized as follows:

- The decay $K_{\rm L} \to \pi^0\nu\bar{\nu}$ alone provides the cleanest determination of the CP violating quantity $\bar{\eta}$, or, equivalently, ${\rm Im}\lambda_t$. Using input from β and γ, also a determination of $|V_{cb}|$ and $|V_{td}|$ becomes possible. All of these statements are, however, valid in the SM only.

- Alternatively, a measurement of $K^+ \to \pi^+\nu\bar{\nu}$ will allow for a determination of R_t and $|V_{td}|$ within the SM.

- Combining information from both decays results in a determination of $\sin 2\beta$ that is independent of $|V_{cb}|$ as well as of contributions from new physics as long one is restricted to the class of minimal flavor violation. Comparing the value thus obtained with the one from $\mathcal{A}_{\rm CP}^{\rm mix}(B_d \to J/\psi K_{\rm S})$ can therefore give some hints as to which kind of new physics one is looking at. Within the SM, both decays combined can be used to construct the entire UT.

For all of these statements to have some impact, one needs rather precise measurements of both decays, in the ball-park of $5-10\%$. These accuracies are rather challenging experimentally and are not to expected in the very near future, even if experimental efforts to measure these decays are actively being pursued nowadays. Still, these efforts should be worthwhile, if not for the precise determination of CKM parameters, then for the search for new physics, to which we have shown that these decays are very sensitive.

Appendix A

Theoretical Expressions

A.1 The $B \to \pi\pi$ System

$$R_{+-}^{\pi\pi} = \frac{1 + 2x\cos\Delta + x^2}{1 - 2d\cos\theta\cos\gamma + d^2} \tag{A.1}$$

$$R_{00}^{\pi\pi} = \frac{d^2 + 2dx\cos(\Delta - \theta)\cos\gamma + x^2}{1 - 2d\cos\theta\cos\gamma + d^2} \tag{A.2}$$

$$\mathcal{A}_{\rm CP}^{\rm dir}(B_d \to \pi^+\pi^-) = -\left[\frac{2d\sin\theta\sin\gamma}{1 - 2d\cos\theta\cos\gamma + d^2}\right] \tag{A.3}$$

$$\mathcal{A}_{\rm CP}^{\rm mix}(B_d \to \pi^+\pi^-) = \frac{\sin(\phi_d + 2\gamma) - 2d\cos\theta\sin(\phi_d + \gamma) + d^2\sin\phi_d}{1 - 2d\cos\theta\cos\gamma + d^2} \tag{A.4}$$

$$\mathcal{A}_{\rm CP}^{\rm dir}(B_d \to \pi^0\pi^0) = \frac{2dx\sin(\theta - \Delta)\sin\gamma}{d^2 + 2dx\cos(\theta - \Delta)\cos\gamma + x^2} \tag{A.5}$$

$$\mathcal{A}_{\rm CP}^{\rm mix}(B_d \to \pi^0\pi^0) = \frac{d^2\sin\phi_d + 2dx\cos(\theta - \Delta)\sin(\phi_d + \gamma) + x^2\sin(\phi_d + 2\gamma)}{d^2 + 2dx\cos(\theta - \Delta)\cos\gamma + x^2}. \tag{A.6}$$

A.2 The $B \to \pi K$ System

$$R = 1 - 2r\cos\delta\cos\gamma + r^2 \tag{A.7}$$

$$\begin{aligned} R_{\rm c} &= 1 - 2r_{\rm c}\cos\delta_{\rm c}\cos\gamma + r_{\rm c}^2 \\ &\quad + qr_{\rm c}\left[2\left\{\cos(\delta_{\rm c} + \omega)\cos\phi - r_{\rm c}\cos\omega\cos(\gamma - \phi)\right\} + qr_{\rm c}\right] \end{aligned} \tag{A.8}$$

$$R_{\rm n} = \frac{1}{b}\left[1 - 2r\cos\delta\cos\gamma + r^2\right] \tag{A.9}$$

$$\begin{aligned} b \equiv \frac{R}{R_{\rm n}} &= 1 - 2qr_{\rm c}\cos(\delta_{\rm c} + \omega)\cos\phi + q^2r_{\rm c}^2 \\ &\quad + 2\rho_{\rm n}\left[\cos\theta_{\rm n}\cos\gamma - qr_{\rm c}\cos(\theta_{\rm n} - \delta_{\rm c} - \omega)\cos(\gamma - \phi)\right] + \rho_{\rm n}^2 \end{aligned} \tag{A.10}$$

$$\mathcal{A}_{\rm CP}^{\rm dir}(B_d \to \pi^{\mp} K^{\pm}) = \frac{2r \sin\delta \sin\gamma}{1 - 2r\cos\delta\cos\gamma + r^2} \tag{A.11}$$

$$\mathcal{A}_{\rm CP}^{\rm dir}(B^{\pm} \to \pi^{\pm} K) = -\left[\frac{2\rho_{\rm c}\sin\theta_{\rm c}\sin\gamma}{1 + 2\rho_{\rm c}\cos\theta_{\rm c}\cos\gamma + \rho_{\rm c}^2}\right] \tag{A.12}$$

$$\mathcal{A}_{\rm CP}^{\rm dir}(B^{\pm} \to \pi^0 K^{\pm}) = \frac{2}{R_{\rm c}}\left[r_{\rm c}\sin\delta_{\rm c}\sin\gamma - q r_{\rm c}\left\{\sin(\delta_{\rm c}+\omega)\sin\phi + r_{\rm c}\sin\omega\sin(\gamma-\phi)\right\}\right] \tag{A.13}$$

$$\begin{aligned}\mathcal{A}_{\rm CP}^{\rm dir}(B_d \to \pi^0 K_{\rm S}) = \frac{2}{b}\Big[& q r_{\rm c}\sin(\delta_{\rm c}+\omega)\sin\phi \\ & -\rho_{\rm n}\left\{\sin\theta_{\rm n}\sin\gamma - q r_{\rm c}\sin(\theta_{\rm n}-\delta_{\rm c}-\omega)\sin(\gamma-\phi)\right\}\Big]\end{aligned} \tag{A.14}$$

$$\begin{aligned}\mathcal{A}_{\rm CP}^{\rm mix}(B_d \to \pi^0 K_{\rm S}) = -\frac{1}{b}\Big[& \sin\phi_d - 2q r_{\rm c}\cos(\delta_{\rm c}+\omega)\sin(\phi_d+\phi) + q^2 r_{\rm c}^2\sin(\phi_d+2\phi) \\ & +2\rho_{\rm n}\left\{\cos\theta_{\rm n}\sin(\phi_d+\gamma) - q r_{\rm c}\cos(\theta_{\rm n}-\delta_{\rm c}-\omega)\sin(\phi_d+\gamma+\phi)\right\} + \rho_{\rm n}^2\sin(\phi_d+2\gamma)\Big].\end{aligned} \tag{A.15}$$

Appendix B

A further SU(3)-Test: $B_s \to K^+K^-$

The decay $B_s \to K^+K^-$ is the U-spin partner of $B_d \to \pi^+\pi^-$, where U-spin is the symmetry that exchanges d and s quarks , in analogy to Isospin. The power of this symmetry has been realized and discussed in [136]. In this case, it allows us to determine the hadronic parameters (d', θ') appearing in the the expressions for $B_s \to K^+K^-$. Therefore, the theoretical expressions for the CP asymmetries are given by

$$\mathcal{A}_{\rm CP}^{\rm dir}(B_s \to K^+K^-) = \frac{2\epsilon d \sin\theta \sin\gamma}{\epsilon^2 + 2\epsilon d \cos\theta\cos\gamma + d^2} \tag{B.1}$$

$$\mathcal{A}_{\rm CP}^{\rm mix}(B_s \to K^+K^-) = \frac{\epsilon^2 \sin(\phi_s + 2\gamma) + 2\epsilon d\cos\theta \sin(\phi_s+\gamma) + d^2 \sin\phi_s}{\epsilon^2 + 2\epsilon d\cos\theta\cos\gamma + d^2}, \tag{B.2}$$

where $\phi_s = 2\beta_s$ is the B_s^0–$\bar{B}_s^0$ mixing phase introduced in 5.7. Numerically, we find that in the SU(3) flavor limit, we expect the direct CP asymmetry to be equal to $\mathcal{A}_{\rm CP}^{\rm dir}(B_d^0 \to \pi^\mp K^\pm) = 0.115 \pm 0.018$, while for the mixing induced CP asymmetry, we update [75] to find:

$$\mathcal{A}_{\rm CP}^{\rm mix}(B_s \to K^+K^-) = (-0.1981)^{+0.0364}_{-0.04480}\,. \tag{B.3}$$

Experimentally, the more interesting quantity on a short-term perspective is the branching ratio. There are two possible ways to obtain a for it, as discussed in [27].

First, we assume that penguin annihilation and exchange topologies are negligible. Then, we can use the branching fraction of $B_d \to \pi^\mp K^\pm$ to obtain

$$\begin{aligned}\frac{\mathrm{BR}(B_s \to K^+K^-)}{\mathrm{BR}(B_d \to \pi^\mp K^\pm)} = &\left[\frac{M_{B_d}}{M_{B_s}} \frac{\Phi(M_K/M_{B_s}, M_K/M_{B_s})}{\Phi(M_\pi/M_{B_d}, M_K/M_{B_d})} \frac{\tau_{B_s^0}}{\tau_{B_d^0}}\right] \\ &\times \left[\frac{F_{B_sK}(M_K^2;0^+)}{F_{B_d\pi}(M_\pi^2;0^+)}\left(\frac{M_{B_s}^2 - M_K^2}{M_{B_d}^2 - M_\pi^2}\right)\right]^2,\end{aligned} \tag{B.4}$$

where

$$\frac{F_{B_sK}(M_K^2;0^+)}{F_{B_d\pi}(M_\pi^2;0^+)}\left(\frac{M_{B_s}^2 - M_K^2}{M_{B_d}^2 - M_\pi^2}\right) = 1.45^{+0.13}_{-0.14} \tag{B.5}$$

corresponds to the factorizable SU(3)-breaking effects and

$$\Phi(x,y) \equiv \sqrt{[1-(x+y)^2]\,[1-(x-y)^2]} \tag{B.6}$$

is the two-body phase-space function. The number in B.5 correspond to ones used in [27] and are determined from Light Cone Sum Rules [216]. In this manner, we find for the branching ratio

$$\mathrm{BR}(B_s \to K^+K^-) = (37 \pm 4)\cdot 10^{-6} \tag{B.7}$$

On the other hand, using U-spin, the quantity H introduced in 3.22 can also be written as

$$H \equiv \frac{1}{\epsilon}\left|\frac{\mathcal{C}'}{\mathcal{C}}\right|^2 \left[\frac{M_{B_d}}{M_{B_s}}\frac{\Phi(M_K/M_{B_s}, M_K/M_{B_s})}{\Phi(M_\pi/M_{B_d}, M_\pi/M_{B_d})}\frac{\tau_{B_s^0}}{\tau_{B_d^0}}\right]\left[\frac{\mathrm{BR}(B_d \to \pi^+\pi^-)}{\mathrm{BR}(B_s \to K^+K^-)}\right], \tag{B.8}$$

where $|\mathcal{C}'/\mathcal{C}|$ is a U-spin-breaking parameter similar to the form factor ratio above:

$$\left|\frac{\mathcal{C}'}{\mathcal{C}}\right|_{\mathrm{fact}} = \frac{f_K}{f_\pi}\frac{F_{B_sK}(M_K^2;0^+)}{F_{B_d\pi}(M_\pi^2;0^+)}\left(\frac{M_{B_s}^2 - M_K^2}{M_{B_d}^2 - M_\pi^2}\right) = 1.76^{+0.15}_{-0.17}. \tag{B.9}$$

In this manner, we obtain

$$\mathrm{BR}(B_s \to K^+K^-) = (49^{+19}_{-18})\cdot 10^{-6} \tag{B.10}$$

which has a much larger uncertainty. In contrast, the current experimental value from CDF is [217]:

$$\mathrm{BR}(B_s \to K^+K^-) = (33 \pm 9)\cdot 10^{-6} \qquad \mathrm{BR}(B_s \to K^+K^-) = (42 \pm 15)\cdot 10^{-6} \tag{B.11}$$

if the ranching ratio is extracted from $B \to \pi^\mp K^\pm$ or $B \to \pi^\mp\pi^\pm$, respectively. The CDF collaboration gives only the branching fraction as normalized to either of the two decays. It will be interesting to compare the prediction with future data, which should give further information on the SU(3)-breaking factors. Further recent theoretical studies of $B_s \to K^+K^-$ can be found in [218, 219].

Bibliography

[1] Glashow, S. L., Nucl. Phys. **22** (1961) 579.

[2] Weinberg, S., Phys. Rev. Lett. **19** (1967) 1264.

[3] Salam, A., *Weak and Electromagnetic Interactions*, published in N.Svartholm, *Elementary Particles Theory*, Proceedings of the Nobel Symposium held 1968 at Lerum, Stockholm 1968, 367-377.

[4] Glashow, S. L., Iliopoulos, J., and Maiani, L., Phys. Rev. **D2** (1970) 1285.

[5] Gaillard, M. K. and Lee, B. W., Phys. Rev. **D10** (1974) 897.

[6] Cabibbo, N., Phys. Rev. Lett. **10** (1963) 531.

[7] Kobayashi, M. and Maskawa, T., Prog. Theor. Phys. **49** (1973) 652.

[8] Christenson, J. H., Cronin, J. W., Fitch, V. L., and Turlay, R., Phys. Rev. Lett. **13** (1964) 138.

[9] Alavi-Harati, A. et al., Phys. Rev. Lett. **83** (1999) 22.

[10] Aubert, B. et al., Phys. Rev. Lett. **87** (2001) 091801.

[11] Abe, K. et al., Phys. Rev. Lett. **87** (2001) 091802.

[12] Aubert, B. et al., Phys. Rev. Lett. **93** (2004) 131801.

[13] Chao, Y. et al., Phys. Rev. Lett. **93** (2004) 191802.

[14] Nir, Y., (2001), hep-ph/0109090.

[15] Fleischer, R., Phys. Rept. **370** (2002) 537.

[16] Ali, A., (2003), hep-ph/0312303.

[17] Battaglia, M. et al., (2003), hep-ph/0304132.

[18] Buras, A. J., (2005), hep-ph/0505175.

[19] Buchalla, G., Buras, A. J., and Lautenbacher, M. E., Rev. Mod. Phys. **68** (1996) 1125.

[20] Beneke, M., Buchalla, G., Neubert, M., and Sachrajda, C. T., Phys. Rev. Lett. **83** (1999) 1914.

[21] Beneke, M., Buchalla, G., Neubert, M., and Sachrajda, C. T., Nucl. Phys. **B591** (2000) 313.

[22] Keum, Y.-Y., Li, H.-N., and Sanda, A. I., Phys. Lett. **B504** (2001) 6.

[23] Keum, Y. Y., Li, H.-N., and Sanda, A. I., Phys. Rev. **D63** (2001) 054008.

[24] Bauer, C. W., Fleming, S., Pirjol, D., and Stewart, I. W., Phys. Rev. **D63** (2001) 114020.

[25] Bauer, C. W., Pirjol, D., and Stewart, I. W., Phys. Rev. **D65** (2002) 054022.

[26] Buras, A. J., Fleischer, R., Recksiegel, S., and Schwab, F., Phys. Rev. Lett. **92** (2004) 101804.

[27] Buras, A. J., Fleischer, R., Recksiegel, S., and Schwab, F., Nucl. Phys. **B697** (2004) 133.

[28] Buras, A. J., Fleischer, R., Recksiegel, S., and Schwab, F., Eur. Phys. J. **C45** (2006) 701.

[29] Buras, A. J., Fleischer, R., Recksiegel, S., and Schwab, F., (2005), hep-ph/0512059.

[30] Buras, A. J., Gorbahn, M., Haisch, U., and Nierste, U., (2006), hep-ph/0603079.

[31] Buras, A. J., Schwab, F., and Uhlig, S., (2004), hep-ph/0405132.

[32] Anisimovsky, V. V. et al., Phys. Rev. Lett **93** (2004) 31801.

[33] Blucher, E., (2005), Talk at Lepton-Photon 2005, Uppsala University, Uppsala, Sweden, June 30-July 5, `http://lp2005.tsl.uu.se/ lp2005/LP2005/programme/index.htm`.

[34] Eidelman, S. et al., Phys. Lett. **B592** (2004) 1.

[35] Wolfenstein, L., Phys. Rev. Lett. **51** (1983) 1945.

[36] Buras, A. J., Lautenbacher, M. E., and Ostermaier, G., Phys. Rev. **D50** (1994) 3433.

[37] Buras, A. J., (1998), hep-ph/9806471.

[38] Buras, A. J., Parodi, F., and Stocchi, A., JHEP **01** (2003) 029.

[39] Charles *et al.* (CKMfitter Group), J., Eur. Phys. J. **C41** (2005) 1, for continuously updated analyses, see `http://ckmfitter.in2p3.fr/`.

[40] Bona *et al.* (UTfit Collab.), M., JHEP **07** (2005) 028, for continuously updated analyses, see `http://utfit.roma1.infn.it/`.

[41] Blucher, E. et al., (2005), hep-ph/0512039.

[42] Branco, G. C., Lavoura, L., and Silva, J. P., Oxford, UK: Clarendon (1999) 511 p.

[43] Bigi, I. I. Y. and Sanda, A. I., Camb. Monogr. Part. Phys. Nucl. Phys. Cosmol. .

[44] Bigi, I. I. Y. and Sanda, A. I., Nucl. Phys. **B193** (1981) 85.

[45] Boos, H., Mannel, T., and Reuter, J., Phys. Rev. **D70** (2004) 036006.

[46] Ciuchini, M., Pierini, M., and Silvestrini, L., Phys. Rev. Lett. **95** (2005) 221804.

[47] Aubert, B. et al., Phys. Rev. Lett. **94** (2005) 161803.

[48] Abe, K. et al., (2005), hep-ex/0507037.

[49] Heavy Flavour Averaging Group, `http://www.slac.stanford.edu/xorg/hfag/`.

[50] Buras, A. J., (2001), hep-ph/0101336.

[51] Buras, A. J. and Jamin, M., JHEP **01** (2004) 048.

[52] Inami, T. and Lim, C. S., Prog. Theor. Phys. **65** (1981) 297.

[53] Buchalla, G., Buras, A. J., and Harlander, M. K., Nucl. Phys. **B349** (1991) 1.

[54] Buras, A. J., Jamin, M., and Lautenbacher, M. E., Nucl. Phys. **B408** (1993) 209.

[55] Buras, A. J., Jamin, M., Lautenbacher, M. E., and Weisz, P. H., Nucl. Phys. **B400** (1993) 37.

[56] Buras, A. J., Jamin, M., and Lautenbacher, M. E., Nucl. Phys. **B400** (1993) 75.

[57] Buras, A. J., Jamin, M., Lautenbacher, M. E., and Weisz, P. H., Nucl. Phys. **B370** (1992) 69.

[58] Chivukula, R. S. and Georgi, H., Phys. Lett. **B188** (1987) 99.

[59] Hall, L. J. and Randall, L., Phys. Rev. Lett. **65** (1990) 2939.

[60] Buras, A. J., Gambino, P., Gorbahn, M., Jager, S., and Silvestrini, L., Phys. Lett. **B500** (2001) 161, hep-ph/0007085.

[61] D'Ambrosio, G., Giudice, G. F., Isidori, G., and Strumia, A., Nucl. Phys. **B645** (2002) 155.

[62] Bobeth, C., Ewerth, T., Kruger, F., and Urban, J., Phys. Rev. **D66** (2002) 074021.

[63] Buras, A. J., Acta Phys. Polon. **B34** (2003) 5615.

[64] Bobeth, C. et al., Nucl. Phys. **B726** (2005) 252.

[65] Beneke, M. and Neubert, M., Nucl. Phys. **B675** (2003) 333.

[66] Aubert, B. et al., Phys. Rev. Lett. **94** (2005) 181802.

[67] Chao, Y. et al., Phys. Rev. **D69** (2004) 111102.

[68] Aubert, B. et al., (2005), hep-ex/0508046.

[69] Abe, K. et al., Phys. Rev. Lett. **94** (2005) 181803.

[70] Aubert, B. et al., Phys. Rev. Lett. **95** (2005) 151803.

[71] Abe, K. et al., Phys. Rev. Lett. **95** (2005) 101801.

[72] Aubert, B. et al., (2004), hep-ex/0408081.

[73] Abe, K. et al., (2005), hep-ex/0507045.

[74] Buras, A. J., Fleischer, R., and Mannel, T., Nucl. Phys. **B533** (1998) 3.

[75] Buras, A. J., Fleischer, R., Recksiegel, S., and Schwab, F., Acta Phys. Polon. **B36** (2005) 2015.

[76] Gronau, M. and London, D., Phys. Rev. Lett. **65** (1990) 3381.

[77] Buras, A. J. and Fleischer, R., Eur. Phys. J. **C11** (1999) 93.

[78] Gronau, M., Pirjol, D., and Yan, T.-M., Phys. Rev. **D60** (1999) 034021, Erratum-ibid. **D69** (2004) 119901.

[79] Gronau, M., Phys. Lett. **B300** (1993) 163.

[80] Buchalla, G. and Safir, A. S., Phys. Rev. Lett. **93** (2004) 021801.

[81] Fleischer, R. and Mannel, T., Phys. Lett. **B397** (1997) 269.

[82] Gronau, M., Lunghi, E., and Wyler, D., Phys. Lett. **B606** (2005) 95.

[83] Grossman, Y., Hocker, A., Ligeti, Z., and Pirjol, D., Phys. Rev. **D72** (2005) 094033.

[84] Gardner, S., Phys. Rev. **D72** (2005) 034015.

[85] Beneke, M., Gronau, M., Rohrer, J., and Spranger, M., (2006), hep-ph/0604005.

[86] Fleischer, R., Eur. Phys. J. **C16** (2000) 87.

[87] Bauer, C. W., Rothstein, I. Z., and Stewart, I. W., (2005), hep-ph/0510241.

[88] Bona *et al.* (UTfit Collab.), M., (2005), hep-ph/0509219.

[89] Buras, A. J. and Fleischer, R., Phys. Lett. **B341** (1995) 379.

[90] Ciuchini, M., Franco, E., Martinelli, G., and Silvestrini, L., Nucl. Phys. **B501** (1997) 271.

[91] Ciuchini, M., Franco, E., Martinelli, G., Pierini, M., and Silvestrini, L., Phys. Lett. **B515** (2001) 33.

[92] Beneke, M., Buchalla, G., Neubert, M., and Sachrajda, C. T., Phys. Rev. **D72** (2005) 098501.

[93] Bauer, C. W., Pirjol, D., Rothstein, I. Z., and Stewart, I. W., Phys. Rev. **D72** (2005) 098502.

[94] Bauer, C. W., Fleming, S., and Luke, M. E., Phys. Rev. **D63** (2001) 014006.

[95] Beneke, M. and Jager, S., (2005), hep-ph/0512351.

[96] Beneke, M. and Yang, D., Nucl. Phys. **B736** (2006) 34.

[97] Bauer, C. W., Pirjol, D., Rothstein, I. Z., and Stewart, I. W., Phys. Rev. **D70** (2004) 054015, hep-ph/0401188.

[98] Li, H.-N., Mishima, S., and Sanda, A. I., Phys. Rev. **D72** (2005) 114005.

[99] Li, H.-N. and Mishima, S., (2006), hep-ph/0602214.

[100] Ciuchini, M. et al., (2004), hep-ph/0407073.

[101] Chiang, C.-W., Gronau, M., Rosner, J. L., and Suprun, D. A., Phys. Rev. **D70** (2004) 034020.

[102] Ali, A., Lunghi, E., and Parkhomenko, A. Y., Eur. Phys. J. **C36** (2004) 183.

[103] Wu, Y.-L. and Zhou, Y.-F., Phys. Rev. **D71** (2005) 021701.

[104] Wu, Y.-L. and Zhou, Y.-F., Phys. Rev. **D72** (2005) 034037.

[105] Du, D.-S., Sun, J.-F., Yang, D.-S., and Zhu, G.-H., Phys. Rev. **D67** (2003) 014023.

[106] Feldmann, T. and Hurth, T., JHEP **11** (2004) 037.

[107] Khodjamirian, A., Mannel, T., and Melic, B., Phys. Lett. **B571** (2003) 75.

[108] Khodjamirian, A., Mannel, T., Melcher, M., and Melic, B., Phys. Rev. **D72** (2005) 094012.

[109] Khodjamirian, A., Nucl. Phys. **B605** (2001) 558.

[110] Cheng, H.-Y., Chua, C.-K., and Soni, A., Phys. Rev. **D71** (2005) 014030.

[111] Baek, S., Botella, F. J., London, D., and Silva, J. P., Phys. Rev. **D72** (2005) 036004.

[112] Baek, S., Botella, F. J., London, D., and Silva, J. P., Phys. Rev. **D72** (2005) 114007.

[113] Yang, Y.-D., Wang, R., and Lu, G. R., Phys. Rev. **D73** (2006) 015003.

[114] Cheng, J.-F., Gao, Y.-N., Huang, C.-S., and Wu, X.-H., (2005), hep-ph/0512268.

[115] Bauer, C. W., Rothstein, I. Z., and Stewart, I. W., Phys. Rev. Lett. **94** (2005) 231802.

[116] Gronau, M., Hernandez, O. F., London, D., and Rosner, J. L., Phys. Rev. **D52** (1995) 6374.

[117] Fleischer, R. and Mannel, T., (1997), hep-ph/9706261.

[118] Buras, A. J. and Fleischer, R., Phys. Lett. **B365** (1996) 390.

[119] Grossman, Y., Neubert, M., and Kagan, A. L., JHEP **10** (1999) 029.

[120] Buras, A. J. and Fleischer, R., Eur. Phys. J. **C16** (2000) 97.

[121] Neubert, M., JHEP **02** (1999) 014.

[122] Aubert, B. et al., Phys. Rev. Lett. **95** (2005) 221801.

[123] Aubert, B. et al., Phys. Rev. **D71** (2005) 111102.

[124] Chao, Y. et al., Phys. Rev. **D71** (2005) 031502.

[125] Fleischer, R. and Matias, J., Phys. Rev. **D61** (2000) 074004.

[126] Fleischer, R. and Matias, J., Phys. Rev. **D66** (2002) 054009.

[127] Lipkin, H. J., Nir, Y., Quinn, H. R., and Snyder, A., Phys. Rev. **D44** (1991) 1454.

[128] Gronau, M., Rosner, J. L., and London, D., Phys. Rev. Lett. **73** (1994) 21.

[129] Fleischer, R., Eur. Phys. J. **C6** (1999) 451.

[130] Fleischer, R. and Recksiegel, S., Eur. Phys. J. **C38** (2004) 251.

[131] Fleischer, R. and Recksiegel, S., Phys. Rev. **D71** (2005) 051501.

[132] Neubert, M. and Rosner, J. L., Phys. Lett. **B441** (1998) 403.

[133] Neubert, M. and Rosner, J. L., Phys. Rev. Lett. **81** (1998) 5076.

[134] Fleischer, R. and Mannel, T., Phys. Rev. **D57** (1998) 2752.

[135] Lipkin, H. J., Phys. Lett. **B445** (1999) 403.

[136] Fleischer, R., Phys. Lett. **B459** (1999) 306.

[137] Ball, P. and Zwicky, R., Phys. Rev. **D71** (2005) 014015.

[138] Buras, A. J., Fleischer, R., Recksiegel, S., and Schwab, F., (2004), hep-ph/0411373.

[139] Williamson, A. R. and Zupan, J., (2006).

[140] Atwood, D. and Hiller, G., (2003).

[141] Yoshikawa, T., Phys. Rev. **D68** (2003) 054023.

[142] Beneke, M., Phys. Lett. **B620** (2005) 143.

[143] Buras, A. J., Fleischer, R., Recksiegel, S., and Schwab, F., Eur. Phys. J. **C32** (2003) 45.

[144] Buras, A. J., Romanino, A., and Silvestrini, L., Nucl. Phys. **B520** (1998) 3.

[145] Buras, A. J. and Silvestrini, L., Nucl. Phys. **B546** (1999) 299.

[146] Buras, A. J., Colangelo, G., Isidori, G., Romanino, A., and Silvestrini, L., Nucl. Phys. **B566** (2000) 3.

[147] Buchalla, G., Hiller, G., and Isidori, G., Phys. Rev. **D63** (2001) 014015.

[148] Arnowitt, R., Dutta, B., Hu, B., and Oh, S., Phys. Lett. **B633** (2006) 748.

[149] Datta, A. and O'Donnell, P. J., Phys. Rev. **D72** (2005) 113002.

[150] Khalil, S., Phys. Rev. **D72** (2005) 035007.

[151] Khalil, S. and Kou, E., Phys. Rev. **D71** (2005) 114016.

[152] Colangelo, G. and Isidori, G., JHEP **09** (1998) 009.

[153] Nir, Y. and Worah, M. P., Phys. Lett. **B423** (1998) 319.

[154] Buras, A. J., Ewerth, T., Jager, S., and Rosiek, J., Nucl. Phys. **B714** (2005) 103.

[155] Barger, V., Chiang, C.-W., Langacker, P., and Lee, H.-S., Phys. Lett. **B598** (2004) 218.

[156] Morozumi, T., Xiong, Z. H., and Yoshikawa, T., (2004), hep-ph/0408297.

[157] Hou, W.-S., Nagashima, M., and Soddu, A., Phys. Rev. Lett. **95** (2005) 141601.

[158] Baracchini, E. and Isidori, G., Phys. Lett. **B633** (2006) 309.

[159] Buras, A. J., Gorbahn, M., Haisch, U., and Nierste, U., (2005), hep-ph/0508165.

[160] Isidori, G., Mescia, F., and Smith, C., Nucl. Phys. **B718** (2005) 319.

[161] Buchalla, G. and Buras, A. J., Phys. Lett. **B333** (1994) 221.

[162] Buchalla, G., D'Ambrosio, G., and Isidori, G., Nucl. Phys. **B672** (2003) 387.

[163] Isidori, G., Smith, C., and Unterdorfer, R., Eur. Phys. J. **C36** (2004) 57.

[164] Buras, A. J., Lautenbacher, M. E., Misiak, M., and Munz, M., Nucl. Phys. **B423** (1994) 349.

[165] Alavi-Harati, A. et al., Phys. Rev. Lett. **84** (2000) 5279.

[166] Alavi-Harati, A. et al., Phys. Rev. Lett. **93** (2004) 021805.

[167] Buchalla, G. and Buras, A. J., Nucl. Phys. **B548** (1999) 309.

[168] D'Ambrosio, G., Isidori, G., and Portoles, J., Phys. Lett. **B423** (1998) 385.

[169] Gomez Dumm, D. and Pich, A., Nucl. Phys. Proc. Suppl. **74** (1999) 186.

[170] Valencia, G., Nucl. Phys. **B517** (1998) 339.

[171] Knecht, M., Peris, S., Perrottet, M., and de Rafael, E., Phys. Rev. Lett. **83** (1999) 5230.

[172] Greynat, D. and de Rafael, E., (2003), hep-ph/0303096.

[173] Isidori, G. and Unterdorfer, R., JHEP **01** (2004) 009.

[174] Batley, J. R. et al., Phys. Lett. **B544** (2002) 97.

[175] Alavi-Harati, A. et al., Phys. Rev. **D67** (2003) 012005.

[176] Barate, R. et al., Eur. Phys. J. **C19** (2001) 213.

[177] `http://www-cdf.fnal.gov/physics/new/bottom/060316.blessed-bsmumu3/`.

[178] Buras, A. J. and Fleischer, R., Phys. Rev. **D64** (2001) 115010.

[179] Grossman, Y. and Nir, Y., Phys. Lett. **B398** (1997) 163.

[180] Lipkin, H. J., Phys. Lett. **B621** (2005) 126.

[181] Gronau, M., Phys. Lett. **B627** (2005) 82.

[182] Gronau, M., Grossman, Y., and Rosner, J. L., Phys. Lett. **B579** (2004) 331.

[183] Grossman, Y., Isidori, G., and Worah, M. P., Phys. Rev. **D58** (1998) 057504.

[184] Hiller, G., Phys. Rev. **D66** (2002) 071502.

[185] Khalil, S. and Kou, E., Phys. Rev. **D67** (2003) 055009.

[186] Ciuchini, M. and Silvestrini, L., Phys. Rev. Lett. **89** (2002) 231802.

[187] Grossman, Y., Ligeti, Z., Nir, Y., and Quinn, H., Phys. Rev. **D68** (2003) 015004.

[188] Fleischer, R. and Mannel, T., Phys. Lett. **B511** (2001) 240.

[189] Buras, A. J., (2004), hep-ph/0402191.

[190] Isidori, G., ECONF **C0304052** (2003) WG304, hep-ph/0307014.

[191] D'Ambrosio, G. and Isidori, G., Phys. Lett. **B530** (2002) 108.

[192] Haisch, U., (2005), hep-ph/0512007.

[193] Adler, S. C. et al., Phys. Rev. Lett. **79** (1997) 2204.

[194] Adler, S. et al., Phys. Rev. Lett. **88** (2002) 041803.

[195] Komatsubara, T. K., (2004), hep-ex/0409017.

[196] Anelli, G. et al., *Proposal to measure the rare decay $K^+ \to \pi^+ \nu\bar{\nu}$ at the CERN SPS*, CERN-SPSC-2005-013.

[197] Littenberg, L., (2005), hep-ex/0512044.

[198] Bryman, D., Buras, A. J., Isidori, G., and Littenberg, L., Int. J. Mod. Phys. **A21** (2006) 487.

[199] Rein, D. and Sehgal, L. M., Phys. Rev. **D39** (1989) 3325.

[200] Hagelin, J. S. and Littenberg, L. S., Prog. Part. Nucl. Phys. **23** (1989) 1.

[201] Lu, M. and Wise, M. B., Phys. Lett. **B324** (1994) 461.

[202] Fajfer, S., Nuovo Cim. **A110** (1997) 397.

[203] Geng, C. Q., Hsu, I. J., and Lin, Y. C., Phys. Rev. **D54** (1996) 877.

[204] Ecker, G., Pich, A., and de Rafael, E., Nucl. Phys. **B303** (1988) 665.

[205] Falk, A. F., Lewandowski, A., and Petrov, A. A., Phys. Lett. **B505** (2001) 107.

[206] Buchalla, G. and Isidori, G., Phys. Lett. **B440** (1998) 170.

[207] Isidori, G., Martinelli, G., and Turchetti, P., Phys. Lett. **B633** (2006) 75.

[208] Buchalla, G. and Buras, A. J., Phys. Rev. **D57** (1998) 216.

[209] Buchalla, G. and Buras, A. J., Nucl. Phys. **B398** (1993) 285.

[210] Buchalla, G. and Buras, A. J., Nucl. Phys. **B400** (1993) 225.

[211] Misiak, M. and Urban, J., Phys. Lett. **B451** (1999) 161.

[212] Buchalla, G. and Buras, A. J., Nucl. Phys. **B412** (1994) 106.

[213] Littenberg, L. S., Phys. Rev. **D39** (1989) 3322.

[214] Buras, A. J., Phys. Lett. **B333** (1994) 476.

[215] Buchalla, G. and Buras, A. J., Phys. Rev. **D54** (1996) 6782.

[216] Khodjamirian, A., Mannel, T., and Melcher, M., Phys. Rev. **D68** (2003) 114007.

[217] Tonelli, D., PoS **HEP2005** (2006) 258, hep-ex/0512024.

[218] Safir, A. S., JHEP **09** (2004) 053.

[219] Descotes-Genon, S., Matias, J., and Virto, J., (2006), hep-ph/0603239.

Acknowledgements

First and foremost I would like to thank Prof. A.J. Buras for the oppertunity to do this work, as well as for all the discussions and advice.

I thank Prof. Wolfgang Hollik for financial support from the Max-Planck Institut.

I thank Andrzej J. Buras, Robert Fleischer, Stefan Recksiegel and Selma Uhlig for the nice and interesting collaborations on the subjects of this thesis. I've learned from all of you.

Anton "Toni P." Poschenrieder, my office-mate, for the great atmosphere we had. All our discussions about physics, life and everything beyond will never be forgotten.

Thanks to everybody who was at T31 during my time, Andrzej Buras, Frank Krueger, Stefan Recksiegel, Luca Silvestrini, Matthias Jamin, Cecilia Tarantino, Diego Guadagnoli, Martin Gorbahn, Sebastian Jaeger, Christoph Bobeth, Thorsten Ewerth, Michael Spranger, Andi Weiler, Anton Poschenrieder, Elmar Wyszomirski, Selma Uhlig, Dominik Bauer, Andi Weinberger, Monika Blanke, Michael Wick, Wolfgang Altmannshofer, Sebastian Schatt, Bjoern Duhling, Christoph Promberger, for the nice atmosphere and interesting discussions

Mark, Anton, Mato, Elmar and Andi Weinberger, for kart-driving, party, pool billiard, cinema and discussions about anything. Special thanks to Andi for beating me at every sport he tried.

Andi Weiler, Vasso, Toby, Selma and Mato: ♫ Thank You for the Music ♫

Diego, for reminding me that "waitresses are more urgent".

Claudia: Surprisingly, we *still* haven't killed each other ;-)

MMM: No, I haven't forgotten the Westzimmer.